EVALUATION OF ANTIOXIDANT PROPERTIES AND NEUROPROTECTIVE EFFECTS OF METHANOLIC LEAF EXTRACT OF *COMBRETUM MOLLE* IN D-GALACTOSE-INDUCED AGING MODEL OF SPRAGUE DAWLEY RATS.

By:

Thandi Mamorapelo Dorothy Fasemore

A Thesis submitted to the Faculty of Health Sciences, University of the Witwatersrand, Johannesburg, in fulfillment of the requirements for the degree of Doctor of Philosophy.

Supervisor: Associate Professor E. F Mbajiorgu

Co-Supervisor: Dr P. Nkomozepi

DECLARATION

I Thandi Mamorapelo Dorothy Fasemore declare that this thesis is my own work. It is being submitted for the degree of Doctor of Philosophy at the University of the Witwatersrand, Johannesburg. It has not been submitted before for any degree or examination at this or any other University.

.....(signature of candidate)

.....5th..... day of…June……,2023

DEDICATION

Ndi bulela konke ku Thixo Bawo, Sonini na nini konke ku vela kuwe. All the Glory and Honor belong to my God for giving me the wisdom to prevail and the strength and the capacity to persevere in the face of adversity, and most importantly for enabling me to keep going in spite of life's challenges and not give up.

To my mother, Tshatiwe Heester Nqinileyo ndi ya bulela nge mfundiso zakho. Jou kind het bo en behalwe die skryf van naam en van gegaan, jou drome word vervul.

To my husband, Dr. Olufemi Fasemore thank you for making “Two are better than one, for they receive the reward for their labor” a reality. Most of all thank you for taking up the roles of being a mother and father to our children. Your labor of love is greatly appreciated.

To my God-given gifts: Olulana Siphoesihle Akinfesi, Ayomide Abiodun Dithapelo, and Isabella Adebanke Vuyolwethu Fasemore thank you for understanding that mommy is studying and working, your presence is like a breath of fresh air to me. I thank God for giving you to me.

In loving memory of my niece Lulama Lucia Mphatho (20 November 1992 – 01 November 2022), though you are gone too soon your efforts and memory will always be with us. Lala ngo xolo ma Mnune Doi xhesibe.

PUBLICATION AND PRESENTATION ARISING FROM THIS STUDY

Conference Proceedings and IBRO schools attended.

1. Ameliorative effect and antioxidant activity of *Combretum molle* in D-galactose induced reactive oxygen species. ***T. M. D. FASEMORE**. P. NKOMOZEPI, E. F. MBAJIORGU. Oral presentation at the 2nd IBRO-ARC Workshop: Oxidative Stress Implication in Neurological Disorders. Faculty of Science, University of Alexandria, 7th - 11th April 2019, Alexandria, Egypt.
2. The efficiency of the *Combretum molle* on antioxidant markers and cognitive performance in D-galactose induced aging rat brain. IBRO-ARC SCHOOL: Neuropharmacology research and drug development. Miklin Hotel, Apamtse Street, East Legon, 31st October - 3rd November 2021, Accra, Ghana.
3. The Neuroprotective effects of *Combretum molle* methanolic leaf extract in the brain of D-galactose induced aging rat model. ***T. M. D. FASEMORE**. P. NKOMOZEPI, E. F. MBAJIORGU. Oral presentation at the 15th Society for Neuroscientist Africa (SONA)/4th Ghana Neuroscience Society (GNS), 27th - 30th October 2021 in Accra, Ghana, West Africa.
4. Adult neurogenesis and protective effect of *Combretum molle* methanolic leaf extract on D-galactose induced aging rat model of Sprague Dawley. ***T. M. D. FASEMORE**. P. NKOMOZEPI, E. F. MBAJIORGU. Virtual Poster Presentation at the 50th Annual Meeting for Society for Neuroscience (SFN), 8th – 11th November 2021 in Chicago, IL, USA.

Publication arising from this study.

No publications accepted yet.

ABSTRACT

Several physical and biochemical changes in the body occur because of the biological process of aging. As part of natural aging, the brain encounters morphological and functional changes that affect dendritic trees and synapses, neurotransmission, circulation, and metabolism. The brain's high metabolism, elevated levels of lipids, and inadequate antioxidant defences make it susceptible to oxidative stress. A reducing sugar called D-galactose (D-gal) causes a significant build-up of reactive oxygen species (ROS). *Combretum molle* (*C.molle*) is a plant rich in compounds that scavenge free radicals and is frequently used to cure a variety of human illnesses in African traditional medicine. This study investigated into the potential impact of *C.molle* on rat brain aging brought on by D-galactose.

Fifty adult male Sprague Dawley rats were treated for 90 days and were composed of 5 groups (n=10) as follows: I) Control group received saline and distilled water, II) *C.molle* only group received intragastric gavage of *C.molle (500 mg/kg)*, III) D-gal only group received a subcutaneous injection of D-galactose (150 mg/kg), IV) CMD 90 group received D-galactose and *C.molle* simultaneously for 90 days, V) CMD 45 group received D-galactose for the first 45 days and *C. molle* for the remaining 45 days. The animals underwent behavioral evaluation post-treatment for a further period of 7 days twice a day. The rat's cognitive function was evaluated through Novel object recognition and object location tests. The lipid peroxidation marker malondialdehyde (MDA), glutathione peroxidase (GSH-Px), glutathione (GSH), superoxide dismutase (SOD), and catalase (CAT) activity were measured by colorimetric assays. The acetylcholinesterase (AchE), Acetylcholine (Ach), Brain Derived Neurotropic Factor (BDNF), and Tumor Necrosis Factor (TNF) alpha were measured using ELISA kits. The effects on adult neurogenesis were assessed through Ki-67 and doublecortin (DCX) immunohistochemistry.

The *C.molle* significantly attenuated the effects of D-galactose-induced changes in the hippocampus and cortex, ranging from cognitive capacity, and oxidative stress among the groups by increasing GSH, BDNF, Ach levels, CAT and SOD activity. Additionally,

C. molle treatment caused a decrease in the levels of MDA, TNF alpha and AchE activity and reduced cell proliferation and neuroblast differentiation brought about by D-galactose.

ACKNOWLEDGEMENTS

This study is the culmination of many years' worth of arduous labor, dedication, and support from men and women from the School of Anatomical Sciences at the University of the Witwatersrand and the Department of Human Anatomy and Physiology at the University of Johannesburg.

My supervisors Associate Professor Felix Mbajiorgu and Dr Pilani Nkomozepi thank you all for the support and guidance rendered to make sure that this study reaches its completion. God bless you all abundantly.

A special appreciation to Ms Hasiena Ali for all the knowledge impacted on me with regard to laboratory techniques and for all the assistance rendered during the study.

To Moratuwa January thanks for availing yourself in my absence and making sure things run smoothly with animal treatment and most importantly thanks for not quitting when things looked impossible for you.

Finally, special gratitude goes to the University of Limpopo, for all the tuition fees paid towards this study for five years and the University of Johannesburg for partial payment of my tuition fees for one year.

Funding

Research Grants and Awards

1. The funding for this study was obtained from the New Generation of Academics (nGap) through the University of Limpopo.
2. DST-NRF Research Development Grant (2016-2017), (nGAP) Ref: NGAP RDG 160504163874.
3. NRF Thuthuka Research Grant (2018-2019) reference TTK190327424705
4. NRF Thuthuka Research Grant (2020-2021) reference TTK190327424705, Grant No: 121982
5. IBRO Travel grant costs for virtual attendance at the Society for Neuroscience annual meeting taking place in Chicago, USA between November 8-11, 2021.

Table of contents

Nomenclature

AB	Avidin-biotin
Ach	Acetylcholine
AchE`	Acetylcholinesterase
AGE	Advanced glycation end products
ANOVA	Analysis of variance
BDNF	Brain Derived Neurotropic Factor
BSA	Bovine serum albumin
CAR	Carnosine
CAT	Catalase
^{o}C	Celcius
ChAT	Choline acetyltransferase
CM	*Combretum molle*
CMD 45	*Combretum molle* and D-Galactose
CMD 90	*Combretum molle* + D-Galactose
C.molle	*Combretum molle*
CU	Copper
CYS	Cystein
DAB	Diaminobenzidine
DCX	Doublecortin
DG	Dentate gyrus
D gal	D-galactose

DI	Discrimination index
DMF	N,N-Dimethylformamide
DNA	Deoxyribonucleic acid
DPX	Distyrene plasticizer xylene
DTNB	Dithiobisnitro benzoic acid
dUTP	Deoxynucleotidyl transferase
EDTA	Ethylene diamine tetra acetic acid
ELISA	Enzyme linked immunosorbent assay
$Fe3^{+}$	Iron III
GABA	Gamma-aminobutyric acid
GCL	Glycine cysteine ligase
GLU	Glutamate
GLY	Glycine
G6P	Glucose 6-phosphate
GS	Glutathione synthase
GSH	Glutathione
GSH-Px	Glutathione peroxidase
GSSG	Glutathione disulfide
GR	Glutathione reductase
h	Hour
H&E	Haematoxylin and Eosin
H_2O_2	Hydrogen peroxide
H_2O	Water

HIV	Human immuno deficiency virus
IGNs	Immature granular neurons
LC	Liquid chromatography
MDA	Malondialdehyde
MS	Mass spectrometry
$NaCO_3$	Sodium carbonate
NADPH	Nicotinamide adenine dinucleotide phosphate
NBT	Nitro Blue Tetrazolium
NGS	Normal Goat Serum
NOR	Novel object recognition
OB	Olfactory bulb
O_2	Oxygen
OFT	Open field test
OLT	Object location test
PFA	Paraformaldehyde
PBS	Phosphate buffer saline
6PGL	6-phosphoglucono-d-lactone
RMS	Rostral migratory stream
RNA	Ribonucleic acid
ROS	Reactive oxygen species
rpm	Revolutions per minute
SAP	IgG-saporin
SOD	Superoxide Dismutase

SGZ	Subgranular zone
SVZ	Subventricular zone
TAU	Taurine
TBA	2- Thiobarbituric acid
TBARS	Thio barbituric reactive substances
TCA	Trichloroacetic acid
TIT	Total Investigation Time
TNF- α	Tumor necrosis factor alpha
TUNEL	Nick end labelling
UWRAF	University of the Witwatersrand research animal facility
Zn	Zinc

List of Figures

List of Tables

Preface

In the world of medicine, aging is a crucial biological process. It is well known that age related conditions like Dementia, Parkinson's disease and Alzheimer's illness and cognitive impairment are major causes of disability and dependency among elderly people worldwide. Numerous neurodegenerative diseases, including schizophrenia, Parkinson's disease, Alzheimer's disease, multiple sclerosis, Huntington's disease, and cognitive conditions in the aged, are influenced by free radical-induced oxidative stress. Antioxidants are a very crucial defense mechanism against free radical-induced damage and are critical for maintaining optimum health and well-being. The brain is more susceptible to oxidative stress, which can lead to structural and functional changes in brain structures because it has lesser antioxidant activity and defenses than other tissues. The use of natural products has increased globally due to their lower adverse effects, affordability, availability, and high efficacy in most human illnesses. Antioxidants in foods are generally considered safe, and studies of antioxidant supplements generally have not reported adverse effects. The usage of *Combretum molle* for the treatment of numerous ailments and disorders is supported by research in literature. The anticholinesterase activity and antioxidant effects of *Combretum molle* in the brain regarding cholinergic function and in learning and memory, however, are little understood.

1 INTRODUCTION

1.1 General Introduction

The natural and biological process of aging is defined by a steady loss of physiological function, a reduced capacity to adjust to environmental cues, a higher propensity for disease, and a rising death rate. Aging consequently leads to several morphological and metabolic alterations in the body. Africa has around 18% of the global population which is estimated to rise to 38% by 2100. Generally, developed nations have a higher percentage of elderly people (those 60 or over), but Africa has a smaller proportion of this population due to a lower median age and a life expectancy of 64 for women and 61 for men (Gyasi and Phillips, 2020, He et al., 2020).

Various factors including quality of public health, medical care, and diet contribute to the lower life expectancy in Africa and other developing countries. The population of the elderly in Africa was estimated to the average of 5.6 % in 2020 compared to world population (Ritchie and Roser, 2019, Mitchell and Walker, 2020). In 2020, the total population and those Aged 60 and Older for Africa by Subregion was estimated to the average of 8.9 % for Southern Africa followed by 7.9 % for Northern Africa (He et al., 2020). In Africa, the distribution of the older population is geographically dispersed between rural and urban area with more elderly in the rural areas (Douglass, 2015, Ritchie and Roser, 2019). In general, aging has developed into a socioeconomic issue that burdens nations all over the world in terms of social security systems, labor markets, health, productivity, and societal growth (Douglass, 2015, He et al., 2020). Certain memory deficiencies, such as delayed verbal recall and decreases in working memory, short-term memory, processing speed, and spatial memory, are linked to aging (Von Bohlen Und Halbach et al., 2006, Currais and Maher, 2013). Dementia, Alzheimer's disease, Parkinson's disease, amyotrophic lateral sclerosis, and glaucoma are among the neurodegenerative illnesses that are most associated with aging (Yin et al., 2016,

Mattson and Arumugam, 2018). These disorders place a burden on public health system in Africa as most countries lack well equipped health care facilities. In Africa, the use of traditional herbal treatments as complementary medicine is significant since it is used to treat a variety of medical disorders as part of primary healthcare (Sofowora, 1996, Adewunmi and Ojewole, 2004, Peltzer et al., 2008, Ogbera et al., 2010, Ozioma and Chinwe, 2019, Paudyal et al., 2022).

It is vitally necessary to increase our knowledge and understanding of the basic mechanisms underpinning both healthy aging and age-related illness. Researching strategies to support healthy aging and creating effective anti-aging therapy interventions are of utmost relevance (Mitchell et al., 2015). There are two distinct aging models namely the naturally aging and the accelerated aging which are used to investigate effects of aging.

Scientifically accelerated aging models are favoured because they can be used quickly and easily, in contrast to naturally aging models that take more time and have higher costs. Shorter study times and low animal mortality rates during the experimental period are additional benefits of the accelerated aging model (Mitchell et al., 2015, Azman and Zakaria, 2019, Cai et al., 2022). Examples of the several accelerated aging models used include D-galactose-induced (D-gal) for *in vitro* and *in vivo* studies, hydroxyurea therapy, radiation-induced, jet lag-induced, senescence-accelerated prone mice, Klotho mice, and thymus-removed mice (Mitchell et al., 2015, Azman and Zakaria, 2019). The most popular and well accepted of these aging models is the D-gal-induced aging model because it is simple to employ, has few adverse effects, and has a low death rate during the experiment.

1.2 Problem statement

Plant extracts are used in traditional medicinal practices around the world to treat a variety of illnesses. However, the scientific bases for the use of these plants, in some instances, are not documented for reference. Poisoning and occasionally death may occur as a result. Currently, South Africa embraces both conventional and traditional medicine. Nonetheless, traditional medicine is widely used, with estimates stating that up

to 80% of the black population consults traditional healers, who outnumber allopathic physicians by a ratio of at least 10 to 1 (McGaw et al., 2001, Babb et al., 2007, Stafford et al., 2008). Cognitive impairment is one of the conditions that puts a burden not only on the patient but also on the family (Morris and Cummings, 2005, Morris et al., 2001). Modern medications are expensive, but they only partially improve the damage to brain cells and partially inhibit the ongoing degenerative process. The above underscore the need for continuous study and documentation of the scientific bases for the use of plant extracts in health care system for development of alternative, affordable and available treatment options.

As earlier on stated, evidence exist in literature on the usage of *Combretum molle* for the treatment of numerous illnesses, such as heart diseases, worm infections as well as wound dressings and treatment of the mentally ill among others (Eloff et al., 2008, Ojewole, 2008, Masoko et al., 2010, Manga et al., 2012, Nair et al., 2012, Mapiye, 2019). However, there is dearth of information on the neuroprotection and anticholinesterase activity of *Combretum molle* in the brain relative to cholinergic function and in learning and memory. Furthermore, the safety profile of *Combretum molle* on neuronal toxicity (oxidative brain damage) has not been studied and documented.

1.3 Aim and Objectives

1.3.1 Aim

To determine whether *Combretum molle* methanolic leaf extract counteracts D-galactose-induced aging in the Sprague Dawley rats' brains.

1.3.2 Objectives

The objectives of this study sought to evaluate:

- The effects of *Combretum molle* on hippocampal-dependent learning and memory in D-galactose-induced aging rats using the Novel Object Recognition (NOR) and Object Location test (OLT).
- The effects of *Combretum molle* on oxidative stress and antioxidant status in the brain by measuring the levels of GSH, MDA and antioxidant defence enzymes (SOD, GPx and CAT).

- The quantities of AchE and Ach in the brain to ascertain the anticholinesterase activity of *Combretum molle*.
- The effects of *C. molle* on neuronal cell division and proliferation in the hippocampus and cortex using the anti-Ki-67 and anti-doublecortin (DCX) antibodies.
- The impact of *C. molle* on brain aging caused by D-galactose on levels of Tumor necrosis factor (TNF alpha).
- The level of Brain Derived Neurotropic Factor (BDNF) in order to ascertain the effect of *C. molle's* methanolic leaf extract on the level of neurotropic factors

2 LITERATURE REVIEW

2.1 Structural modifications in the brain due to aging

The brain changes both morphologically and functionally as it ages, impacting dendritic trees and synapses. Reduced sensitivity of the catecholaminergic, dopaminergic, cholinergic, and opioid systems are among the changes that occur throughout normal aging (Mariani et al., 2005, McDaniel et al., 2007). The effects of aging process also impact adversely on neural structures, manifesting in functional alterations associated with circulation, neurotransmission, and metabolism (Schliebs and Arendt, 2006, Mattson and Arumugam, 2018). These structural and functional modifications can alter the sensory and motor systems, affecting sleep, learning and memory (Kumar et al., 2011, Dorszewska, 2013).

The free radical neurological damage hypothesis (Haman's theory) is one of the aging theories which proposes that free radical and reactive oxygen species production can cause cell and tissue damage, along with changes in gene function that cause aging and premature cell death (Knight, 2001, Wickens, 2001, Lee et al., 2004, Mariani et al., 2005). Moreover, age-related deficits are mostly caused by the brain's increased vulnerability to the negative effects of oxidative stress (Knight, 2001, Mariani et al., 2005).

Various studies established that aging processes leads to accumulation of waste products of metabolism resulting in physiological changes, decline in biological function and less ability to adapt to metabolic stress which will eventually affect all bodily organs to varying degrees with different disease endpoints (Song et al., 1999, Wei et al., 2005a, Lobo et al., 2010, Lu et al., 2010, Zhen et al., 2016a).

Damage to all cellular components (proteins, lipids, and nucleic acids) is caused by free radicals and peroxides, which are produced when normal metabolic processes (oxidative metabolism) of cells are disrupted (Song et al., 1999, Wei et al., 2005b, Zhang et al., 2008, Haider et al., 2014). In numerous age-related neurodegenerative disorders, reactive oxygen species (ROS) production has been connected to an important phase in the death of neuronal cells (Cui et al., 2006, Lu et al., 2007), suggesting that the accumulation of

these free radicals gradually destroys brain structures and eventually results in functional impairments (Mariani et al., 2005, Cui et al., 2006, Lei et al., 2008a).

One of the major risk factors for neurodegenerative conditions linked to cognitive decline and memory dysfunction is the increase of free radicals known as oxidative stress (Lu et al., 2006, Hsieh et al., 2009., Haider Saida et al., 2014 , Shwe et al., 2018).Thus a heightened vulnerability to the long-term effects of oxidative stress has been reported as a major contributing factor in the pathogenesis of aging (Sen and Chakraborty, 2011, Haider et al., 2014). Incidences of stroke, white matter lesions, dementia, level of memory impairment and changes in levels of neurotransmitters amongst others have been associated with aging (Peters, 2006, Rattan, 2008). Aging is mainly due to the result of lipid peroxidation, DNA damage, protein oxidation by free radical action (Sen and Chakraborty, 2011).

Among most models of aging, D-galactose has been successfully used *in vivo and in vitro* to simulate the effects of aging by causing oxidative stress, mitochondrial malfunction, and intracellular damage to neurons. These effects also help accelerate aging and affect age-related cognitive decline (Park et al., 2011, Shwe et al., 2018, Nam et al., 2019, Wang et al., 2020).

2.2 D-Galactose metabolism

D-galactose (D-gal) is a reducing sugar that is abundant in milk products and other non-dairy foods including fruits and vegetables. It occurs naturally in the body and is completely metabolized at normal physiological concentrations (Lei et al., 2008a, Hsieh et al., 2009). The maximum daily intake of D-galactose for an adult human in good health is 50 g, and the normal concentration of D-galactose in the blood is thought to be less than 10 mg/dL (Shwe et al., 2018, Azman and Zakaria, 2019). At normal concentrations, D-gal is converted to glucose by two enzymes namely galactokinase and uridyl transferase (Song et al., 1999, Lei et al., 2008b, Ji et al., 2015). However, at high levels, D-gal (see Figure 2.1 below) is metabolized into hydrogen peroxide by the enzyme galactose oxidase, which ultimately results in the generation of superoxide anions and oxygen-derived free radicals that damage macromolecules and cell function (Haider et al.,

2015, Zhen et al., 2016a). Furthermore, When D-gal levels are high, it alters the structure of proteins and peptides by reacting with their free amine groups. This non-enzymatic glycation process leads to the accumulation of advanced glycation end (AGE) products and, eventually, Reactive Oxygen Species (ROS), which results in oxidative stress and neurotoxic effect on the brain (Song et al., 1999, Zhang et al., 2005, Cui et al., 2006, Lei et al., 2008a, Ji et al., 2015).

For brain research and the screening of anti-aging agents, D-galactose is frequently used to mimic aging in animal models. It causes brain aging that is analogous to human brain aging in many aspects, including conditions such as cognitive impairment, increased oxidative stress and mitochondrial malfunction, neuronal degeneration, and apoptosis (Azman and Zakaria, 2019, Aydın et al., 2016b) in several parts of the brain, including the cerebral cortex and hippocampus (Rehman et al., 2017).

2.2.1 Studies on D-galactose induced aging.

Studies have shown that oral D-gal exposure in housefly (*Musca domestica*) and 6.5 % in culture medium of fruit fly (*Drosophila melanogaster*) shortened the lifespan (Cui et al., 2004). Also chronic subcutaneous injections of D-gal with doses ranging from 50mg/kg to 200mg/kg in mice and rats induced cognitive dysfunction (Xu and Zhao, 2002, Lu et al., 2007, Wang et al., 2011, Haider et al., 2014, Ji et al., 2015), and malfunction in the mitochondria (Lin and Beal, 2006, Long et al., 2007, Yousuf et al., 2009, Kumar et al., 2010), oxidative stress (Hsieh et al., 2009, Liu et al., 2010, Aydın et al., 2016c, Budni et al., 2016), through formation of AGE (Song et al., 1999, Ramasamy et al., 2005), decreases in neurogenesis (Zhang et al., 2005, Cardoso et al., 2015) and neurological impairments including increased apoptosis, decreased density of synapses and reduction in the neural progenitor cells migration in the subgranular zone (SGZ) of the dentate gyrus (DG) (Song et al., 1999, Zhang et al., 2005, Cui et al., 2006, Lei et al., 2008a, Zhu et al., 2014, Zhen et al., 2016b, Zhang et al., 2017, Shwe et al., 2018).

According to other studies, basal forebrain cholinergic neurons are impaired by prolonged exposure to high amounts of D-gal, which impairs cognition and memory (Xu and Zhao, 2002, Wei et al., 2005b, Hua et al., 2007, Lei et al., 2008b, Lu et al., 2010, Ji et al., 2015).

Therefore, protective agents against aging induced changes in the brain should potentially mitigate these D-galactose effects.

There are various studies that were done recently using plant-based extract to determine whether they attenuate the effects of D -galactose on aging rat brains. A study by Firdaus et al., 2022 reported that the adult rat brain is protected from neurodegeneration, oxidative stress, and cognitive impairments by *Centella asiatica* (Firdaus et al., 2022). The effects of Chrysin, a flavonoid extract, on a D-galactose-induced model were examined in a different study by Prajit et al., (2020), and they found that it protected against memory loss and the reduction of hippocampal neurogenesis (Prajit et al., 2020). According to a different study, supplementing with cocoa powder prevents oxidative stress, cholinergic dysfunction, and cell death in the D-galactose-induced aging rat brain (Yoo and Kim, 2021). By lowering levels of reactive oxygen species, these plant extracts have been demonstrated to be beneficial in maintaining the antioxidant status of the brain.

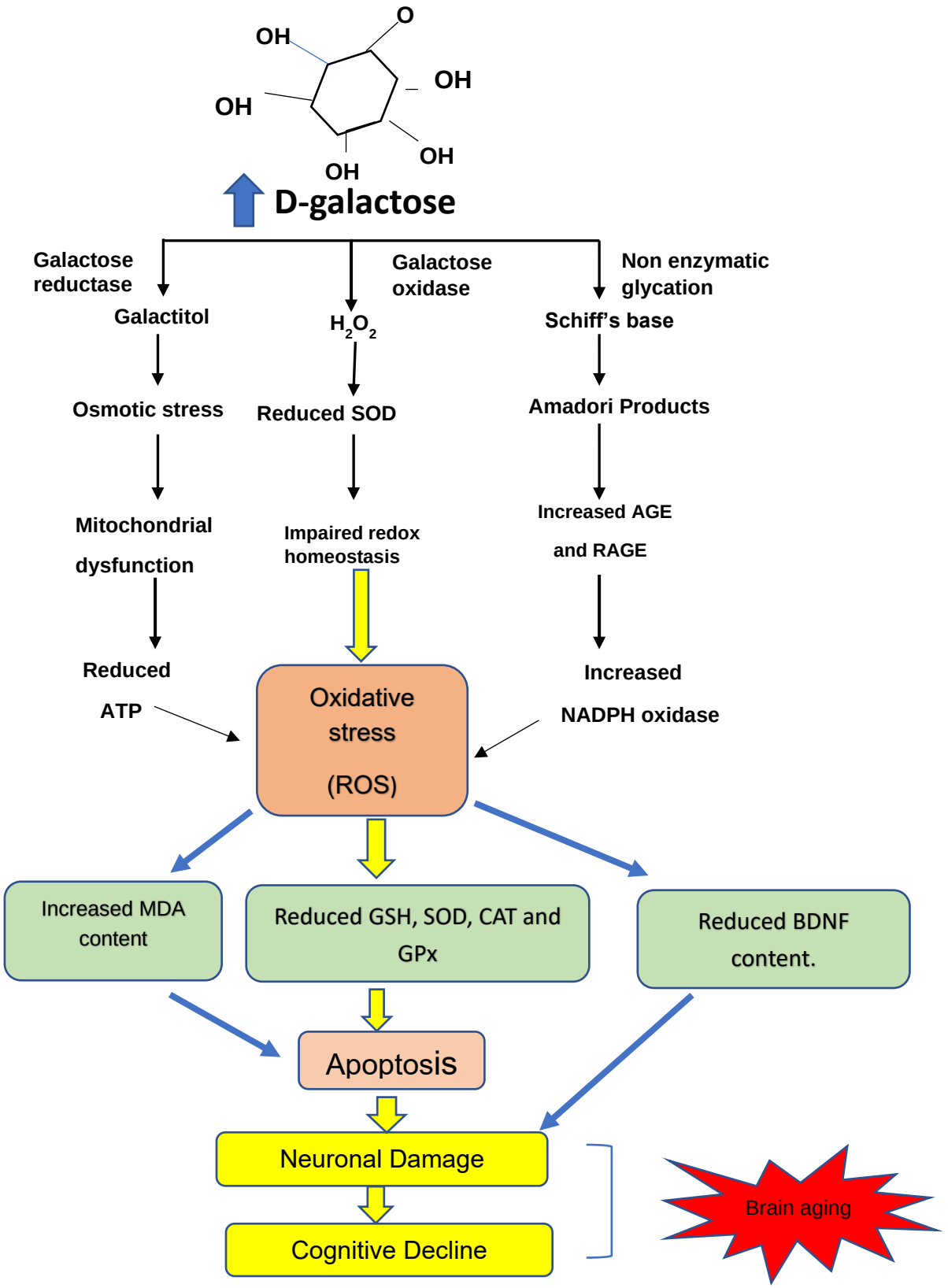

Figure 1.1: Flow Diagram showing mechanism involved in D-galactose induced aging. Adopted from Azman and Zakaria., 2019 and modified

2.3 Reactive oxygen species (ROS)

Reactive oxygen species (ROS) are a variety of molecules and free radicals produced from molecular oxygen. They are toxic byproducts of aerobic metabolism that are primarily formed in mitochondria, peroxisomes and other cellular components that includes proteins or molecules that support activities of the respiratory chain with a sufficiently high redox potential to excite or donate an electron to the atmospheric oxygen (Mittler, 2017). Lower ROS concentrations are reported to have some beneficial effect in plants as they can act as important mediators of cell signaling events, such as supporting cellular proliferation, physiological function, and cell viability (Mittler, 2017, Fattman et al., 2003). Despite their beneficial effect, they are also toxic in the presence of Fe^{3+} (Fenton reaction) causing the disruption of cell membranes and inappropriate activation or inactivation of enzymes (Fattman et al., 2003). The excessive production of ROS results in oxidative stress and has been linked to the pathogenesis of various conditions and identified as one of the causal factors in the aging process (Li et al., 2010). Because of the brain's high oxygen demand and rapid metabolic rate, ROS progressively increase with age, which causes a decrease in the amount of ATP available for reductive synthesis and an increase in peroxidation damage (Von Bernhardi et al., 2010). In an animal cell, ROS target proteins, carbohydrates, lipids, deoxyribonucleic acid (DNA) and ribonucleic acid (RNA) molecules.

2.4 Lipid peroxidation

The brain has multiple factors such as it has high oxygen demand per unit weight, a high content of easily peroxidizable unsaturated fatty acids, the presence of Fe3+ (Fenton reaction) and ascorbate (key ingredients in causing membrane lipid peroxidation) and is not highly enriched in antioxidant protective defenses (Floyd and Hensley, 2002). These factors, makes the brain prone to oxidative damage. Malondialdehyde (MDA), a key byproduct of lipid peroxidation that interacts with free amino groups in proteins, phospholipids, and nucleic acids to modify their structural composition, is the most widely used biomarker to study oxidative damage (Ho et al., 2003, Aly et al., 2011a, Sridharamurthy et al., 2012, Haider et al., 2014, Zhen et al., 2016b).

Malondialdehyde, is a highly reactive dialdehyde, produced by arachidonic acid catabolism or lipid peroxidation of unsaturated fatty acids, and has been associated to the generation of age-related pigments and is believed to be accelerated by oxidative stress (Dei et al., 2002). Reactive oxygen species cause the oxidative destruction of lipids, which produces highly reactive and unstable lipid peroxides that can be fragmented to produce a variety of reactive intermediates, including malondialdehyde which increases with increasing chronological age in tissue samples (Dei et al., 2002, Zhu Yuangui et al., 2006). Due to its fast metabolic rate, high lipid content, and weak antioxidant defense system, the brain is particularly susceptible to oxidative stress. Thus, Increased MDA is a well-known indicator of oxidative damage. Therefore, it has become more crucial in recent years to identify therapeutic agents such as antioxidants that can retard the lipid peroxidation process by preventing the development of free radical chain reactions.

2.5 Antioxidant defence system

2.5.1 Antioxidant enzymes

Antioxidant enzymes have been postulated to defend against biological oxidative damage by scavenging oxygen free radicals. Superoxide dismutase (SOD), glutathione peroxidase (GPx), and catalase (CAT) are the three main antioxidant enzymes that prevent or treat cellular damage caused by ROS (Ighodaro and Akinloye, 2018). There are three different SOD isoforms found in mammalian species: the cytosolic Cu/Zn SOD (SOD 1), Mn SOD (SOD2), and extracellular Cu/Zn SOD (SOD3) and among these isoforms SOD1 and SOD2 are expressed in all cells, whilst SOD3 is only significantly expressed in a few tissues, including the blood vessels, lungs, kidneys, and heart (Wang et al., 2018).

Superoxide radicals are converted into hydrogen peroxide (H_2O_2) and molecular oxygen (O_2) by SOD, acting as the body's first line of defense against oxidative stress (Fattman et al., 2003). The GPx and CAT further scavenge H_2O_2, which may result in the formation of water (H_2O) (Ighodaro and Akinloye, 2018, Wang et al., 2018). However, failure to convert H_2O_2 by CAT and GPx leads to accumulation of H_2O_2 in the body which eventually leads to the insufficiency or modification of antioxidant defense system. This insufficiency or modifications of antioxidant enzymes in metabolism result in an excessive amount of reactive oxygen species (ROS), which can damage macromolecules (proteins, lipids, and

DNA) and cell membranes leading to apoptosis and necrosis (Ho et al., 2003, Zhang et al., 2008, Aly et al., 2011b, Bhatnagar et al., 2012, Carocho and Ferreira, 2013, Zhen et al., 2016a, Wang et al., 2018).

Many clinical conditions, including some of the most prevalent age-dependent diseases like cardiovascular diseases, neurological diseases, and cancer, have been linked to reduction in the expression level or catalytic activity of SODs (Wang et al., 2018). Reduced ROS generation and ROS neutralization by antioxidants are essential for lowering oxidative stress. Antioxidants are molecules that directly scavenge ROS or upregulates antioxidant defenses (Carocho and Ferreira, 2013). The human antioxidant system is divided into non-enzymatic and enzymatic defenses of which the latter is further divided into primary and secondary enzymatic defense. Its antioxidant capacity also decreases with age. Antioxidants obtained from plants, animals, and minerals can be consumed exogenously and have been shown to improve human health and lower the incidence of diseases caused by free radicals (Ho et al., 2003, Wei et al., 2017, Carocho and Ferreira, 2013, Zhen et al., 2016a, Shwe et al., 2018).

For instance, a research report by Zhang et al., (2016) revealed that in mice with D-gal-induced aging, antioxidant products such hydrolysates protein of the Big Yellow Croaker (*Pseudosciaena crocea*) promoted an increase in SOD, CAT, GPx, and GR activity and triggered a decrease in MDA (Zhang et al., 2016). Another study by Aydin et al., (2016) found that the antioxidant defense mechanisms SOD, CAT, and GPx were increased by carnosine (CAR; -alanil-L-histidine) and taurine (TAU; 2-aminoethanesulfonic acid) and that MDA levels were decreased in the D-galactose-induced aging rat model (Aydın et al., 2016a).

Age-related disorders can be effectively treated with a variety of plant extracts that have antioxidant efficacy and cholinesterase activity. For example the following plant extracts: Iriodoide glycoside catalpol, derived from fresh roots of *Rehmannia* (Zhang et al., 2007*)*, *Centella asiatica* leaf extract (Kumar et al., 2011, Firdaus et al., 2022), purple sweet potato (*Dioscorea alata*) a naturally occurring anthocyanin (Zhang et al., 2009, Lu et al., 2010), Troxerutin a natural bioflavanoid (Lu et al., 2011), soy isoflavones (Hsieh et al., 2009.), *Ginkgo biloba* (Abd-Elhady et al., 2013), Stevia (*Stevia rebaudiana Bertoni*) (Zhao et al., 2019), Piperine (Wang et al., 2019), walnut (*Juglans*) (Rusu et al., 2020), *Moringa oleifera*

(Jamari et al., 2020), Cacao powder (*Theobroma cacao*) (Yoo and Kim, 2021) and *Sarcococca saligna* (Saleem et al., 2023) have been shown to ameliorate the consequences of brain aging in models of D-gal-induced aging.

2.5.2 Glutathione (GSH)

GSH is one of the most important small-molecule antioxidants in somatic cells. It is a tripeptide that is synthesised sequentially by glutamate cysteine ligase (GCL) and glutathione synthase (GS) from glutamate (glu), cysteine (cys), and glycine (gly) (Zhu Yuangui et al., 2006, Ighodaro and Akinloye, 2018, Iskusnykh et al., 2022). It is part of a second line defense antioxidants, due to its vital role in eliminating both ROS and their harmful by-products, serves as a significant antioxidant defense mechanism against reactive free radicals and serves as a marker of changes in oxidative stress (Currais and Maher, 2013).

In the central nervous system, GSH plays many important roles, such as protein synthesis, prevention of oxidative cell damage, involved in transport of metals across membranes including the modulation of cellular differentiation and proliferation, apoptosis, enzyme activation, and neurotransmission (Suh et al., 2004, Kumar et al., 2012, Iskusnykh et al., 2022). Moreover, it plays a crucial role in eliminating ROS from a reaction that glutathione peroxidases (GPx) catalyze to produce glutathione disulfide (GSSG) which is subsequently transformed back into GSH by glutathione reductase (GR) (Zhu Yuangui et al., 2006, Ghosh et al., 2014, Iskusnykh et al., 2022). For the latter process to take place, glucose 6-phosphate (G6P) must be converted into 6-phosphoglucono-d-lactone (6PGL), which then activates GR (Currais and Maher, 2013, Ghosh et al., 2014).

The age-related neuronal loss in the brain is associated with impaired glutathione function (Iskusnykh et al., 2022). Microglial activation and endothelial dysfunction, both of which can contribute to deficits in brain function, are linked to the age-related decline in GSH (Currais and Maher, 2013, Kumar et al., 2012). The concentration of GSH varies in different tissues of adult mammals. In the brain, it is present at high levels with a total GSH content estimated to 0.5–3.4 µmol/g with the highest concentration discovered in the cortex's glial cells (Zhu Yuangui et al., 2006, Ghosh et al., 2014). Maintenance of GSH

levels is developing as an important therapeutic target both to reduce the impact of aging and treatment of age-associated neurodegenerative diseases.

Studies reported on antioxidant enzymes in the brain, compared the activities of antioxidant enzymes and glutathione (GSH) concentrations in several tissues of different mammalian species, relationship between the generation of oxygen free radicals or oxidative defense systems across different age groups and the relationship between aging and antioxidant defense (Sohal et al., 1990, Hussain et al., 1995, Kaushik and Kaur, 2003, Zhu Yuangui et al., 2006, Hermes-Lima et al., 2012, Gu et al., 2015, Iskusnykh et al., 2022). Studies by Zhu Yuangui et al, (2006) and Gu et al., (2015) reported decreased GSH levels across midbrain, cortex, and cerebellum in aged rats, and concluded that this may be caused by the decrease in GSH synthesis which may be directly responsible for the reduced levels of GSH.

2.6 Tumor Necrosis Factor alpha

Natural aging is characterized by a mild chronic inflammatory state with increased levels of cytokines in the brain and an imbalance between pro- and anti-inflammatory cytokines. Tumor necrosis factor-a (TNF-a), interleukin-1b (IL1b), and systemic IL-6 are early proinflammatory cytokines that are secreted at higher levels in the CNS than anti-inflammatory cytokines like IL-10 (Von Bernhardi et al., 2010). TNF-alpha, a multifaceted proinflammatory cytokine, has been associated with neurodegenerative disorders. It works by positively activating the dual signaling cascades through these receptors TNFR 1 and TNFR 2 that may lead to apoptosis, proliferation, and differentiation (Shohami et al., 1999, Trembovler et al., 1999, Wajant et al., 2003, Figiel, 2008, Chu, 2013, Naude et al., 2014, Dong et al., 2015). While the controlled release of TNF-alpha may have beneficial physiological consequences (Figiel, 2008, Ortí-Casañ et al., 2022), the unregulated production of TNF-alpha may cause organ failure and even death (Wajant and Siegmund, 2019, Cacci et al., 2005). Cellular processes and dendritic structures are negatively affected by prolonged proinflammatory cytokine activity (Meissner et al., 2015). Anti-TNF antibodies, soluble TNF receptors, and associated fusion proteins may be administered to prevent organ damage and lower mortality rates (Dong et al., 2015, Naude et al., 2014). The creation of a new class of anti-TNF medicines with fewer side effects

will be made possible by knowing TNF's actions and the mechanisms causing pathologies due to TNF-alpha.

2.7 The Brain Derived Neurotropic Factors

The brain-derived neurotrophic factor (BDNF) belongs to a family of small proteins called the neurotrophins. Neurotropic factors have been reported to regulate the survival and differentiation of selective populations of neurons during embryonic development and the maintenance of specific functions of those neurons in adulthood (Thoenen, 1995, Bathina and Das, 2015). Among the neurotrophic family, BDNF is the most abundant as it is produced in the brain by different types of cells (Molinari et al., 2020) and is expressed in regions of the brain with a high plasticity level (i.e. the hippocampus, cerebral cortex) (Arancibia et al., 2008, Silhol et al., 2008, Erickson et al., 2010, Miranda et al., 2019, Zhong et al., 2019). It is produced in sensory neurons' endoplasmic reticulum as a precursor protein (Pro BDNF) during development and in adult animals (Bathina and Das, 2015).

Brain-derived neurotrophic factor (BDNF) is a growth-promoting protein primarily responsible for stimulating the axonal growth, neuron survival, synapse assembly and phenotypic maintenance including differentiation of mature and fully developed neurons (Zhong et al., 2019, Bathina and Das, 2015, Nam et al., 2019, Molinari et al., 2020). It stimulates neural stem cells to differentiate into neurons and supports the survival of newly formed neurons throughout the development of the cerebral cortex and hippocampus (Arancibia et al., 2008, Zhong et al., 2019). It can be found in the olfactory bulb (OB), cortex, hippocampus, basal forebrain, mesencephalon, hypothalamus, brainstem, and spinal cord, among other parts of the brain (Katoh-Semba et al., 1997, Yamada et al., 2002).

2.7.1 Exogenous BDNF Administration

Studies indicated that BDNF can be transported outside the brain through the blood–brain barrier (BBB) (Pan et al., 1998, Alcalá-Barraza et al., 2010, Molinari et al., 2020, Zhang and Pardridge, 2001). However, the issue of whether the BDNF can cross the BBB has sparked some controversy because some studies have reported that it does not (Knusel et al., 1992, Williams et al., 2008) while some studies have reported that it does (Klein et al.2010). (Zhang and Pardridge, 2001) confirmed the latter findings by indicating that BDNF can cross the BBB through receptor-mediated transport (RMT) when it is coupled to a molecular Trojan horse (a second peptide or peptidomimetic monoclonal antibody that binds a particular receptor). This allows the conjugated BDNF to enter the brain and have the desired pharmacological effect. The authors confirmed that the conjugated BDNF resulted in complete neuroprotection of the pyramidal neurons of the CA1 sector of the hippocampus in transient forebrain ischemia.

2.7.2 The role of BDNF on Adult Neurogenesis and Learning and Memory

The BDNF and its receptors have an important role during aging, and its mediated protection involves Tyrosine receptor kinase B (TrkB) receptor activation (Mizuno et al., 2003, Wu et al., 2020). The signaling of BDNF at synapses enhances long-term potentiation (LTP), a process of synaptic strengthening associated with learning and memory (Jia et al., 2010, Baroncelli et al., 2010, Lalo et al., 2020). The effect of BDNF on LTP is apparently mediated by cAMP-response-element-binding protein (CREB), which regulates the expression of genes involved in LTP and memory formation (Mattson and Arumugam, 2018, Mattson, 2004, Baroncelli et al., 2010, Lalo et al., 2020).

BDNF plays a crucial role in protein neuroprotection and neurogenesis by stimulating cell differentiation, maturation, neuron survival and maintenance (Pan et al., 1998, Yamada et al., 2002, Mattson, 2004, Yamada and Jinno, 2019). Additionally, BDNF ensures the functionality of hippocampal neurons, cholinergic neurons, and peripheral sensory neurons (Yeltekin et al., 2022) which suggests its potential role in the therapeutic treatment of age-related neurodegenerative disorders.

Plant extracts are attracting increased attention as novel therapeutic alternatives and supplemental candidates for the treatment of oxidative stress and aging related cognitive decline. Plant products such as Ginseng (*Panax ginseng*), blueberry and Curcumin (turmeric) (*Curcuma longa*) demonstrated to restore D-galactose induced cognitive deficits by increasing the BDNF levels and enhancing adult neurogenesis (Wu et al., 2020, Rendeiro et al., 2012, Zhong et al., 2019)).

2.8 Neuronal Plasticity

Neuronal plasticity is defined as the capacity of neurons or glial cells to modify themselves, functionally and structurally and improve or to depress the synaptic efficacy by adapting to biochemical or morphological changes which evolve in a dynamic manner during development and aging (Cramer et al., 2011) (Von Bernhardi et al., 2017)). Brain plasticity can be in various levels depending on the stage of life, namely the developmental plasticity is more involved with the formation of neuronal connections in the embryo or a child, synaptic modulation plasticity which is involved in modification of neuronal connections throughout life and postlesional plasticity which is involved in repair post injuries or pathological insults (Malabou, 2009).Neuronal plasticity was first described by Ramon y cajal as a non-pathological changes that occur in the adult brain (Fuchs and Flügge, 2014). These changes involve morphological, neuronal networks, neuronal connectivity, neurobiochemical as well as neurogenesis.

2.9 Adult neurogenesis and Neuroplasticity

The cerebral and cerebellar cortex, hippocampus, basal nucleus of Meynert, locus ceruleus, and substantia nigra are among the areas of the aging brain where alterations in the metabolism of neurons may result in decreased numbers of neurons, synapses, and impaired stimulation of synaptic plasticity (Dorszewska, 2013). The adult mammalian brain was believed to be a non-renewable organ. In contrast to this belief, earlier studies on adult brain have proven that the adult brain can repair itself but cannot completely generate new neurons and establish connections among surviving neurons (von Bohlen und Halbach, 2011). The first evidence of neurogenesis in adults was provided by Josef

Altman who detected the creation of adult-born neurons and glia in the rat brain by labelling proliferating cells with tritiated thymidine (Altman, 1969).

Adult neurogenesis is a multi-step process which neural progenitor cells are generated in the sub ventricular zone and in the dentate gyrus of the hippocampus (Ihunwo and Pillay, 2007), (von Bohlen und Halbach, 2011). Various factors are involved in regulating the rate of adult neurogenesis. Factors including stress, mental illness, aging, excess alcohol and opioid use, and neurodegenerative diseases have the opposite effect and impede adult neurogenesis (Klempin and Kempermann, 2007),(Sánchez-Huerta et al., 2022). Other factors such as neurotransmitters including glutamate, gamma-aminobutyric acid (GABA), acetylcholine (Ach), dopamine and serotonin (5-HT) influence proliferation and differentiation of cells within neurogenic zones (Shohayeb et al., 2018). The rostral migratory stream (RMS) carries the neuro epithelial progenitor cells from the subventricular zone of the cerebral cortex to the olfactory bulb (OB), where they differentiate into mature neurons and are integrated as useful components into the neuronal olfactory circuitry (Klempin and Kempermann, 2007). In the hippocampus, the neural progenitor cells are located in the SGZ of dentate gyrus. These cells which proliferate and differentiate into immature neurons which extend their dendrites in the direction of the molecular layer of the DG (von Bohlen und Halbach, 2011).

The cell cycle progresses through four critical phases namely the G0/G1 phase, DNA synthesis (S), G2 phase and mitosis ((Zambón et al., 2010), (Sobecki et al., 2017)). Ki67 is a 360 kDa nuclear protein that is expressed during all active phases of cell division except during DNA repair or the cell quiescent (G0) ((Kee et al., 2002), (Zambón et al., 2010). It is activated when inactive arrested cells transition into the G1-S phase and is maintained throughout the G2 and M phases ((Bruno and Darzynkiewicz, 1992, Zambón et al., 2010). Other than detecting and quantify proliferating cells, Ki-67 plays a beneficial part in regulating cellular proliferation and exhibits phase-specific staining patterns(Zambón et al., 2010, Tartt et al., 2018)., The Ki67 expression pattern in T cells is used to assess antigen-specific T cell growth for several chronic disorders, including HIV infection, cancer, and autoimmune diseases. Ki-67 is an endogenous marker that has no negative effects on living cells and is commonly used to quantify proliferative cells

in tissues (Kee et al., 2002, Zambón et al., 2010, Sobecki et al., 2017). In cancer research, Ki-67 is used to estimate Tumor aggressiveness (Sobecki et al., 2017).

During normal aging, one of the brain areas that is significantly impacted by neurodegeneration and functional deterioration is the hippocampus (Klempin and Kempermann, 2007). Doublecortin (DCX), a protein that is widely expressed in migrating neuroblasts both tangentially and radially, is necessary for proper neuronal migration in the developing brain structures. Neuroblasts that express doublecortin (DCX), a marker also found in immature granular neurons (IGNs), are formed in the SGZ of the dentate gyrus from neural progenitor cells (Tartt et al., 2018, Vaz et al., 2022).

Several studies have provided evidence of neurogenesis and age-related changes in the subgranular zone (SGZ) and subventricular zone (SVZ) of the adult mammalian brain. In the Investigation of age-related adult hippocampal alterations in Sprague Dawley rats by (Wati et al., 2006) found that aging decreases the survival of neonatal neurons both in baseline conditions and following the survival-promoting stimulation of contextual fear conditioning. Another study by (Cameron and Mckay, 2001) reported that adrenalectomy can prevent a decrease in hippocampal neurogenesis. More recent studies such as in human cancer patients by (Tartt et al., 2018), mice(Nkomozepi P. Mazengenya P, 2019), ra (Saenno et al., 2022), focused on age-related changes in adult neurogenesis. Therefore, the neuronal regenerative, cognitive, and locomotive effects are central to aging induced changes and require investigation into natural protective agents that could ameliorate these changes.

2.10 Cognitive Behaviours

Cognitive behavioural tests have been an integral part of psychopharmacology and psychological resear(Nkomozepi P. Mazengenya P, 2019)ch. Learning can be evaluated with repeated training trials to measure acquisition, and memory can be repeatedly assessed across time to evaluate retention (Moser et al., 2011). Although it is not a disease, aging is marked by cognitive impairments, which are frequently unrelated to neurodegeneration, which in the hippocampus may involve changes in adult neurogenesis, loss of neurons, or the breakdown of circuits and synapses. Over the years animals have been used in scientific studies to study the effectiveness of various drugs

developed for various ailments. Cognitive behaviour of the animal is one of the principal characteristics studied to evaluate the effectiveness of the administered drug. Various animals such as mice, rats and fish are used for this purpose. (Sarter, 2004)describes cognitive behavioural study as a validation step of drugs developed to redress the impacts of cognitive impairments and disorders. Cognitive tests are designed to assess the diverse neuronal activity in various brain areas. One of the drivers of utilization of animals for cognitive behavioural studies is most of the drugs developed are not yet ethically certified to be used on human beings. The development and usage of animal models creates room for better control and experimental adjustments such as gene expression, inducing wounds and modulation of circuitry activities (Denninger et al., 2018).

The hippocampus, which is a component of the limbic system, is a crucial structure for studying how memories are formed. It is particularly involved in the establishment and maintenance of spatial learning and memory as well as exploratory behaviour (D'Hooge and De Deyn, 2001, McDaniel et al., 2007, Moser, 2011, Calton and Taube, 2009). Also, the hippocampus is essential for declarative memory, which entails representing particular events and knowledge accumulated across a number of episodes (Genzel et al., 2019). There are, however, complex interactions amongst the other components of the limbic system (Calton and Taube, 2009, McDaniel and Moser, 2004). The non-spatial memory task involves the hippocampus, perirhinal, entorhinal and parahippocampal and cortices While the spatial memory is majorly dependent on the hippocampus (Squire et al., 2007, Tuscher et al., 2014). Cognitive tests often used to assess hippocampal function include spontaneous alternation, Fear conditioning, Object Recognition test, Object location, Morris water maze, and radial-arm maze (Gerlai, 2001, Rattan, 2008). In this study, the following test: open field test, novel object recognition test and object location test were employed. The advantages of the three tests are that these involve an animal in its natural form as there are no rule learning is required; nor any rewarding or punishing stimuli involved that may influence motivational rather than mnemonic aspects of task performance; and no rigorous training is required.

2.10.1 Open field test (OFT)

The open field test ascertains the relative anxiety levels and exploratory behaviors (cognition) of the animals during the test. It is a valuable instrument for analyzing animal behavior, such as locomotor impairment in animal models of neuromuscular disease and effectiveness of medicinal medications that may enhance locomotion and or muscle function (Tatem et al., 2014). Measurements of open field activity vary by animal strain, age, sex, and circadian rhythm. (Hattiangady et al., 2014). In addition, room temperature, humidity, lighting, noise, and even odour can affect assessment outcomes (Quinn et al., 2014). Key parameters for the test depend on which parameter is most relevant or specific to one's investigation such as location, body part movement and autonomic nervous system.

2.10.2 Novel object recognition test (NORT)

The novel object recognition test is considered analogous to human declarative (episodic) memory (Rajagopal et al., (2014) and the test is used for recognition memory. The test is based on rodents' innate propensity to spend more time exploring unfamiliar objects than they do familiar ones. The decision to investigate the novel object shows how learning and recognition memory are used. The hippocampus, amygdala, and parahippocampal regions are among the structures in the medial temporal lobe that play a significant role in the process of memory recognition. In humans, monkeys, and rodents, any type of damage to these brain structures impairs performance in the capacity to recognize memory obligations or tasks (Squire et al., 2007).

2.10.3 Object location test (OLT)

The OLT test is a simplified and accurate test that determines the hippocampus spatial memory (Denninger et al,2018). It utilizes the animal emotional innate natural preference, hence, avoiding external influences which may cause complications and lead to differential emotional results from the test. For example, food is used as a positive reinforcer in the radial maze test and water immersion is used in the water maze test in the majority of spatial memory tasks. Several studies investigated on the ability of various

agents in enhancing both spatial and non-spatial memory. For example, in an exploratory investigation, Akkerman et al., (2012) used male Wistar rats that had been saline-treated and those that had not, and they discovered that there was no change in the ability to distinguish between a novel object and an old object. Another study by Cai et al.,(2012) used selective cholinergic immunotoxin 192 IgG-saporin (SAP) to treat Sprague Dawley rats, and the results showed that NORT memory was unaffected while OLT memory was considerably reduced. Also, Wang et al.(2009) used Swiss albino mice treated with saline (control) or D-galactose for the NORT and OLT, and they found no changes in the cognitive abilities of the two groups based on the amount of time spent stumbling around in the object locating and object recognition tests. According to results obtained by Wang et al (2009), the OLT and NORT showed that nonspatial and spatial cognition were both negatively affected by chronic D-galactose administration in various ways.

2.11 Cholinergic markers

The cholinergic system is involved in many different brain activities and is essential for controlling learning and memory functions. In both the central and peripheral nervous systems, acetylcholine (Ach) is a vital neurotransmitter. The cholinergic hypothesis postulates that many of the cognitive, functional, and behavioural symptoms experienced by patients with cognitive dysfunction results from a deficiency in Ach neurotransmitter, and thus a reduction in cholinergic neurotransmission (Ballard et al., 2005, Elufioye, 2017). The central cholinergic neurons are subdivided into projection neurons that are primarily found in the forebrain and upper brain stem, and interneurons that are found in the caudate-putamen, nucleus accumbens, hippocampus, cerebral cortex, hypothalamus, and spinal cord (Schliebs and Arendt, 2006). Cholinergic projection system originates in the pedunculopontine and laterodorsal tegmental nuclei of the brainstem with projections to thalamus whereby its reticular nucleus plays a role in controlling consciousness and general attention (Herholz, 2008, Anand et al., 2012). Loss and severe functional impairment of basal forebrain cholinergic neurons are associated with reduction of Ach and choline acetyltransferase (ChAT), which is responsible for its synthesis (Herholz, 2008, Anand et al., 2012, Anand and Singh, 2013, Meda et al., 2014, Yang et al., 2014), thus results in reduction of synaptic availability of Ach leading to cognitive impairment in neurodegenerative disorders (Herholz, 2008, Herholz et al., 2008).

Acetylcholinesterase (AchE) is an enzyme involved in terminating nerve impulse transmission at cholinergic synapse (Mukherjee et al., 2007a) and a hydrolase belonging to carboxylesterase family of enzymes. It plays a crucial role in regulating cholinergic neurotransmission that metabolizes acetylcholine (Ach) into acetic acid and choline after its release in the synaptic terminals (Mukherjee et al., 2007a, Lionetto et al., 2013, Wang et al., 2016). There are several molecular variations of AchE. These forms can be categorized into two groups:(1) globular forms, which have monomer (G1), dimer (G2), and tetramer (G4) structures with 1,2, or 4 subunits each, and (2) asymmetric forms, which have a tail that resembles collagen and have 4 (A4), 8 (A8), or 12 (A12) catalytic subunits (Rakonczay, 2003). Additionally, the G4 form is functionally crucial for the breakdown of Ach and in the human brain the most abundant AchE forms are G4 (membrane bound) and G1 (cytosolic) (Khan et al., 2012). Measurement of AchE activity in organisms is used worldwide as a biomarker of cholinergic metabolism, environmental contamination, and exposure to neurotoxins (Kaizer et al., 2005, Lionetto et al., 2013).

Numerous studies found that aged rats had decreased AchE activity (Park et al., 2011, Haider et al., 2014), while other studies showed defects in acetylcholine (Ach) synaptic transmission and revealed that it is linked with the oxidative damage (Haider et al., 2014, Wang et al., 2020). Therefore, inhibition of AchE is needed for deceleration of neurodegenerative disorders ((Anand et al., 2012)Anand et al., 2012, Meda et al., 2014). Cognitive dysfunction due to loss or decline of cholinergic activity in the brain areas involved in cognition, is considered a normal biological process associated with aging as well as some forms of progressive neurodegenerative disorders (Campanari et al., 2014, Shin and Dixon., 2015). A growing number of studies has demonstrated that the cholinergic system's impairment was linked to the decline in memory function brought on by D-galactose (Sha et al., 2019,). Using anti-choline acetyltransferase immunohistochemistry, Lei et al., (2008b) found that both the medial septum and the diagonal band of Broca's nucleus' vertical limb showed relatively small number of cholinergic neuronal loss and atrophy, while in the hippocampus cholinergic neurons were severely lost. Another investigation by Lu et al., (2010a) showed that prolonged administration of troxerutin reduced the levels of AGEs and ROS in the basal forebrain, hippocampus, and frontal cortex of D-gal-induced animals while inhibiting AchE activity.

Kaur et al., (2008) found that older green tea-treated rats' cerebrums had decreased acetylcholinesterase activity compared to younger green tea-treated rats.

Most of the approved cholinesterase inhibitors (eserine, tacrine, donepezil, rivastigmine and galantamine) used for treatment of neurodegenerative diseases are synthetic and known to have a short half-life which will require multiple daily dosing (Rakonczay., 2003, Ballard et al., 2005, Haake et al., 2020). They have unfavourable side effects like diarrhoea, nausea, vomiting, headache, seizures, and insomnia (Mukherjee et al., 2007a, Mukherjee et al., 2007b, Vinutha et al., 2007, Haake et al., 2020). Moreover, these acetylcholinesterase inhibitors were reported to only remedy the neurodegenerative disorder instead of reversing it completely. Older people are vulnerable to cognitive deficits caused by the anticholinergic drugs. Most of the elderly are vulnerable due to use of multiple prescribed medications they use to treat comorbidities, and this can be compounded by using over-the-counter medications (Boustania et al., 2008) Therefore a search for acetylcholinesterase inhibitors with less side effects, high efficacy and improved bioavailability sparked more studies to be conducted in various laboratories.

Acetylcholinesterase inhibitors have been found from screening plant extracts from leaf, seed, stem, flower, and rhizome of medicinal plants (Ferreira et al., 2006, Mukherjee et al., 2007a, Adewusi and Steenkamp, 2011, Talić et al., 2014, Owokotomo et al., 2015). Various plant extract such as the leaves of the following plants: *Croton zambesicus, Jatropha curcas, Jatropha tangorensis, Jatropha curcas, Jatropha gossypiifolia , Combretum kraussii* , including the leaves, roots and bark of *Combretum molle* (Ferreira et al., 2006, Mukherjee et al., 2007a, Adewusi and Steenkamp, 2011, Anand et al., 2012, Colovic et al., 2013, Dhivya et al., 2014, Haider et al., 2014, Owokotomo et al., 2015, Elufioye, 2017) possibly exhibit anticholinesterase activity. An in vitro phytochemical study by Elufioye (2017) reported the anticholinesterase inhibition of *Combretum molle* leaves and stem bark to be 90.42% and 88.13%, respectively.

2.12 The Traditional Medicinal Plants

Almost 80% of the world's population still receives health coverage from traditional medicine, particularly in underdeveloped countries (Ndip et al., 2007). Traditional healers

are reputedly consulted by 80% of the black population in South Africa, since traditional medicine is so widely practiced (Stafford et al., 2008). This high percentage patronage is ascribed to readily available and affordable cheap traditional health care system which offers culturally acceptable alternative to unaffordable allopathic system. Moreover, traditional health care is easily accessible, especially, to those living in the rural areas.

2.13 Combretum molle

Over 24 different species of Combretum are widely used in traditional medicine in Africa as therapeutic treatments for a wide range of illnesses and diseases, including heart conditions, worm infections, wound dressings, mental illness treatment, and scorpion stings. (Masoko and Eloff, 2005, Fyhrquist, 2007, Ojewole, 2008, Masoko et al., 2010). Several studies have shown that many Combretum species possess antifungal, antibacterial, anti-parasitic, antioxidant, antitussive activity, anti-HIV type 1 reverse transcriptase, anti-inflammatory, and anti-asthmatic, (Asres et al., 2001, Eloff et al., 2005, Bessong, 2008, Ojewole, 2008, Masoko et al., 2010, Dodehe et al., 2010, Njume et al., 2011, Simon et al., 2012, Bessong et al., 2005). *Combretum molle (C. molle)*, is a semi-deciduous tree of about 6 to 10m high, with a spreading crown (Ojewole, 2008, Njume et al., 2011). It exists throughout tropical Africa as well as most of South Africa especially found in Venda (Limpopo Province), North of Pretoria (Gauteng) and Nelspruit (Mpumalanga province) (McGaw et al., 2001, Masoko and Eloff, 2007, Masoko et al., 2007, Njume et al., 2011).

2.13.1 Phytochemical compounds in *Combretum molle*

The *Combretum molle* plant has been found to contain significant amounts of phenolic compounds (including tannins, quinines, coumarins, phenolic acids, flavonoids, lignins, and stilbenes) and other endogenous metabolites with high antioxidant activity (McGaw et al., 2001, Bhatnagar et al., 2012,). Using solvents like methanol and acetone, Ntshanka

et al., (2020) conducted research on C. molle and found that secondary metabolites such alkaloids, steroids, coumarins, essential oils, flavonoids, terpenoids, and anthraquinones are present. Furthermore, their result showed that methanolic solvent extraction yields a higher percentage of phenolic compounds compared to the acetone solvent extraction. Also, Miaffo et al., 2020 reported additional metabolites such as saponins on phytochemical screening of *C. molle*. The presence of carbohydrates and glycosides was also noted in a more recent study by Hamza et al., (2021) that examined the effect of *C. molle* leaves on diabetic foot wound healing.

2.13.2 Pharmacological properties of *Combretum molle*

In African traditional medicine, *C.molle* 's roots, leaves, seeds, and stem bark are frequently used to cure a variety of human illnesses, including as leprosy, hookworm, dysmenorrhea, and infertility in women, as well as abdominal pain, body aches, respiratory problems, colds, and fevers (McGaw et al., 2001, Fyhrquist, 2007, Masoko and Eloff, 2007, Manga et al., 2012, Njume et al., 2011, Simon et al., 2012, Mensah et al.,2020, Shibeshi et al.,2021). According to another study, the methanol and acetone extracts of *C. molle* twigs have been shown to have anti-diabetic potential in dexamethasone-induced insulin resistance (Miaffo et al., 2014)

Despite the various uses of *Combretum molle*, there is no documented data or studies on the exact mechanism on neuroprotective effects of methanolic leaf extract of Combretum molle. This study was designed against this backdrop, whereby a D-gal induced rat model was used to underscore the effects of *Combretum molle* in learning and memory. The methanolic leaf extract of *Combretum molle*, used in this study, has shown to have neuroprotective properties in a rat model of D-galactose-induced aging. Consequently, this work looked at the effects of the *Combretum molle* methanolic leaf extract on adult neurogenesis, oxidative stress, and related neurotransmitters in D-galactose-induced aging brains.

3 MATERIALS AND METHODS

3.1 Plant Preparation and Extraction

Combretum molle leaves were harvested from a field farm plot located in the North of Pretoria, GPS coordinates 25°40’07.70S 28°01’03.30E, Gauteng province, South Africa between the months of October to January 2018. The leaves and seeds were sent for identification at the University of Johannesburg Herbarium (voucher number: DFC/MDP-04). The accurately identified leaves were rinsed with tap water, dried at room temperature for 72 hours or more until they are dry and crispy. The leaves were grounded into powder using a commercial laboratory blender (Logik) in 3 cycles at the speed of 2 . The method of extraction was adopted from studies by Dodehe et al., (2010), Bhatnagar et al., (2012) and Miaffo et al., (2014). A total of 200g of grounded *C.molle* powder was soaked in 1000ml of 100 % Methanol and placed on a shaker (Labcon) at a speed of 150 rpm 72 hours. The mixture was first filtered using cotton wool followed by filtration using No. 1 Whatman filter paper. A rotary evaporator (Buchi R II) was then used to concentrate the filtrate at speed of 5 rpm at the temperature of 80 °C. The concentrate was freeze dried (Virtris benchtop K) at -80 ^{o}C. The extract (freeze dried concentrate) was weighed and kept at 4 ^{o} C until used for treatment. The yield percentage of the extract was calculated as per the formula below.

$$\textbf{\% Yield} = \frac{\text{Percentage of extract yield}}{\text{Extract weight (g)}} \times \frac{100}{\text{Powdered weight (g)}}$$

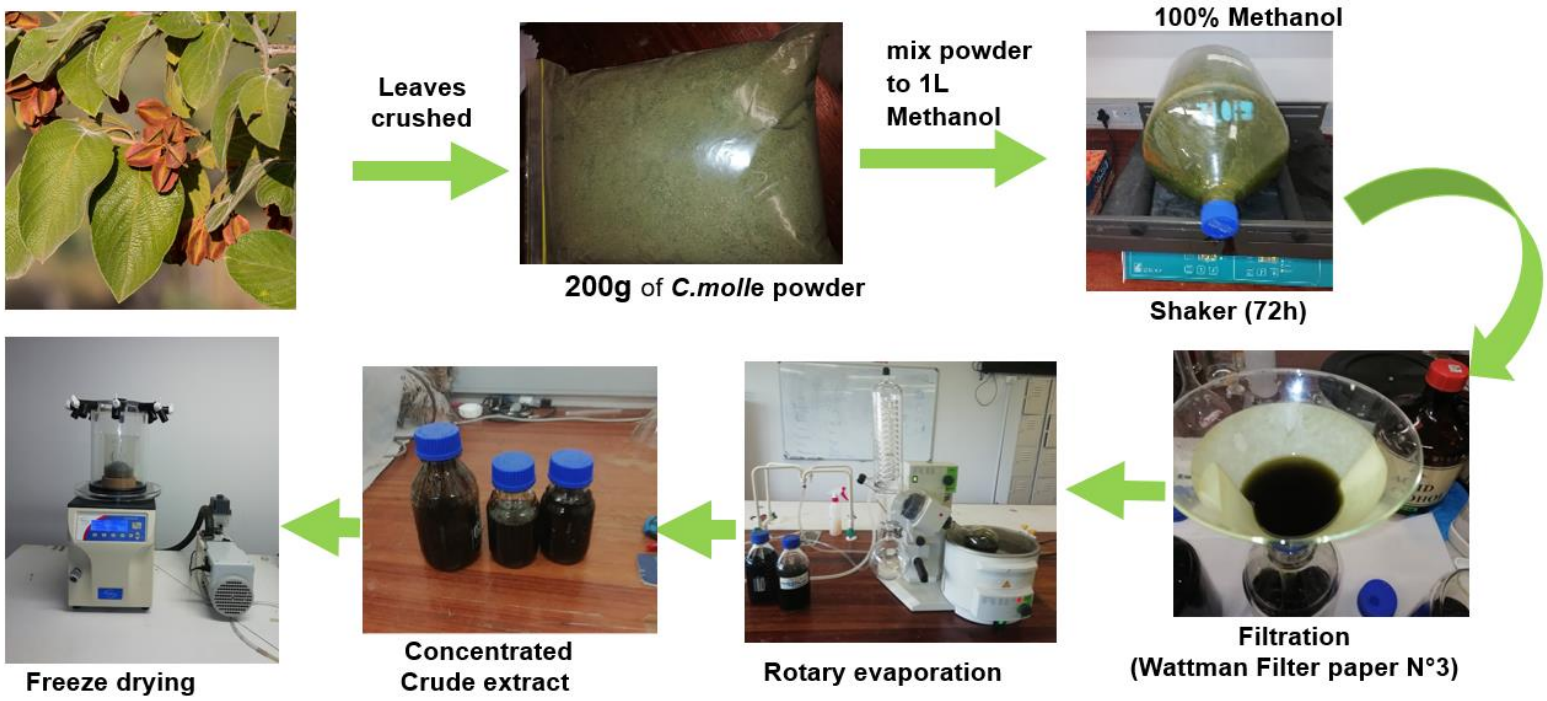

Figure 3.1. Photomicrograph outlining the process of extraction

3.2 Experimental Animals

Fifty male inbred Sprague Dawley rats were purchased and procured at 8 weeks of age weighing between 300 - 350g from the University of the Witwatersrand research animal facility (UWRAF) and the permission to undertake animal research was granted by the Animal Ethics Research Committee (Arec: 2017/08/51/C) of the University of the Witwatersrand. The animals were housed in a standard cage wired-net top dimensions: Top surface is 26.5 cm x 42 cm, lower surface is 22cm x 37.5 cm, height is 18cm. Two rats were housed in a physically enriched cage containing a non-chewable PVC under controlled temperature (24 ± 2°C) with a relative humidity of 60^{o}C and a 12-hour light/dark cycle. Prior to experiments, animals underwent a two-week acclimatization phase and a variety of handling techniques to neutralize any psychological effects of the surroundings and to lessen the stress associated with novelty and handling.

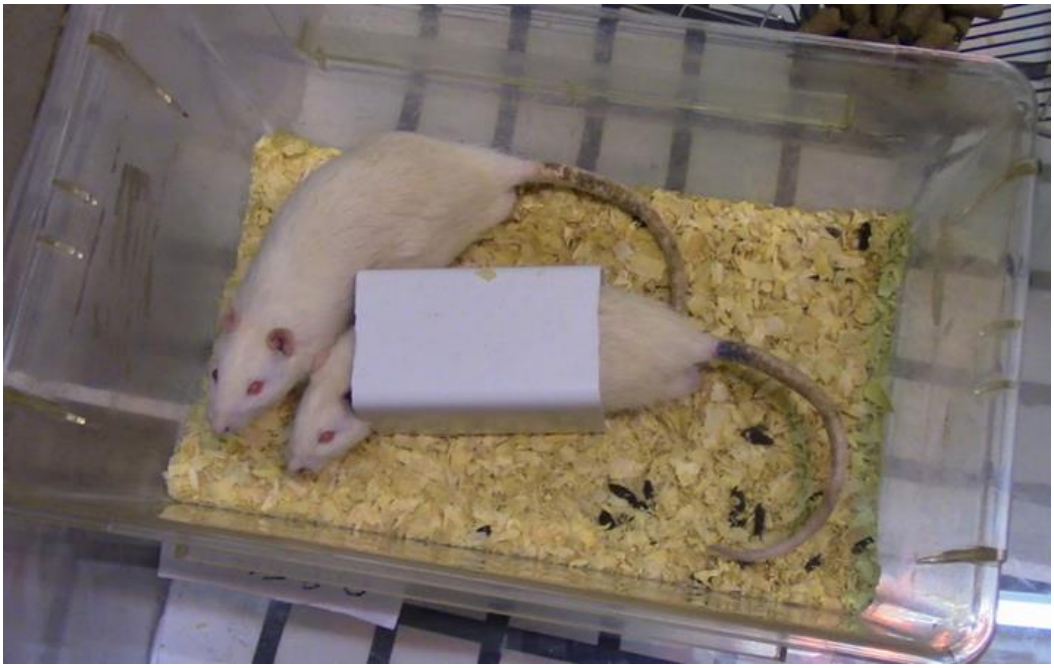

Figure 3.2. Photomicrograph showing the housing of the experimental animal.

.

3.3 Experimental Design

The rats were randomly allocated to five equal groups after two weeks of acclimation (n=10). The groups were allocated as the Control group received 1 mL of distilled water by oral gavage and subcutaneous injections of 1 mL/kg of saline daily for 90 days The prophylactic group (CM) received 500mg/kg/1ml/kg of *C. molle* orally and 1ml/kg saline subcutaneously daily for 90 days. The accelerated aging (Dgal-90) group received 1ml/kg subcutaneous injections of D-galactose and 1ml/kg distilled water orally daily for 90 days. The combination treatment (CMD 90) group received 1ml/kg of *C. molle* orally and 1ml/kg D-galactose subcutaneously daily for 90 days. The induction treatment (CMD 45) group received 1ml/kg of D-galactose subcutaneously and 1ml/kg distilled water orally for the first 45 days, and on day 46 received 1ml/kg of saline subcutaneously and 1ml/kg of *C.molle* orally for another 45 days.

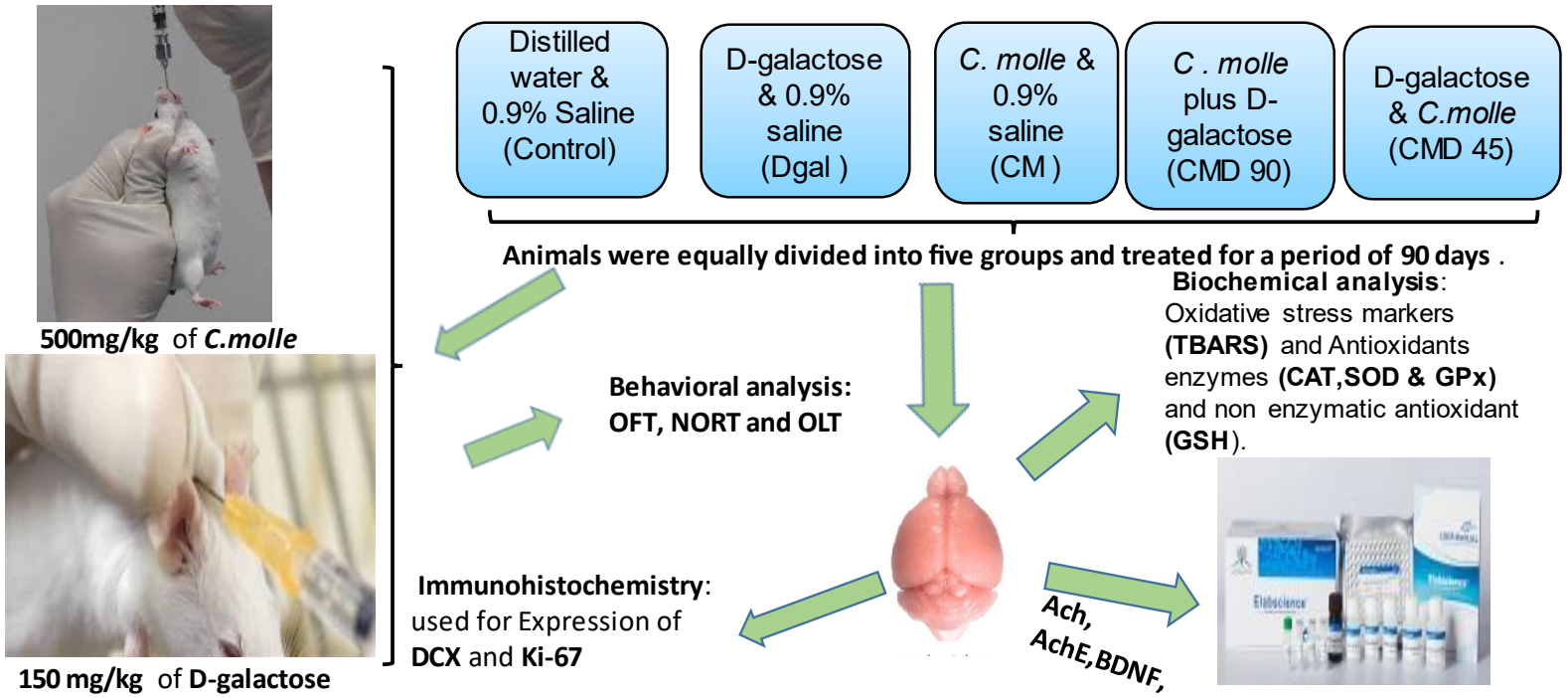

Figure 3.3. Flow diagram showing the experimental design

3.4 Cognitive Behavioural Test

On ninety- first day (91) the animals were subjected to a series of the cognitive behavioural tests, such as the Open Field test (OFT), Object Location Test (OLT) and Novel Object Recognition Test (NORT) on the 91st day.

3.4.1 The open field test.

The rat's behaviour and the drug effects on it were evaluated using the OFT. White plexiglass was used to build the open field maze, which had walls that were 40 cm high and measured 70 by 70 cm. The apparatus's floor was divided into squares (10 cm x 10 cm), with a centre square (30 cm x 30 cm) drawn in the middle of the open field. One of the walls was made of translucent Plexiglas so that the rat could be seen inside the apparatus (Figure 3.4). The movement of the rats was videotaped after they were placed in the centre square.

The open field maze apparatus was set up in a test room with a background light source of a 60-watt red bulb, a video recorder mounted 2.1 meters above the apparatus, and the maze cleaned with 70% ethyl alcohol in between each animal experiment. By capturing the spontaneous behavioral variables in 2 minutes, 5 minutes, and 10 minutes for each rat, the locomotion of the animal was observed and recorded. Each trial was videotaped and graded further for these behavioral factors for later study. Two observers who were unaware of the experimental groups manually analysed all the parameters. The following behavioral variables/parameters were measured: the number of squares crossed by the four paws during locomotion; the frequency of rearing; the duration (in seconds) of grooming, which included washing or mouthing of the forelimbs, hind paws, face, body, and genitalia (Tatem,2014).

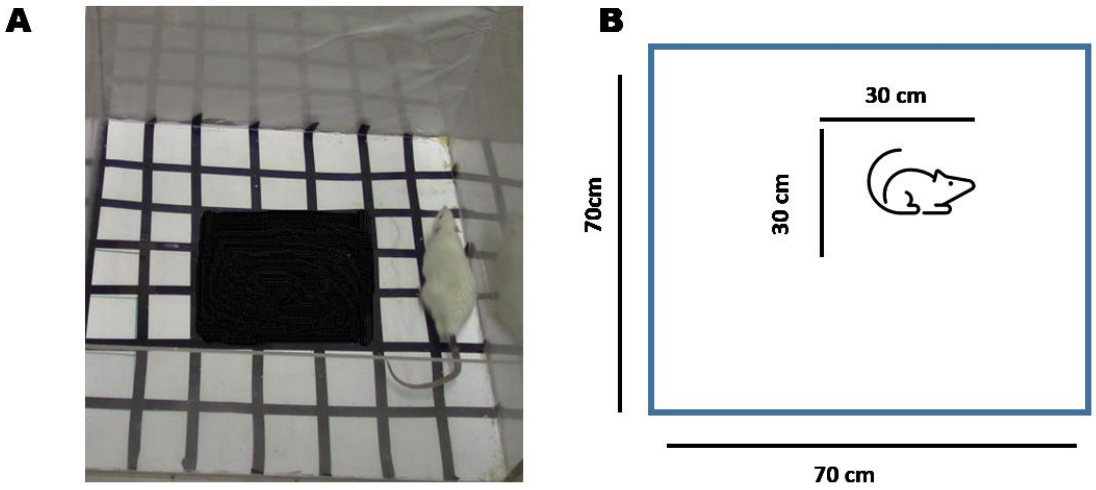

Figure 3.4. Photomicrograph showing the open field apparatus (A) and the diagram indicating the dimensions of the open field test (B).

3.4.2 Scoring and interpretation of results in the OFT

The number of lines crossed (Horizontal activity), and rearing frequency (vertical activity) usually used as a measure of locomotor activity and exploration of the novel environment (Tatem et al., 2014). A higher frequency is an indication of higher locomotion or exploration while a lower frequency or rate indicates anxiety (Brandao et al., 2000). Grooming behaviour is a non-cognitive behaviour that serve a role in care of body surface and measure displacement response in the novel environment (Spruijt et al., 1992). Grooming was scored as time spent by the animal washing or mouthing of forelimbs, hind paws, face, body, licking genitals and scratching the body using fore and hind limbs.

3.4.3 Novel object recognition test

The Novel object recognition task was conducted in the same box (Figure 3.5) used for open field maze on six randomly selected rats from each group. The rats (n=6 each group) were habituated to the open field arena and allowed to explore the empty arena for 5 min for two consecutive days with no external cues to assist learning and memory. The discriminated objects (A, B, and C) were cylindrical and cuboid wood blocks that were all the same size (5 cm× 5 cm× 5 cm). The colors of objects A and C were blue, but object B featured a pattern in red and silver. The three items were all too heavy for the rat to knock down. Twenty-four hours after habituation, the animals underwent two days of exposure to the same arena with two identical objects set 30 cm apart for the duration of 10 minutes. Twenty-four hours after training, one familiar object was switched out for a novel one, and the rats were then free to explore an open field while being exposed to both the familiar and unfamiliar objects.

3.4.3.1 Calculations in NORT

The amount of time spent investigating each object or location was recorded, and the discrimination index (DI) percentage and total investigation time (TIT) were calculated to determine the preference for each object as per the formulas adopted from Tuscher et al., (2014) and Denniger et al., (2018).

$$\textbf{DI} = \frac{(\text{Total time at novel object} - \text{Total time the familiar object})}{(\text{Total time at the novel} + \text{familiar object})} \times 100$$

The percentage of total investigation time (TIT) was calculated as follows:

$$\textbf{TIT} = \frac{\text{Time at the novel object}}{\text{Time at the novel object} + \text{time at the familiar object}}$$

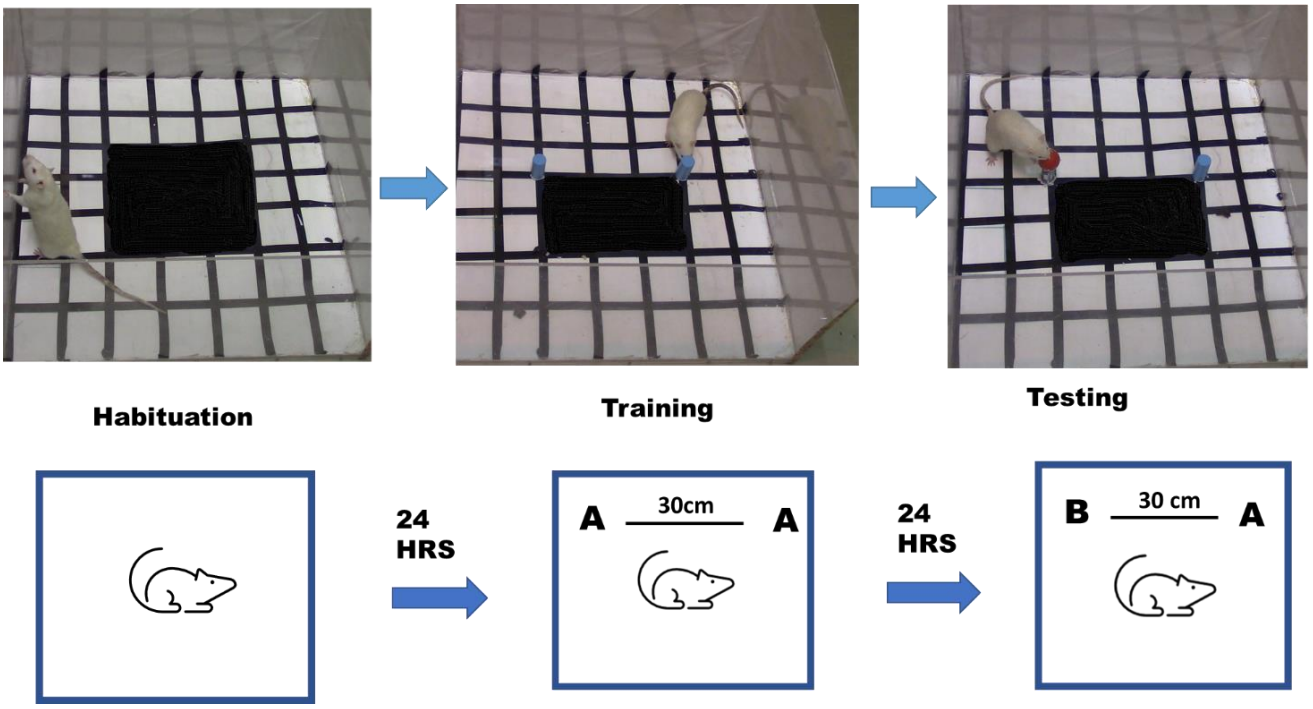

Figure 3.5. Photomicrographs and schematic flow diagrams showing the overview of novel recognition object.

3.4.4 Object location task

The object location is a stress-free hippocampus dependent memory test. This test assesses the spatial memory which relies primarily on the hippocampus. The habituation and training for object location test is identical to Novel object recognition except, one of the identical objects in the testing area is relocated to a new location. Since the behavioural test were conducted on the same cohort of animals, the object location task was conducted 4 days after the object recognition task.

Prior to training or familiarization phase, each rat (n = 6 in each group) was acclimated to the testing equipment for two days in a row without the presence of any objects for 5 minutes each day. Rats were then introduced to the experimental setup during the training phase, where they were exposed to two identical objects to explore for 10 minutes each over the course of two days. After 24 hours of training, the test phase involved exposing rats to the experimental apparatus again for 10 minutes while moving one of the two objects to a different place (Figure 3.6). When a rat's nose touched an object or its head was pointing in that direction within 1 cm of the object, exploration of that object was scored (Tuscher et al., 2014).

3.4.4.1 Calculations in OLT

To measure the preference for each location, we calculated the discrimination index (DI) and Total investigation time (TIT) as follows:

$$DI = \frac{(\text{Total time at the novel location} - \text{total time at the familiar location})}{(\text{Total time spent at the novel + familiar location})} \times 100$$

$$TIT = \frac{\text{Time at novel location}}{\text{Time at novel location + time at familiar location}}$$

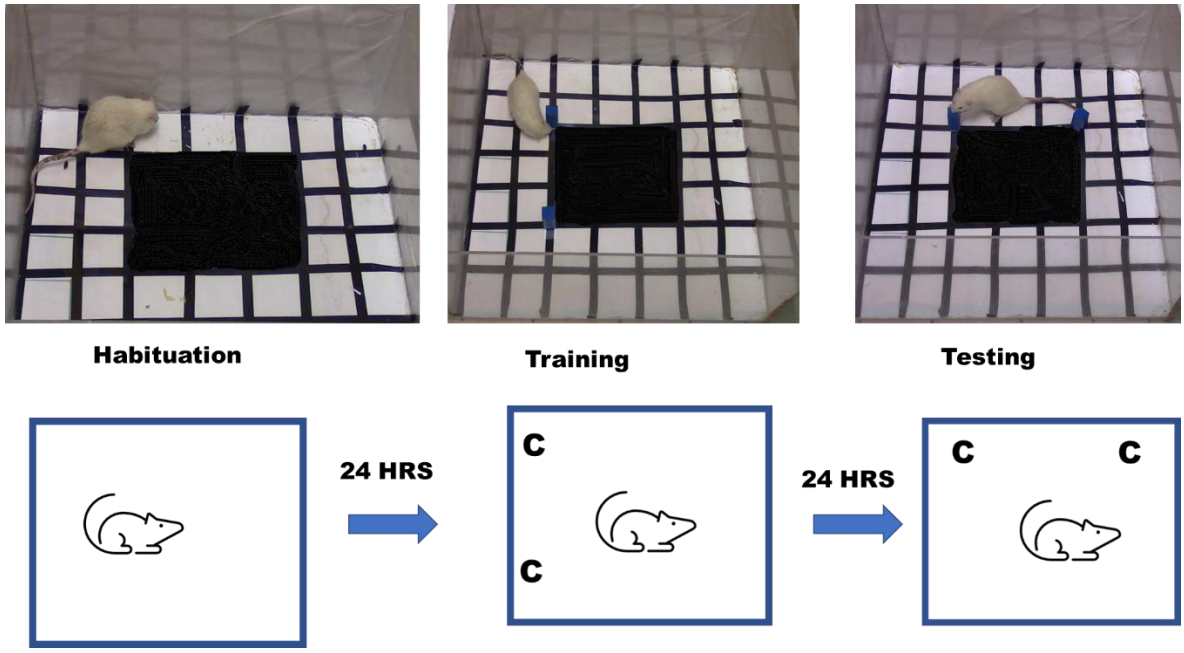

Figure 3.6. Photomicrograph and schematic flow diagrams showing the overview of object location task

3.4.5 Exclusion criteria of scoring behaviours in NORT and OLT

1. Rats that spent a total of less than 5 sec exploring objects or location during the testing phase
2. If a rat is not approaching the object but accidentally touch it with part of its body such as nose or tail.
3. The rat knocks down the object.
4. The rat is not exploring the object but on top of it and use it for rearing.
5. The rat is around the object touching it with part of the body or tail but not facing the object or focusing on the object.

3.4.6 Scoring and results interpretation in NORT and OLT.

A value more than 50 % indicates greater investigation of the novel object or location and a positive value of Total Investigation Time (TIT) indicates more time investigating the novel object or location while a zero indicates equal time spent with both subjects hence no preference. A negative value indicates preference for familiar object or location. Exploration of an object was scored when a rat's nose touched it or when its head was pointed in that direction within 1 cm of the object.

3.5 Termination of Animals

At the end of behavioural tests, the rats were injected with Euthanaze (1ml/kg sodium pentobarbitone; 200mg) and were scarified by cervical dislocation. In heparinized tubes, blood samples were drawn and stored at room temperature for 30 minutes before being centrifuged at 1,500 g for 10 minutes. Until biochemical assays were performed on all blood samples, they were all kept at - 80 °C. The euthanised rats were perfused with phosphate buffer saline (PBS), the brains were immediately removed from the skull within 30 seconds of decapitation and weighed, one hemisphere was dissected into regions on ice and rapidly frozen in liquid nitrogen and stored at -80°C until assayed.

The other hemisphere of the brain was preserved in 4 % Paraformaldehyde (PFA) for overnight. It was then cryoprotected in sucrose for 72 hours then transferred to antifreeze until utilized for immunohistochemical analysis, were kept at -20°C.

3.6 Biochemical Methods

3.6.1 Reagents and Chemicals

The Rat AchE, Ach, TNF- α and BDNF Enzyme Linked Immunosorbent Assay (ELISA) Kits were bought from Elabsciences Biotechnology Inc, USA, through our regional supplier Biocom Africa. The levels of GSH, SOD, CAT, TBARS and GSH-PX were measured colorimetrically using the following chemicals: Hydrogen peroxide (H_2O_2) stock (35 %) solution, 2- Thiobarbituric acid (TBA) (Sigma T5500), Trichloroacetic acid (TCA) (Sigma T9159), Potassium dichromate, glacial acetic acid, Nitro Blue Tetrazolim (NBT), N,N-Dimethylformamide (DMF), Sodium carbonate ($NaCO_3$), EDTA (Ethylene diamine tetra acetic acid), Hydroxylamine hydrochloride, Reduced Glutathione (G4251) and 5,5'-dithiobisnitro benzoic acid (DTNB) (D8130), were purchased from Sigma Aldrich through our local supplier Merck laboratories.

3.6.2 Tissue Preparation

Each animal's dissected brain sample was homogenized in PBS (0.01M, pH7.4) using an Omni Tissue Master 125 homogenizer at a ratio of 1:10 (w/v), at a speed of 4 rpm, and the supernatant was collected and used for Ach, AchE, TNF, and BDNF assays. Some of the brain tissue was frozen immediately in liquid nitrogen during termination and was stored in -80 ^{o}C until used for biochemical analysis. The cortex and hippocampus were dissected in cold ice, weighed, and homogenized in ice-cold 0.01 M PBS at pH 7.4 to give a 10 % (w/v) homogenate. This homogenate was centrifuged as per the requirements of the test to be undertaken. The supernatant was stored at –80 °C and used for measurement of BDNF, GSH, TNF-alpha, oxidative stress biomarker (MDA), antioxidant status (GSH, GPx, CAT and SOD), and cholinergic markers (Ach and AchE).

3.6.3 Measurement of Ach, AchE, TNF alpha and BDNF

The Ach concentration levels in the hippocampus and cerebral cortex were quantified according to the manufacturer's protocol of each assay kit from Elabscience Biotechnology Inc., USA, Cat No. E-EL- 0081, E-EL-R0355, E-EL-R0019 and E-EL-R1235 respectively. The procedures followed the manufacturer's guideline for sandwich and competitive methods (Appendix B).Using a microplate reader, the optical density value for each parameter was read at 450 nm.

3.7 Oxidative stress Biomarkers

The whole hemisphere of the brain tissue was weighed and prepared by crushing brain tissue in ice cold 0.01 M Phosphate Buffer (pH 7.4), using tissue homogenizer (Omni International Tissue Master 125). The samples were centrifuged for 10 minutes at 8000xg.

3.7.1 Measurement of lipid peroxidation (MDA)

Malonaldialdehyde (MDA) levels were determined as a marker of lipid peroxidation by detecting thiobarbituric acid reactive substances (TBARS), using the procedure outlined by Akthar et al., (2012) with a few minor modifications made for use in a plate reader.

Reaction mixture

The reaction mixture composed of brain homogenate (0.5 ml), 0.25 ml of 30% Trichloroacetic acid (TCA) (Sigma T9159) and 0.25 ml of 0.8% 2- Thiobarbituric acid (TBA) (Sigma T5500) were mixed. The blank contained the distilled water (0.5 ml), 0.25 ml TCA and 0.25 ml TBA.

Procedure

To produce a pink coloured MDA chromogen, the reaction mixture was incubated in 80 ^{o}C Thermo shaker (MS 100 thermo shaker incubator) for 30 min, cooled with ice cold water at 4 °C for 30 min, then centrifuged at 3,000×g for 15 min. The 200µl of supernatant was added to each well in the 96 well plate in duplicates, and the absorbance was read

at 540 nm and 620 nm. The difference in absorbance value at 540nm and 620 nm was used to calculated MDA concentration.

Calculation for MDA concentration

The malondialdehyde (MDA) concentration was calculated using its molar extinction coefficient = 0.156 x 10^6 Moles/Litre/cm and the data was calculated as μmoles of MDA per gram of brain using the formular below:

$$C = \frac{Abs_{Corrected\ (540 - 620)}}{0.156 \times g \text{ of tissue used in homogenate}}$$

3.7.2 Measurement of non- enzymatic antioxidant glutathione (GSH)

The glutathione was measured by the method of Ellman reagent with volumes modified for use in the plate reader.

Reaction mixture

The reaction mixture was as follows 0.05 ml supernatant, 0.5 ml of 0.1 M phosphate buffer (PB) (pH 7.4), 0.25 ml 5,5'-dithiobisnitro benzoic acid (DTNB) (D8130) and 0.2 ml of double distilled water was added. The blank contained 1ml of 5,5'-dithiobisnitro benzoic acid (DTNB) (D8130).

Procedure

To separate the proteins and produce a reaction supernatant, equal quantity of 10 % homogenate (w/v) and 10% Trichloroacetic acid (TCA) (Sigma T9159) were mixed and centrifuged. To make the 1 ml reaction mixture 0.05 supernatant was collected and mixed with 0.25 ml 5,5'-dithiobisnitro benzoic acid (DTNB) (D8130), 0.2 ml of double distilled water and 0.5 ml PB vortexed and 200 µL was transferred into duplicates in a universal 96 well plate and the absorbance were read at 420 nm with a plate reader.

Calculations of GSH

Measurement of glutathione (GSH) concentration was calculated using molar extinction coefficient: 1.36 x 10^4 Moles/litre/cm of the formula below and values were expressed as μmoles GSH per mg of brain.

$$C = \frac{\text{Abs x dilution factor}}{13600 \times B} \times 1000$$

Abs: absorbance
B: mg of brain tissue used in homogenate

3.8 Measurement of antioxidant enzymes

All the antioxidant enzymes were measured through the colorimetric methods. The whole brain was crushed in various ice-cold buffers as per the requirements of each test to be run. All buffers were prepared the day before the test is run and kept in 4 ^{o}C refrigerator.

3.8.1 Determination of SOD activity

SOD is so important in the studies of ROS and antioxidant that a rapid and accurate method to determine its activity is required. Because the substrate O_2^- is unstable, SOD activity is mainly determined by indirect methods. Most of these indirect assays depend on competition between SOD and an O_2^- scavenging indicator such as hydroxylamine hydrochloride, nitroblue tetrazolium (NBT), cytochrome c, or water-soluble tetrazolium (WST) (Zhang et al., 2016). The methodology by Beauchamp and Fridovich (1971) and Murthy et al., (2002) based on the reduction of Nitro Blue Tetrazolium (NBT) to water-insoluble Blue Formazan was used to measure brain SOD activity.

Reaction mixture

Since NBT is not soluble in water, the NBT stock solution was prepared by dissolving NBT in 70% Dimethyl Formaldehyde (DMF). The reaction mixture contained 0.5 ml of Brain homogenate (10 %), 0.4 ml of 24µM NBT, 1 ml of 50 mM sodium carbonate, and 0.2 ml of 0.1 mM EDTA (Ethylene diamine tetra acetic acid).

Procedure

0.4 ml of 1 mM hydroxylamine hydrochloride was added to the reaction mixture to initiate the reaction. The change in absorbance was recorded at time 0 min, 5 min, 10 min, 15min and 30 min at 620nm nm at 25 °C. Each batch of samples was run along a suitable control

without brain homogenate. Units of SOD activity were expressed as the amount of enzyme required to inhibit the reduction of Nitro blue tetrazolium (NBT) by 50 %. Units per gram of brain served as an expression for the specific activity.

Calculations of SOD activity

The SOD activity of the original sample will be presented as the following formula (Zhang et al., 2016) :

$$\text{SOD activity} = \frac{A_0 - A_1}{A_1} \div 50\ \% \times \frac{\text{System Volume}}{\text{Sample Volume}} \times \text{Dilution Factor}$$

where A_0 is the absorbance without SOD, A_1 is the absorbance with SOD present, and the amount of enzymatic activity that results in 50% inhibition in the system is specified as 1 unit (U). In other words, the SOD activity causing $A_1 = 0.5$, A_0 is defined as 1 U. SOD activity was estimated against linear standard curve of Bovine Superoxide dismutase (Sigma).

3.8.2 Determination of catalase (CAT) activity

The amount of catalase activity was measured as per (Sinha, 1972). The method is based on the reduction of Potassium Dichromate $K_2Cr_2O_7$ to chromic acetate when heated in the presence of H_2O_2.

Reaction mixture

The stock solution of potassium dichromate and glacial acetic was prepared by mixing 5 % potassium dichromate with glacial acetic acid (1 in 3). The stock solution was further diluted (1 in 5) in distilled water to make a dichromate-acetic acid working solution. The volumes were modified for use in the plate reader. The reaction mixture included 0.13 ml of 0.2 M H_2O_2, 0.33 ml of 10% brain homogenate, and 0.3 ml of 0.01 M phosphate buffer (PB) (pH 7.4).

Procedure

The tubes were incubated for 90 s at 37 °C. Samples were then incubated for 15 minutes at 100 °C in a thermoshaker (Allsheng MB 100 2A). Duplicate additions of 200ul of the sample were added to the 96-well plate, and the amount of H_2O_2 consumed was calculated by measuring absorbance at 540 nm with a microplate reader (Allsheng AMR 100).

Calculation of Catalase activity

CAT activity was expressed as micromoles of H_2O_2 consumed per minute per gram of brain using the formula below adopted from (Hadwan and Albert, 2016). Catalase activity is calculated using a first-order reaction(k) equation and its rate constant.

$$\text{Catalase activity (U/g)} = \frac{2.303}{t} \quad X \left[\log \frac{S^0}{S-M} \right] X \frac{V_s}{V_t}$$

Where V_t is the total volume of chemicals in the Eppendorf tube, V_s is the volume of homogenates, S^0 is the absorbance of the standard, S is the absorbance of the test sample, M is the absorbance of the control test, and T is the time.

3.8.3 Determination of glutathione peroxidase (GPx) activity

The activity of Glutathione peroxidase was measured by Flohe and Gunzler (1984) method as described in Haider (2014) with modification of volumes for use in the plate reader.

Reaction mixture

One millilitre of reaction mixture was prepared from 0.3 ml of brain supernatant ,0.3 ml of phosphate buffer (0.1 M, pH 7.4), 0.1 ml of Sodium azide (10 mM), 0.2 ml of GSH (2 mM), , 0.1 ml of H_2O_2 (1 mM). A blank without homogenate was prepared along sample.

Procedure

For 15 minutes, the reaction mixture was incubated at 37 °C. The reaction was stopped by adding 0.5 ml of 5% TCA after incubation. After centrifuging the tubes at 1,500 g for five minutes, 0.1 ml of supernatant was extracted. To 0.1 ml of reaction supernatant, 0.2

ml of phosphate buffer (0.1 M, pH7.4) and 0.7 ml of DTNB (0.4 mg/ml) were added. After mixing, the absorbance was read at 420 nm.

Calculation of GPx activity

The activity of GPx was expressed as micromoles per milligram of brain.

$$\text{GPx activity} = \frac{(\text{Blank} - \text{Sample}) \times \text{dilution factor} \times 1000}{13600 \times C}$$

3.9 Protein determination

Bovine serum albumin was utilized as the standard for all samples used in colorimetric tests for the detection and quantification of total protein using the Coomassie G-250 dye colorimetric reagent (Bradford, 1976).

3.10 Immunohistochemistry

Phosphate buffer saline (PBS) was used to perfuse the animals. The brain was then removed, weighed, and stored in 4% PFA overnight before being transferred to 30% sucrose for 72 hours. Frozen 1 in 5 serial sagittal 50 µm thick sections were cut on a cryostat (Thermo Scientific HM 525 NX) for free floating method of immunohistochemistry.

3.10.1 Cresyl violet staining

The first set of sections were mounted on 0.5% gelatine-coated slides, dried, cleaned in a 1:1 solution of 100% ethanol and 100% chloroform overnight, and then rehydrated in alcohol by submerging the slides in a succession of gradually lower alcohol baths. For five minutes, the slides were set to100%, followed by 100% again for five minutes, 95% for two minutes, 70% for two minutes, and 50% for two minutes. After spending 2 minutes in 1% Cresyl Violet, the slides were transferred to distilled water for another 2 minutes. After that, sections were dehydrated for the same lengths of time as previously noted in graduated alcohol baths of increasing concentration (i.e., starting in 50% alcohol and ending in 100% alcohol).

The only exception was the 70% alcohol bath, which serves as a differentiation phase; as a result, the length of time the slides were in the bath depended on how strongly the slides were stained with cresyl violet. After achieving the best staining, dehydration was continued while the staining was being evaluated under a stereomicroscope. The slides were cleaned in xylene following the final dehydration process (5 minutes in 100% alcohol), and then DPX mountant was applied to the cover slips.

3.10.2 Immunohistochemistry for Doublecortin and Ki-67

Adult neurogenesis investigation was done through Doublecortin (DCX) and Ki-67 Immunohistochemistry. To lower endogenous peroxidase activity, the sections were incubated in a solution of 1.6% H_2O_2, 49.2% methanol, and 49.2% 0.1 M PB for 30 minutes. This was followed by three 10-minute rinses in 0.1 M PB. The sections were incubated in a 1.6% H_2O_2, 49.2% methanol, 49.2% 0.1 M PB solution, for 30 minutes to reduce endogenous peroxidase activity, which was followed by three 10 minutes rinses in 0.1 M PB. To block unspecific binding sites the sections were pre incubated for 2 hours, at room temperature, in blocking buffer (3% normal goat serum – NGS, plus 2% bovine serum albumin - BSA, and 0.25% Triton X-100 in 0.1 M PB).

Following that, the sections were incubated with a primary antibody solution (1:1000, goat anti-doublecortin, DCX, ab18723, California, USA) for DCX and (1:1000, rabbit anti-Ki-67, ab15580) for Ki-67 for 48 hours at 4 degrees Celsius. There were three 10-min rinses in 0.1 M PB after the primary antibody incubation. After that, sections were incubated for 2 hours at room temperature with a secondary antibody solution for DCX and Ki-67 (1:1000 dilution of anti-goat IgG, BA1000, Vector Laboratories, Burlingame, California, USA, in a mixture of 3% NGS and 2% BSA in 0.1 M PB). Sections were then incubated in an avidin-biotin solution (AB complex) (1:125; Vector Laboratories, PK 6100) for 1 hour before being rinsed three times for 10 minutes each time in 0.1 M PB.

The sections were then incubated for 5 minutes in a solution containing 0.05% diaminobenzidine (DAB,) in 0.1 M PB, followed by the addition of 3.3 µl of 30% hydrogen peroxide per 1 ml DAB solution. On a low power stereomicroscope, chromatic precipitation was observed until the background stain reached a level that would permit precise

architectonic matching to the Nissl sections without masking the immunopositive structures. Sections were soaked to 0.1 M PB for 10 minutes, rinsed twice for 10 minutes, and then the reaction was terminated.

3.10.2.1 Microscopy

All images were analysed with a research microscope Leica DM 500, with camera Leica ICC 50 HD (Leica microsystem, Germany). The Leica Acquire (Macintosh) software was used for image capture.

3.10.2.2 Volume measurements

A total of 2.5 times of magnification was used to mark the dentate gyrus (DG) and the contour of the hippocampus. Using Image J software, evaluations were performed on an average of 10 routinely sampled portions of each animal's hippocampal region.

3.10.2.3 Quantification of immunopositive cells

Using the average cell count across six sections per animal, cell density was estimated. The cell count was conducted using seven camera fields per section at a magnification of x40. The area of the camera field was divided by the total count for each region. Only those cells in the dentate gyrus were counted.

3.11 Statistical analysis

Results are shown as the mean and standard Error of the Mean (SEM). Version 9 of GraphPad Prism was used for the statistical analysis (GraphPad Software, CA, USA). Before doing any additional statistical analysis, outliers were discovered using the ROUT test (Q = 1%) and eliminated. The Komolgrov-Smirnov test was used to determine whether the data were normal. The Tukey's post hoc test for multiple comparisons among the groups was used after the One-Way analysis of variance (ANOVA) for normally distributed data between the five groups. Using the use of Two-way ANOVA, some of the biochemical and behavioral tests were analyzed. after a meaningful p was reached. The threshold for statistical significance was set at $p < 0.05$. If $p > 0.05$ but < 0.1, a tendency is considered.

4 RESULTS

4.1 Combretum molle leaf extract yield and phytochemical content

The yield percentage of plant extraction was 9.26%. Liquid chromatography/mass spectrometry (LC/MS) analysis was used to isolate the chemicals. The National Institute of Standards and Technology (NIST14) and Willey library were used to match the compound spectra. The compounds that were isolated were alkaloids, Saponins, Tannins and Flavonoids with some of the flavonoid subclasses isolated from the extract presented in Table 4.1

Table 4.1 List of flavonoids phytochemical isolated from methanolic leaf extract of *Combretum molle.*

Name of the compound	**Isolated**
Astragalin (kaempferol-3-O-β-D-glucoside)	Positive
Isovitexin	Positive
Hyperoside (quercetin-3-O-D-galactoside)	Positive
Myricetin-3-Galactoside	Positive
(+)-Catechin	Positive
Phloretin	Positive
Quercetin	Positive

4.2 Effects of *C.molle* and D-galactose on General health, food and water intake of rats during treatment period.

To prevent erroneous false positives, the overall health of each rat was first assessed when it was received and during the acclimatization period. For this reason, daily food and fluid intake was recorded, and body weight assessed once a week during treatment. General health was unaffected following the administration of the *C.molle* and D-galactose, and there was no mortality linked with it. The treatment groups did not differ substantially ($F_{4, 20} = 0.518$; $P=0.7234$; Figure 4.1*,* Appendix C, Table 4.3) in terms of the weekly average food intake. The weekly average of food intake was not significantly different among the treatment groups ($F_{4, 20} = 0.518$, $P=0.7234$, Figure 4.1, Appendix C, Table 4.3). Similarly, during the treatment, there was no discernible difference in the amount of fluid consumed by the rats between the groups ($F_{4, 20} = 0.1805$, $P = 0.9458$, Figure,4.2, Appendix C, Table 4.2.).

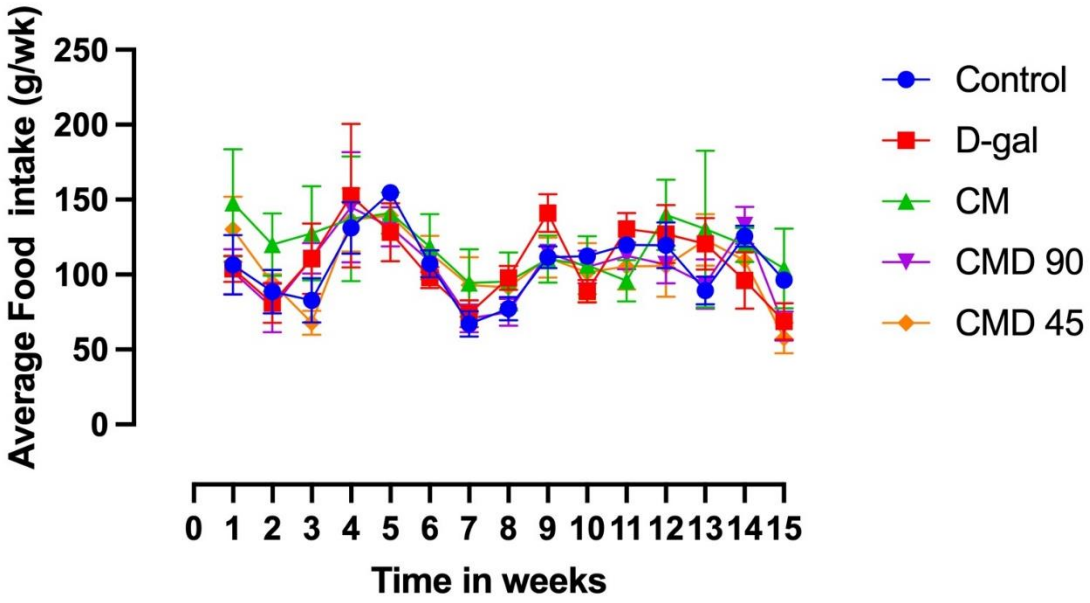

Figure 4.1. Average food intake in grams/week during the first two weeks of acclimatization and thirteen weeks of treatment period Values represent mean ± SEM. The level of significance ($p<0.05$)

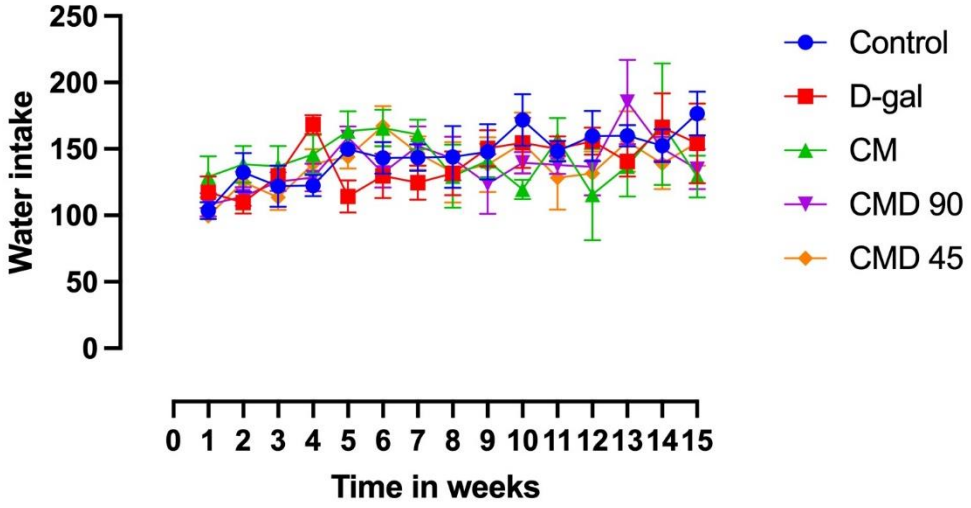

Figure 4.2. Fluid intake (ml/week) during the first two weeks of acclimatization and the thirteen weeks of treatment period. Values represent mean ± SEM. The level of significance ($p<0.05$)

4.3 Effects of *C. molle* and D-galactose administration on Body Weight

The rats experienced no weight loss as there was weight gain across the groups throughout the treatment period (Figure 4.3). There was significant weight gain (P = 0,01) across the groups with CM and CMD 90 groups showing significant differences from the 3rd to 13th week compared to the Control, D-gal and CMD 45 groups (F4,35 = 4,802, P = 0,0034).

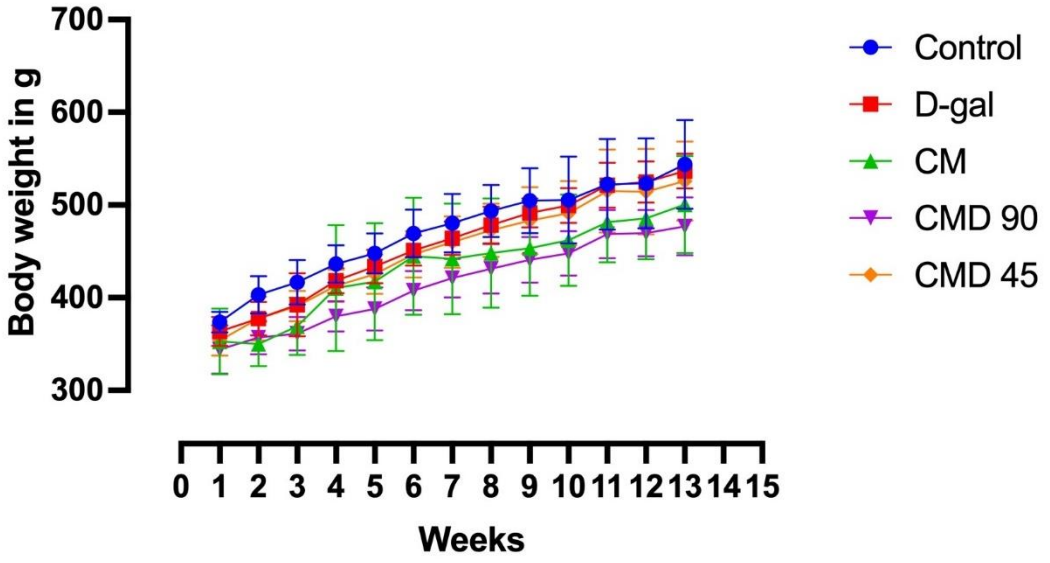

Figure 4.3. Average body weight (g) measured weekly during the first two weeks of acclimatization and thirteen weeks of treatment period. Values are expressed as mean ± SEM, n= 8. Level of significance ($P<0.05$).

The initial body weights of the groups didn't differ significantly during the first week of treatment (F4, 35 = 1,351, P= 0,271, Table 4.2). However, the average final body weights showed significant difference (F4,35 = 3,752, P = 0,0121, Table 4.2) in the CMD 90 and CM group, having significantly lower body weights compared to D-gal (P = 0,0044; P = 0,012) and Control (P = 0,0011; P = 0,032) groups respectively. Comparing the CM and CMD 90 group to the other groups, the percentage of weight gain was also noticeably lower in the CM and CMD 90 group.

Table 4.2. Effect of D-galactose and *Combretum molle* administration on body weight.

Treatment Groups	**Initial week body weight (g)**	**Final week body weight (g)**	**Weight gain (g)**	**%Weight gain**
Control	374.4 ± 3.77	553.5 ± 17.11	189.3 ± 17.67	41.49 ± 4.39
D-gal	370.9 ± 6.92	541.8 ± 4.85	171.8 ± 6.858	47.09 ± 2.53
CM	360.4 ± 9.86	488.2 ± 8.17***\#\#**	132.8 ± 7.953	38.39 ± 1.57****\#\#**
CMD 90	355.3± 7.89	476.8 ± 11.03***\#\#**	159.2± 11.89	36.71 ± 4.21****\#\#\#**
CMD 45	357.6 ± 6.57	525.9 ± 15.07	171.8 ± 14.11	46.29 ± 4.75 **f, a**

All data are shown as mean ± SEM, n = 8. $^{\#}p < 0.05$ or $^{\#\#}p < 0.01$ vs the **Control group**, *****p < 0.05 or ******p < 0.01 vs **D-gal** group. f< 0.00001 vs CM; a< 0.05 vs CMD 90.

4.4 Effect of Combretum molle and D-galactose administration on the open field activity and non- cognitive parameters.

4.4.1 Effect on locomotor activity.

In the habituation trial, the animals were exposed to the open field environment for 2 minutes and there were no significant differences (F 4, 22 = 0,3773; P=0,8223, Figure 4.4A, Table 4.3) in terms of the average line crossed. Also, in the Rearing frequency, no significant difference (F 4, 22 = 1,825; P=0,1600, Figure 4.4B, Table 4.3) was observed in the averages among the groups. During the familiarization phase, the rats were exposed to the open field for a longer period (5 min) and no discernible change was found in the lines crossed (F4,25 = 2,732; P= 0,0516; Figure 4.4A) and in the rearing frequency (F4, 25 = 2.2; P = 0.0907, Figure 4.4B) for all the groups. Similarly, during the testing phase of 10 min there was no discernible difference observed in the line crossing (F4, 21 = 0,7317; P =0.5789; Figure 4.4A) and Rearing frequency (F4,25 = 0.1831; P = 0.9450; Figure 4.4B).

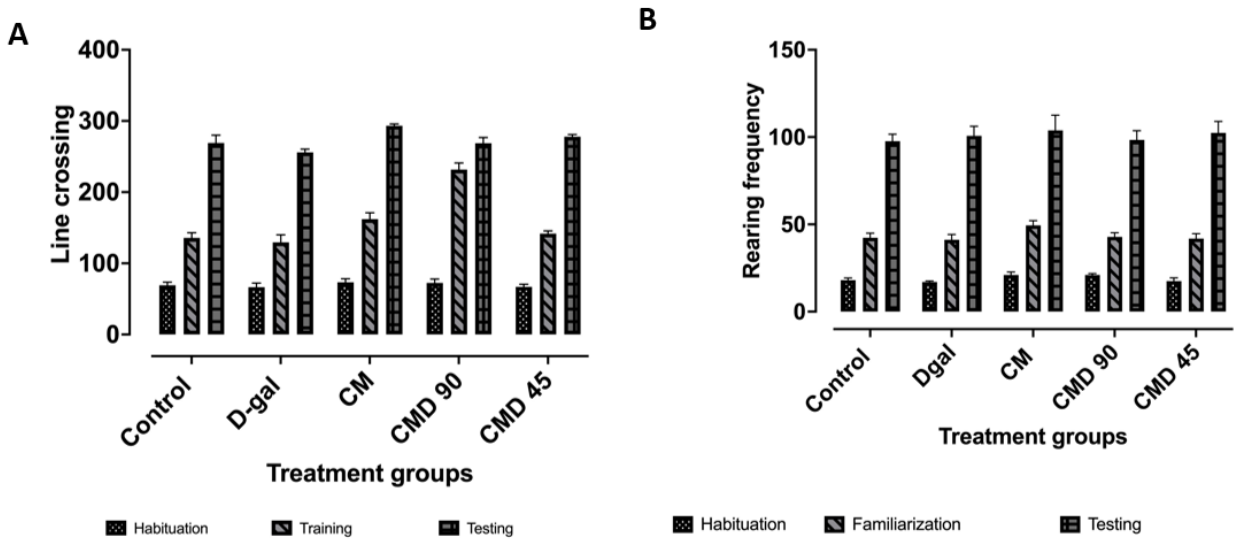

Figure 4.4. Summary of results showing the number of lines crossed (horizontal) and the rearing frequency (vertical) during the different trials in the open field test. All data are shown as mean ± SEM, n = 6. No significance was observed at **P> 0.05.**

Table 4.3. Mean values of locomotor activity (line crossing and rearing frequency) during an open field test

	LINE CROSSING			REARING FREQUENCY		
Groups	**Habituation**	**Familiarization**	**Testing day**	**Habituation**	**Familiarisation**	**Testing day**
Control	69.17 ± 4.39	135.7 ± 7.39	248.2 ± 20.23	18.00 ± 1.29	40.4 ± 2.272	97.60 ± 4.02
D-gal	66.50 ± 5.77	154.7 ± 13.98	247.2 ± 14.23	17.00 ± 0.58	41.17 ± 3.049	95.60 ± 2.79
CM	78.00 ± 6.15	154.7 ± 10.37	268.0 ± 7.04	21.00 ± 2.10	49.40 ± 2.73	103.8 ± 8.76
CMD 90	76.67 ± 6.26	165.3 ± 16.15	254.7 ± 7.20	21.00 ± 0.86	42.83 ± 2.39	98.40 ± 5.31
CMD 45	69.67 ± 3.99	140.0 ± 4.16	252.0 ± 11.07	17.50± 1.84	41.83.67 ± 2.85	102.4 ± 6.59

All data are shown as mean ± SEM, n = 6. All values were not significant (p> 0.05) was observed.

4.4.2 Effect of *C.molle* and D-galactose on non-cognitive behaviour parameters in the open field

Freezing is another open field indicator used to gauge activity absence. This is a widely used parameter which is usually taken as an indicator of a high-stress state in the animal when exposed to the novel environment (Boliver et al.,2000). During the testing trial (10 minutes), the average time spent freezing was not significantly different ($F_{4,25} = 1,014$; $P = 0.4193$; Figure 4.5A, Appendix C, Table 4.6) observed among the groups.

Grooming is another parameter in the open field that indicates the animal activity using a body part. There was no significance difference ($P > 0,9999$) observed when the Control was compared to D-gal and the CMD 45 group. The rats in this group spent less time grooming themselves. However, there was significant difference ($F_{4,25} = 10,38$; $P < 0,0001$; Figure 4.5B, Appendix C, Table 4.6) in the grooming time among other groups, whereby the CMD 90 group had significantly higher average grooming time with significance at $P = 0,0007$; $P=0,006$ and $P= 0,0005$ when compared to the control, D-gal and CMD 45 respectively. The CM group and the CMD 90 group did not differ substantially from one another ($P= 0.5919$) but significantly different when compared to the control group ($P=0,0242$), D-gal ($P= 0,0221$) and CMD 45 ($P= 0,0183$).

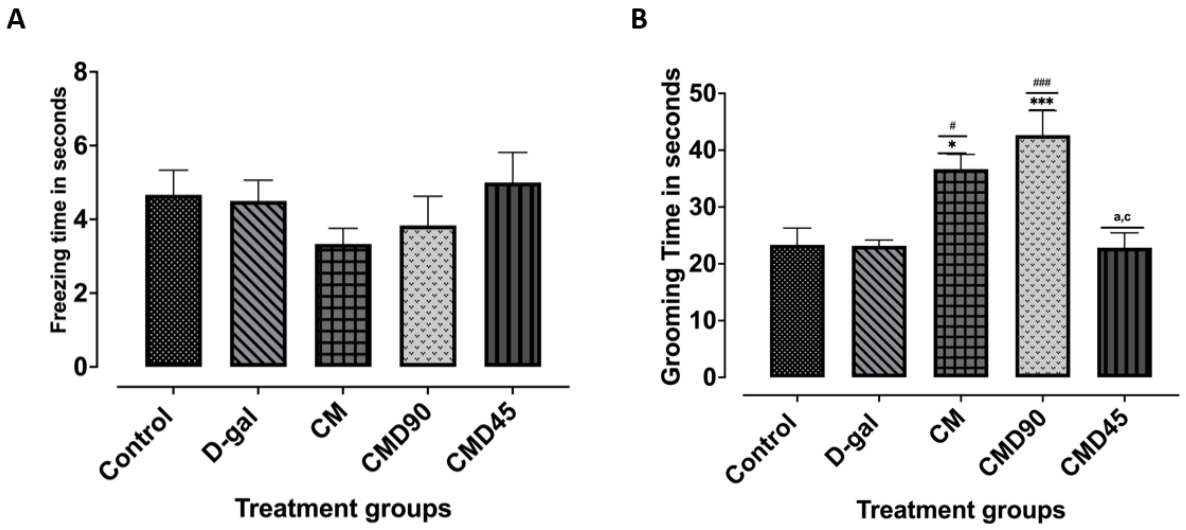

Figure 4.5. Showing the time spent by animals Freezing (A) and Grooming (B). All data are expressed as mean ± SEM, n = 6. Level of significance set at p< 0.05. Data represented as mean ± SEM (n=6). Significant difference set at P< 0,05 was obtained by ANOVA followed by Turkeys multiple comparison test for normally distributed data and were expressed as ###P <0.001, ##P < 0.01, #P< 0.05 vs. **D-gal group**; ***P<0,001, **P< 0.01, *P< 0.05 vs. **Control group**. a< 0.05, c < 0.01, d < 0.001 vs **CM group**. b < 0.05, d< 0.01 vs **CMD 90 group**.

4.5 Effects of D-galactose and *Combretum molle* on memory

4.5.1 Object recognition test

4.5.1.1 Familiarization phase

There was no substantial difference in the groups' exploration times for objects A and B during the familiarization (training) trial ($F_{4, 25}=3.537$; $P=0.0537$, Figure 4.6A, Appendix C, Table4.8) and ($F_{4, 25}=1.795$; P=0,162; Figure 4.6B, Appendix C, Table 4.9), respectively. The average mean values for objects A and B exhibited no discernible difference, indicating that there was no preference for objects A and B among the treatment groups.

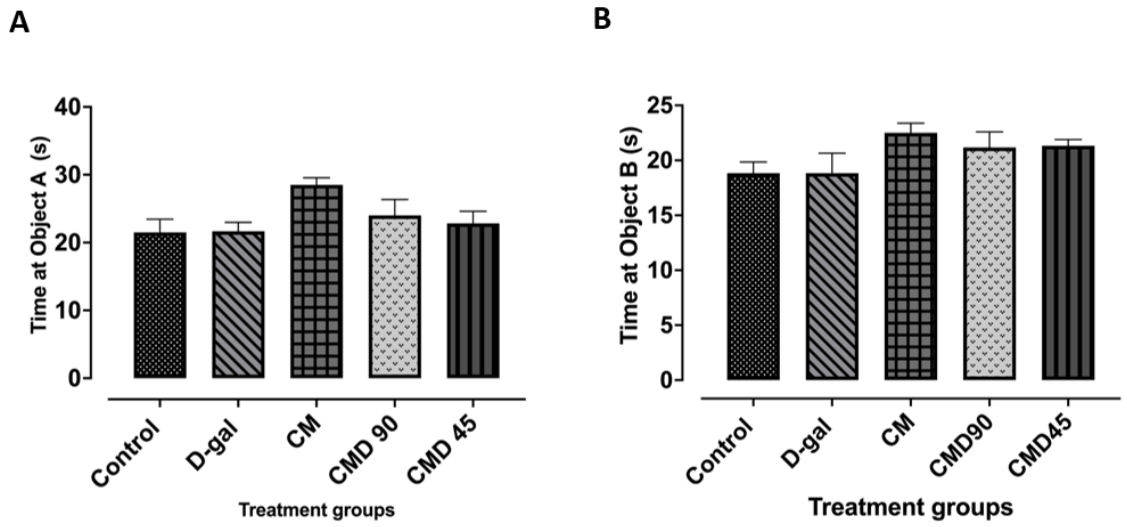

Figure 4.6. Exploration time of similar objects during the familiarization phase of object recognition. Data represented as mean ± SEM (n=6). Significant difference set at P< 0,05 was obtained by ANOVA followed by Turkeys multiple comparison test for normally distributed data. No significant difference was observed as P> 0.05.

4.5.1.2 The Discrimination index during familiarization

The Discrimination index between the groups during familiarization (Figure 4.7A) was statistically significant (F 4,25 = 2,541, P = 0,0422, Appendix C, Table 4.10). The average for *C.molle* (CM) only group was 44.63, while for the D-galactose only group was 31.15 (Appendix C, Tale 4.10) . The percentage of total investigation time of a Novel object (Figure 4.7B) as depicted in Appendix C, Table 4.11 was as follows 71.23 (CMD 90),69.81 (CM), 66.86 (Control), 66.54 (CMD 45) and 62.24 (D-gal), however no significant difference (F4,25 = 1.056, P = 0.394) was observed among all the groups.

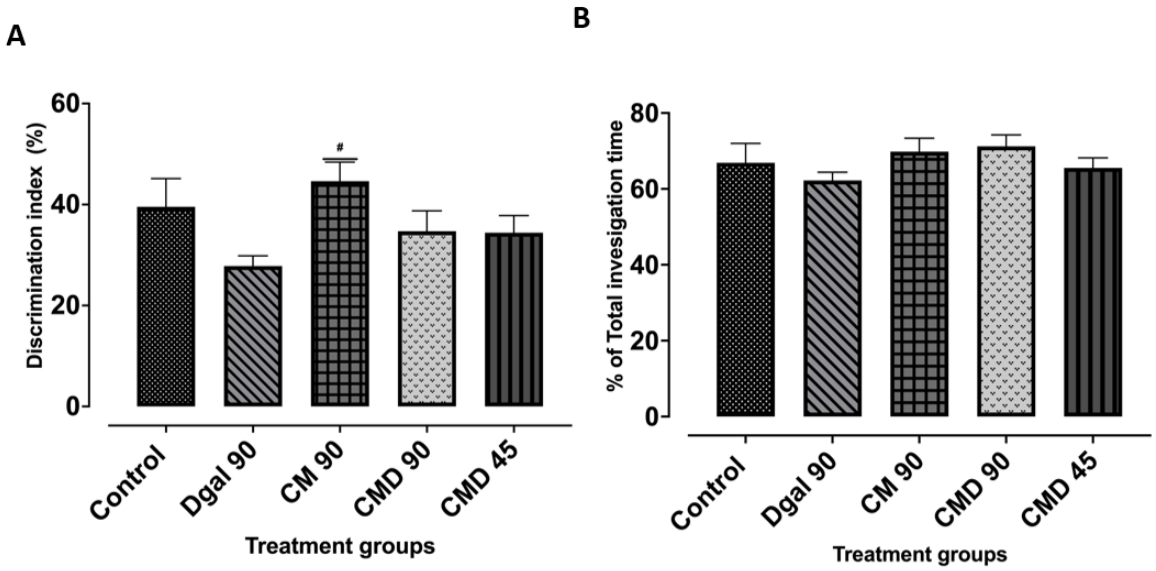

Figure 4.7. Discrimination index and total investigation time of objects during the familiarization trial. Data represented as mean ± SEM (n=6). Significant difference set at P< 0,05 was obtained by ANOVA followed by Turkeys multiple comparison test for normally distributed data and were expressed as $^{\#}$P< 0.05 vs. D-gal group.

4.5.1.3 Testing phase

The duration of the novel object's exploration in the test phase was significantly different (F 4,25 = 7.349; P = 0,0005, Figure 4.8A) among the groups. The D-galactose only (D-gal) group (P = 0,0351) and the CMD 45 (P =0,0260) spent significantly shorter time (33.67s ± 2.87 and 33.80s ± 4.25 respectively) with the novel object compared to other groups. The exploration time of Novel object for the CM, CMD 90 and control was 53,83s ± 3,74; 48,83s ± 3.73 and 49,33s ± 3,13 (Appendix C, Table 4.12) respectively was significantly longer compared to the D-gal group. When comparing D-galactose (D-gal) only to *C. molle* (CM) only and CMD 90 group, time spent with the novel object was significantly higher at P = 0,0043 and 0,0437 respectively. Contrary to the exploration of novel object, the D-galactose group explored the familiar object longer (24.67 ± 1.15, Appendix C, Table 4.13) with the level of significance at (F 4, 25 = 8,206; P = 0,0002; Figure 4.8B), compared to the animals that received *C. molle* (CM, CMD 90 and CMD 45).

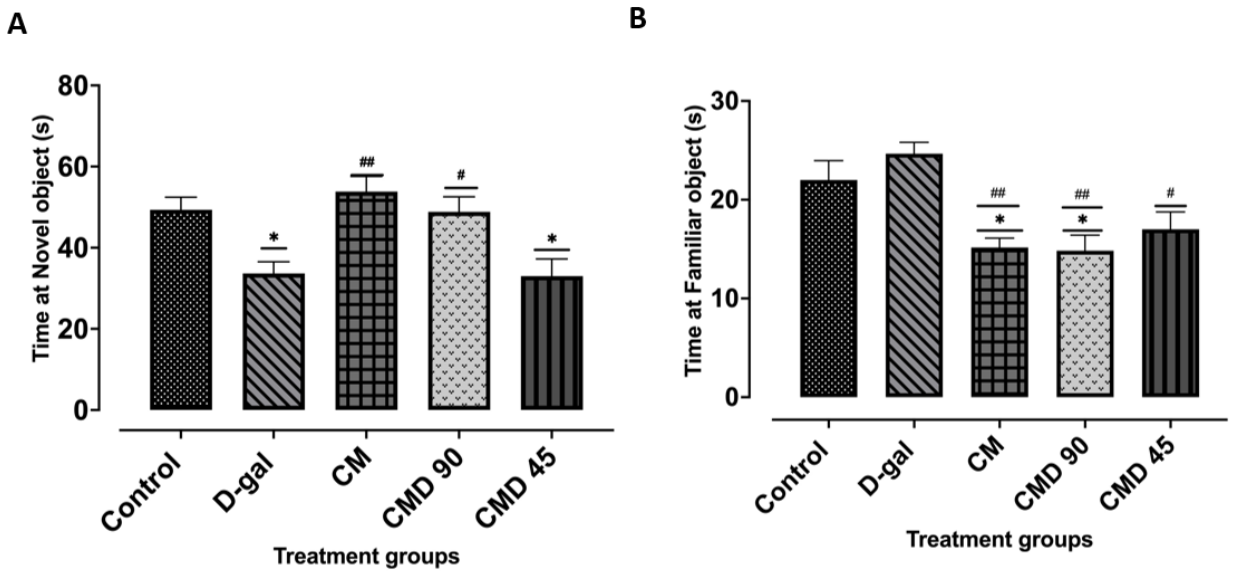

Figure 4.8. Exploration time of the novel object and the familiar object during the novel object recognition test. Data represented as mean ± SEM (n=6). Significant difference set at P< 0,05 was obtained by ANOVA followed by Turkeys multiple comparison test for normally distributed data and were expressed as ##P < 0.01, #P< 0.05 vs. D-gal group; *P< 0.05 vs. Control group.

4.5.1.4 The Discrimination index in the testing phase

The Discrimination index as shown in Figure 4.9A, demonstrated that the control, CM, CMD 90 and CMD 45 groups differed significantly from the D-galactose Group ($F_{4,25} = 4,79$; $P = 0,0052$). The discrimination index mean value of the D-galactose group was -19.26 while for the Control, CM, CMD 90 and CMD 45 were 6.64, 26.40, 16,05 and 16,61 respectively (Appendix C, Table 4.14). The percentage of Total investigation time of the novel object (Figure 4.9B) as depicted in Appendix C, Table 4.15 were as follows: in the control (53,32 %), CM (63,20 %), CMD 90 (54,40 %), CMD 45 (58.30 %) and the D-galactose group (40,37 %). The D-gal group had less than 50% total investigation time with the novel object while for other groups was significantly more than 50 %. This demonstrates that recognition memory deficit was developed in the D-gal-treated rats, but that it was corrected after either 45 or 90 days of *C. molle* treatment.

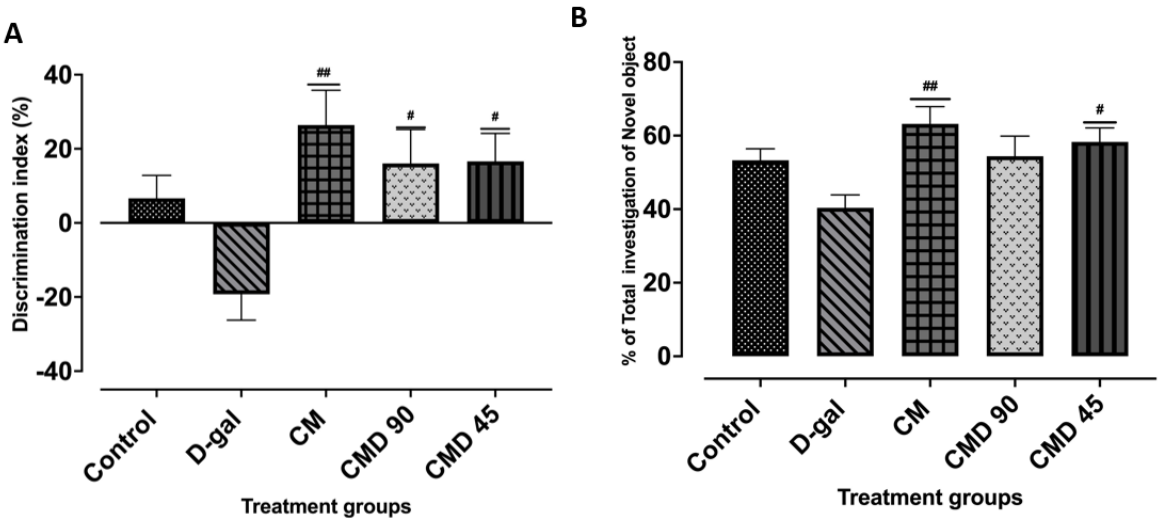

Figure 4.9. Discrimination index and total investigation time of the novel object during the novel object recognition test. Data represented as mean ± SEM (n=6). Significant difference set at P< 0,05 was obtained by ANOVA followed by Turkeys multiple comparison test for normally distributed data and were expressed as $^{\#\#}P < 0.01$, $^{\#}P< 0.05$ vs. D-gal group.

4.5.2 Object location test

4.5.2.1 Familiarization phase

Animals in all groups explored the objects at locations A (F 4,21 = 2,031; P = 0.7300, Figure 4.10 A) and B (F 4,19 = 2.312; P = 0,0950, Figure 4.10B) for almost the same amount of time during the familiarization trial, therefore there was no evidence of a significant difference between them. The average times exploring object in location A were 25.60 (control), 21.20 (D-gal), 23.17 (CM), 24.50 (CMD 90) and 21.67 (CMD 45) (Appendix C, Table 4.16). While for location B, the average exploration times were 22.80 (control), 28.00 (D-gal), 20.17 (CM), 16.00 (CMD 90) and 21.00 (CMD 45) (Table 4.17). The Discrimination Index was not significantly different for both Location A and B among all groups (F 4,20 = 1,715; P = 0,1861). The average DI were 19.50 (control), 19.50 (D-gal), 25.00 (CM), 21.50 (CMD 90) and 20.00 (CMD 45) (Appendix C, Table 4.18) The total investigation time (TIT) on locations A and B was not significantly different (F4,25 = 1,892; P = 0.1432) in all the groups. The average percentages of TIT were 53.02 (control), 48.09 (D-gal), 54.14 (CM), 57.30 (CMD 90) and 49.14 (CMD 45) (Appendix C, Table 4.19). This shows that the animals did not have preference of location during familiarization trial.

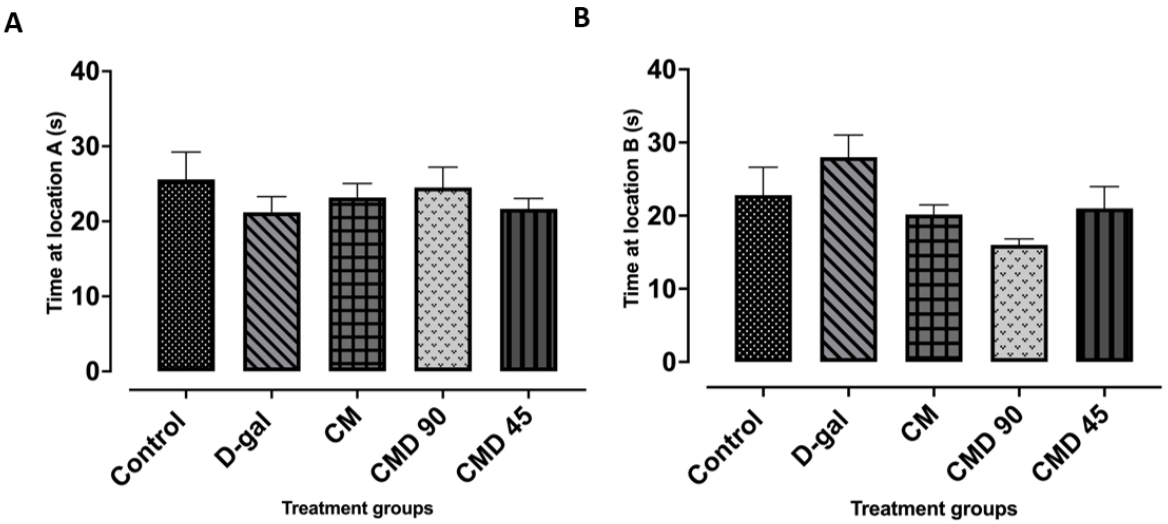

Figure 4.10. Exploration of location A and B in the familiarization trial of the object location Data represented as mean ± SEM (n=6). Significant difference set at P< 0,05 was obtained by ANOVA followed by Turkeys multiple comparison test for normally distributed data and no significant difference was observed as P> 0.05 for all groups.

4.5.2.2 Exploration of locations during the Testing phase

The Control, CM, CMD90, and CMD 45 groups, respectively, spent an average of21.80,24.00,25.80, and 23.80 seconds exploring objects in location A (Novel) during the test trial while for D-gal group the exploration time of object at location A was 16.00 (Appendix C, Table 4.20). The average exploration time for location B (Familiar) were 19.50, 15.33, 16.50 and 17.50 for the Control, CM, CMD 90 and CMD 45 groups respectively while for the D-gal group the exploration time of familiar location B was 27.20. The animals in the Control, CM, CMD 90, and CMD 45 groups spent substantially more time examining the object in the new location than they did in the familiar location ($F_{4,19}=4,549$; $P=0.0096$, Figure 4.11A), but the D-galactose group spent less time exploring the novel object. The time spent by the *C. molle*, CMD 90 and CMD 45 differed significantly at P = 0,0306; 0,0064 and 0,0362 respectively to the D-galactose group. The D-galactose group spent longer time exploring the familiar object ($F_{4,24} = 7,436$; P = 0,0005) while the Control (P = 0,0285), *C.molle* (P = 0,0004), CMD 90 (P = 0,0014) and CMD 45 (P = 0,0040) spent lesser time exploring the familiar location. Based on these findings, treatment with C. molle attenuated the effects of D-gal on spatial memory.

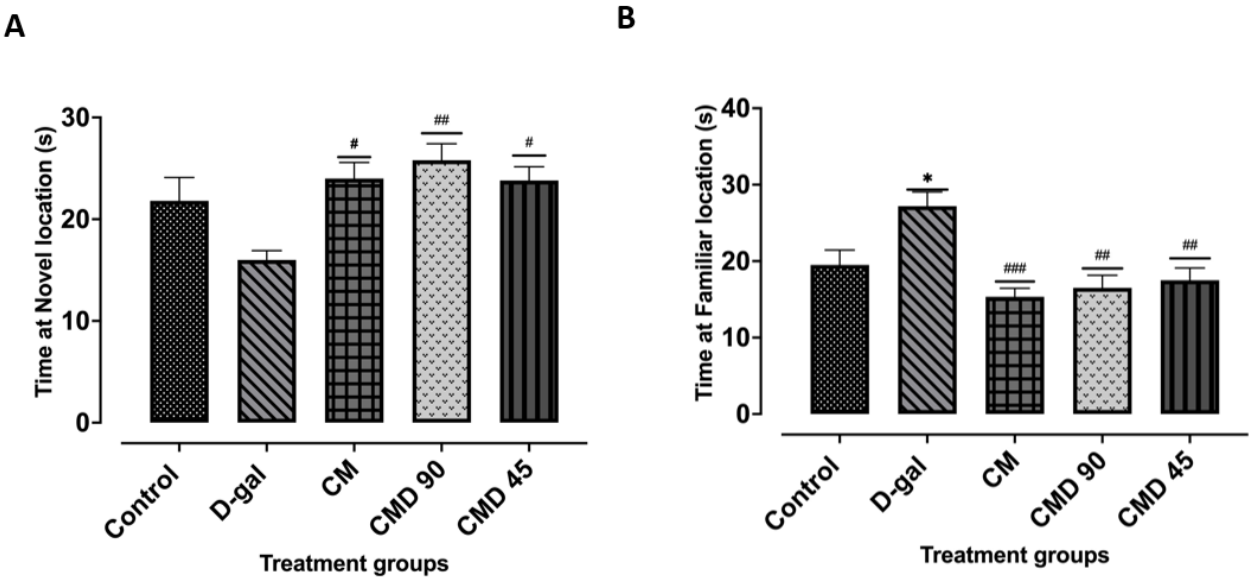

Figure 4.11. Exploration of the object location A and B in the object location test trial. Data represented as mean ± SEM (n=6). Significant difference set at P< 0,05 was obtained by ANOVA followed by Turkeys multiple comparison test for normally distributed data and were expressed as $^{###}P < 0.001$, $^{##}P < 0.01$, $^{#}P < 0.05$ vs. D-gal group; *P< 0.05 vs. Control group.

4.5.2.3 The Discrimination index and Total investigation time during the testing phase of OLT

The Discrimination index of the Control, CM, CMD 90, CMD 45 and D-gal groups were 6.97, 27.92, 37.79, 13.95 and -7.80 respectively (Appendix C, Table 4.22). The Control, CM, CMD 90 and CMD 45 were significantly different to D-galactose group ($F_{4,22}$ = 5.134; P = 0,0045, Figure 4.12A). Similarly, the total investigation time of the novel location was significantly more than 50% probability in the CM (63,96 %), CMD 90 (67,07 %) and CMD 45 group (55,14 %) compared to the D-galactose group (46,83%) (Appendix C, Table 4.23). These results indicate that spatial memory deficits caused by D-galactose exist.

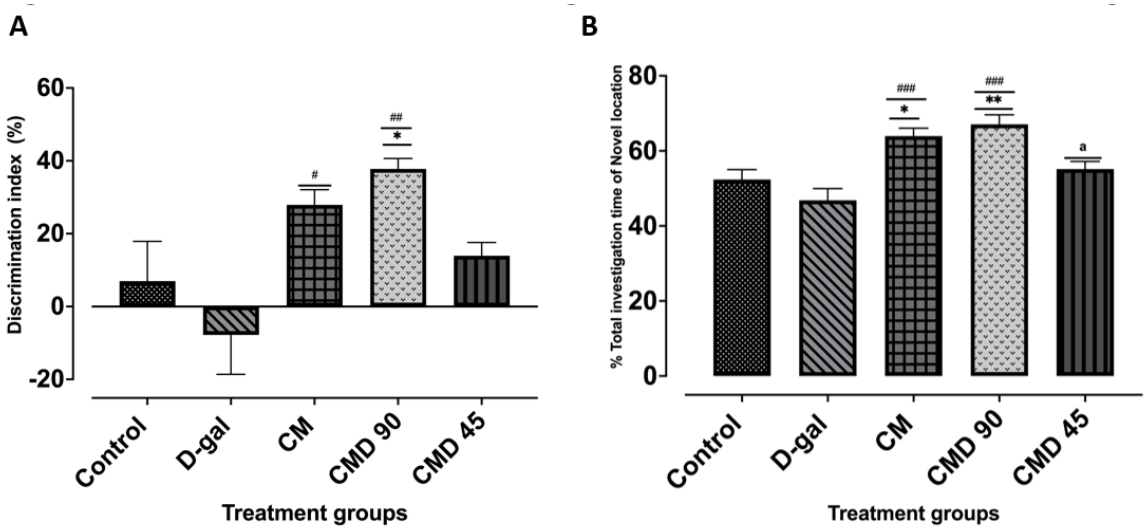

Figure 4.12. Discrimination index and total investigation time of novel location during the object location testing phase Data represented as mean ± SEM (n=6). Significant difference set at P< 0,05 was obtained by ANOVA followed by Turkeys multiple comparison test for normally distributed data and were expressed as $^{###}$P <0.001, $^{##}$P < 0.01, $^{#}$P< 0.05 vs. D-gal group; **P< 0.01, *P< 0.05 vs. Control group. a< 0.05 vs *C.molle* only (CM) group.

4.6 Biochemical Analysis

4.6.1 Acetylcholine levels in the brain

According to the findings in Figure 4.13, the amounts of acetylcholine were significantly higher in the cortical ($p < 0.0001$) and hippocampal ($p < 0.01$) regions of the brain in the CM and CMD 90 groups than in the D-gal and control groups. For the CMD 45 there was some level of significant difference when compared to the CM and CMD 90 group both in the cortex ($p< 0.001$) and hippocampus ($p< 0.05$). However, no significance ($p> 0.05$) was observed in both the cortex and hippocampus when comparing control group, D-gal group and CMD 45**.**

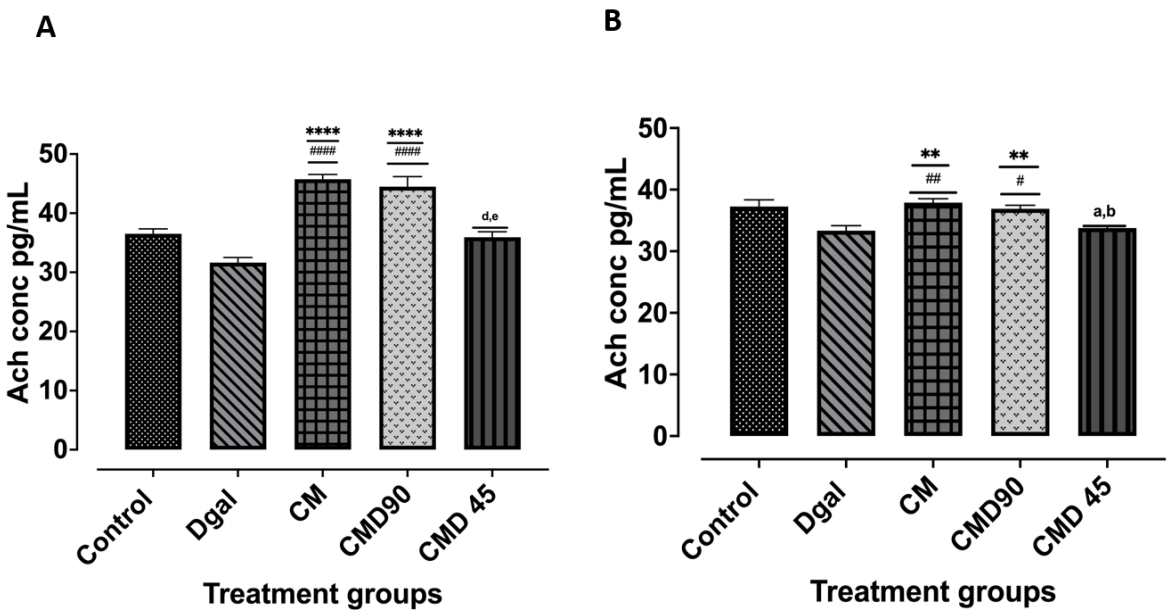

Figure 4.13. The effect of *C.molle* and D-galactose administration on Ach levels in the A cortex and B Hippocampus of D-galactose induced aging adult rats. Each column represents mean ± SEM (n=8). Significant difference was obtained by ANOVA followed by Turkeys multiple comparison test and were expressed as ####P < 0 .0001, ###P <0.001, ##P < 0.01, #P< 0.05 vs. D-gal; ****P < 0.0001, ***P<0,001, **P< 0.01, *P< 0.05 vs. (Control) animals. a< 0.05, c < 0.01, d < 0.001 vs CM. b < 0.05, d< 0.01, e < 0.001 vs CMD 90.

4.6.2 Activity of Acetylcholinesterase

A marker of cholinergic neuron loss in the forebrain is AchE. According to the findings as shown in Figure 4.14 and Table 4.24 in Appendix C, the D-gal group had higher AchE activity in the hippocampus (3.98 ± 0.11) than did the CM (2.61± 0.083) and CMD 90 (3.04± 0.072) groups ($p < 0.0001$ and $p< 0.001$, respectively).Similarly in the cortex, the high activity of AchE was observed in the D-gal group (3.91 ± 0.17) in comparison to CM group (2.57 ± 0.068) ($p < 0.001$) and CMD 90 group (2.65 ± 0.088) ($p< 0.001$). There was a difference in AchE activity in the hippocampus between the control group and the CM and CMD 90 groups that was statistically significant at the significance level of $p < 0.0001$ and $p< 0.001$ respectively, while in the cortex the significant difference was at $p < 0.01$ for both groups.

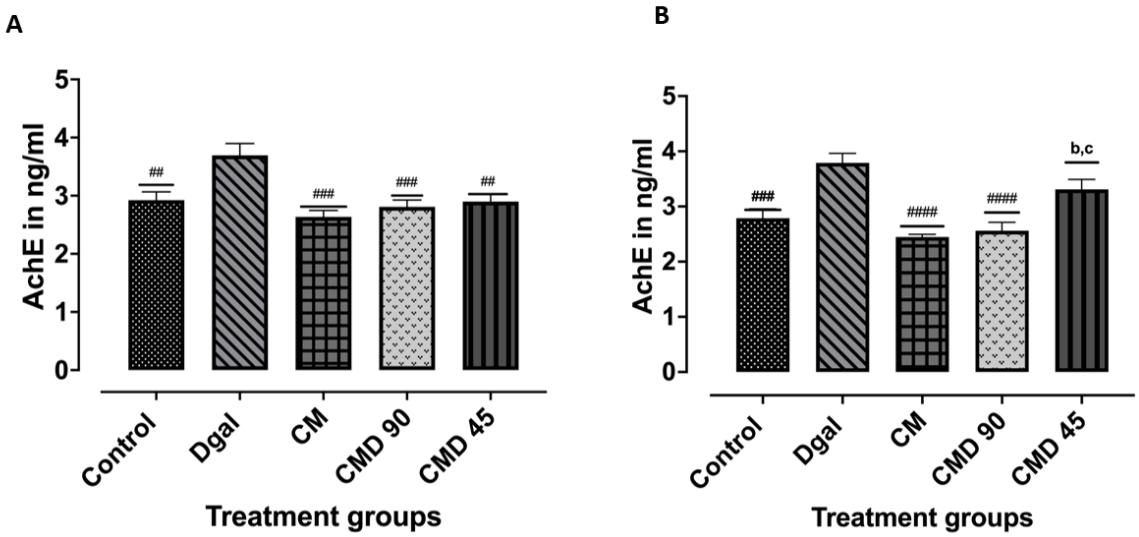

Figure 4.14. Effect of *C.molle* administration on AChE activity in the A cortex and B Hippocampus of D-galactose induced aging rats. Each column represents mean ± SEM (n=8). Significant difference expressed as ####P < 0 .0001, ###P <0.001, ##P < 0.01, #P< 0.05 vs. D-gal. c < 0.01, vs CM. b: p < 0.05 vs CMD 90.

4.6.3 Levels of Brain Derived Neurotropic factor.

According to the findings in Figure 4.15 and Table 4.25 in Appendix C, the CM and CMD 90 group had significantly higher levels of BDNF in the cortex (93.81±8.25 and 92.33±8.40; $p< 0.01$) and hippocampus (95.21±6.83; $p<0.001$ and 86.88±6.67; $p< 0.01$). In the cortex and hippocampus of the Control, D-gal, and CMD 45 groups, BDNF levels were significantly reduced, although there was no statistically significant difference ($p>0.05$) across the groups.

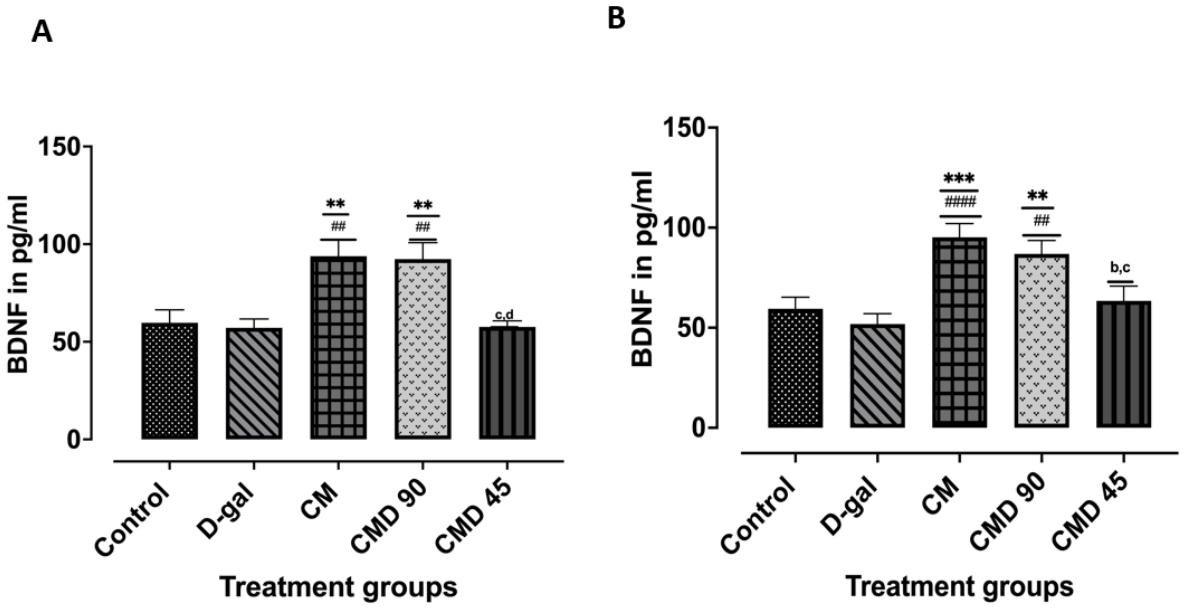

Figure 4.15. The effect of *C.molle* administration on Brain Derived neurotropic factor levels in the cortex A and B. Hippocampus of D-galactose induced aging adult rats. Each column represents mean ± SEM (n=8). Significant difference expressed as $^{\#\#\#\#}P < 0.0001$, $^{\#\#\#}P < 0.001$, $^{\#\#}P < 0.01$, $^{\#}P < 0.05$ vs D-gal ; ****P < 0.0001, ***P<0,001, **P< 0.01, *P< 0.05 vs. Control. a< 0.05, c < 0.01, d < 0.001 vs CM. b: p < 0.05, d< 0.01, vs CMD 90.

4.6.4 Levels of Glutathione (GSH)

The GSH content in the CM group was considerably ($p<0.0001$) higher than in any other group, according to the results shown in Figure 4.16 and Table 4.25 in Appendix C. The GSH concentration in the cortex (0.025) and hippocampus (0.028) of the D-gal group was substantially lower. GSH levels in the cortex and hippocampus of the Control (0.030 and 0.041, $p< 0.001$), CMD45 (0.035 and 0.041; $p < 0.001$), and CMD 90 (0.044; $p < 0.05$ and 0.045; p0.01) groups were all substantially lower than those in the CM group.

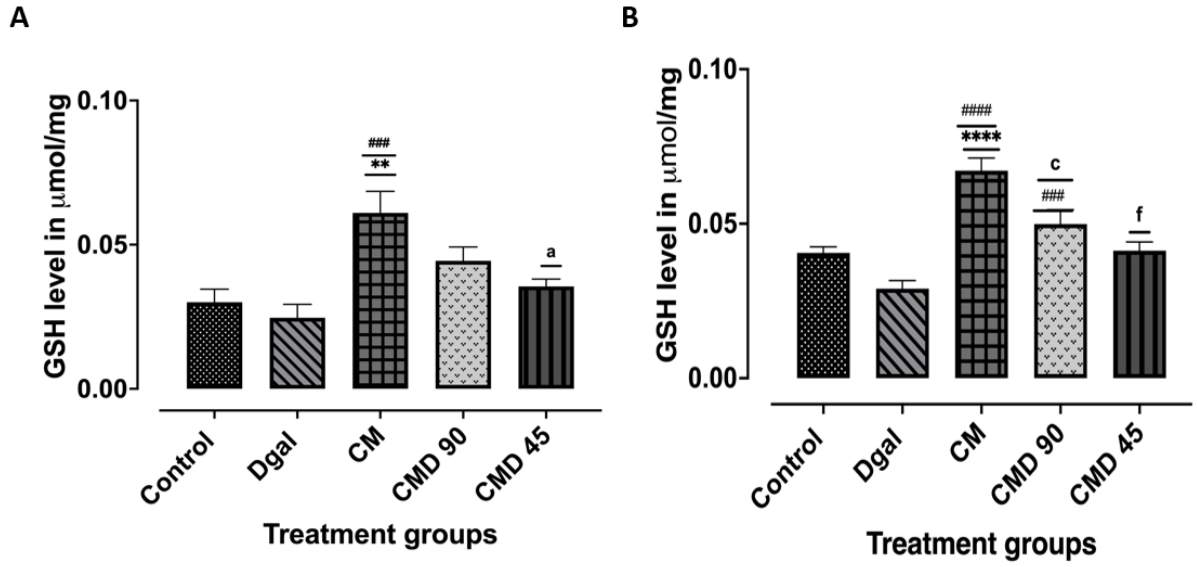

Figure 4.16. The effect of *C.molle* administration on Glutathione (GSH) levels in the A. cortex and B. Hippocampus of D-galactose induced aging adult rats. Each column represents mean ± SEM (n=8). Significant difference expressed as $^{\#\#\#\#}P < 0.0001$, $^{\#\#\#}P < 0.001$, $^{\#\#}P < 0.01$, $^{\#}P < 0.05$ vs. D-gal; ****P < 0.0001, ***P<0,001, **P< 0.01, *P< 0.05 vs. Control . a< 0.05, c < 0.01, vs CM; f < 0.0001 vs CMD 90)

4.6.5 Lipid Peroxidation Levels

The results in Figure 4.17 and Table 4.25 in Appendix C, revealed significantly elevated levels of MDA content in the cortex and hippocampus for the D-gal group (1.61; $p< 0.001$ and 1.63; $p<0.0001$), Control group (1.57; and 1.06; $p < 0.01$) and CMD 45 group (1.23 and 1.08; $p< 0.001$). The MDA levels in the were significantly lower in the cortex of CM group (0.92) and CMD 90 (1.04) including the hippocampus of both the CM group (0.44) and CMD 90 (0.45).

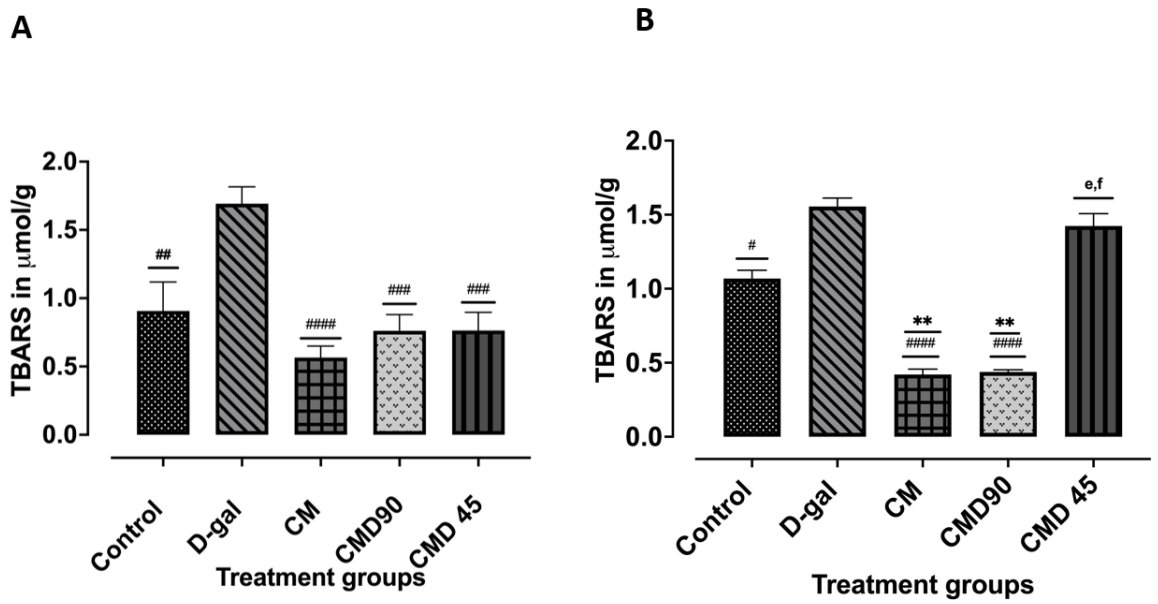

Figure 4.17. The effect of *C.molle* and D-galactose administration on lipid peroxidation levels in the A. cortex and B. Hippocampus of D-galactose induced aging adults. Each column represents mean ± SEM (n=8). Significant difference expressed as $^{\#\#\#\#}P < 0.0001$, $^{\#\#\#}P < 0.001$, $^{\#\#}P < 0.01$, $^{\#}P < 0.05$ vs. D-gal $^{**}P < 0.01$, $^{*}P < 0.05$ vs. control. a< 0.05, c < 0.01, d < 0.001, f < 0.0001 vs CM. b: p < 0.05, d< 0.01, e < 0.001 vs CMD 90.

4.7 Effects of *Combretum molle* and D-galactose administration on levels of Tumour Necrosis factor alpha (TNF α).

According to the results in Figure 4.18 and average values in Table 4.26 in Appendix C, the D-gal group (363.9 and 446.4) had significantly higher levels of TNF α content in the cortex ($F_{4,53}= 10.11$; $P < 0.0001$) and hippocampus ($F_{4,35}= 46.13$; $P< 0.0001$) than the Control group(304.6 and 245.9) and CMD 45 group (284.3 and 302.4), CMD 90 (262.1 and 243.1), and CM (267.1 and 231.5).

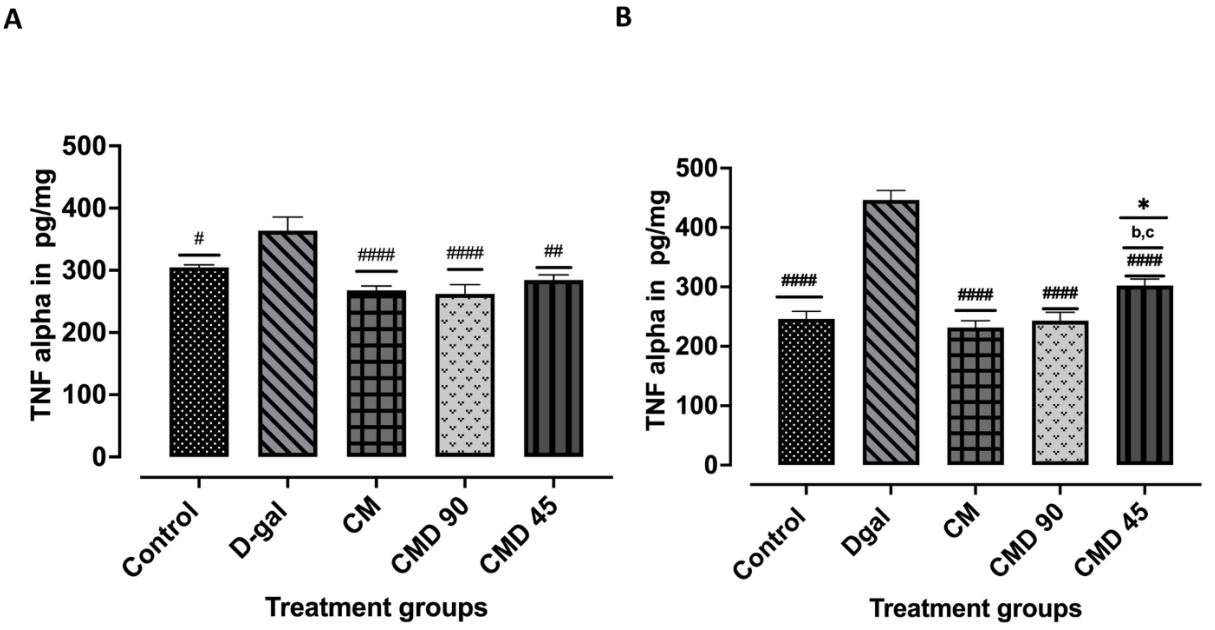

Figure 4.18. The effect of *C.molle* and D-galactose administration on Tumor Necrosis Factor alpha levels in the A. cortex and B. Hippocampus of D-galactose induced aging adults. Each column represents mean ± SEM (n=8). Significant difference expressed as ####P < 0 .0001, ###P <0.001, ##P < 0.01, #P< 0.05 vs D-gal; *P< 0.05 vs control. c < 0.01 vs CM. b: p < 0.05 vs CMD 90.

4.8 Effects of Combretum molle and D-galactose administration on antioxidant enzymes

4.8.1 Superoxide dismutase activity (SOD)

Antioxidant defence mechanism, superoxide dismutase catalyses the dismutation of superoxide and anions. Activity of SOD was measured at 0mins, 5mins, 10mins and 15 mins among the test groups as shown on Figure 4.19. The two-way ANOVA results revealed significant difference in the time factor ($F_{3, 140} = 9.49$. $P < 0.001$) among the groups. At 0 minutes there was no significant difference in the enzyme activity in Control, D-gal, CMD 90 and CMD 45 whereby the activity was less than 1u/mg compared to the CM group which the activity was more than 1 u/mg (Figure 4.16). At 5 min the minutes the activity of the Control, CMD 90 and CMD 45 increased to more than 1u/mg compared to the D-gal group which remained at less than 1 u/mg. At 10 minutes the CMD 90 and CMD 45 enzyme activity decrease to 1u/mg, however they increased again to more than 1u/mg at the at 15 minutes. The D-galactose group activity peaked at 10 minutes to 1u/mg however the activity decreased to below 1umg at 15 min. The enzyme activity kept on increasing for the CM group until it peaked at 2 u/mg at 15^{th} minutes.

Treatment groups were significantly different ($F_{12,140} = 9.43$ $P < 0.001$). No interaction among the groups was observed ($F_{12,140} = 0667$. $P=0.81$). The results in Figure 4.19 and average values in Table 4.27 in Appendix C showed that SOD activity was significantly higher in the CM group when compared to D-gal group ($P < 0.0001$) and Control ($P=0.002$). Additionally, significant difference was observed when the D-gal group was compared to CMD 90 ($P=0.01$) and CMD 45 ($P=0.04$). When CM group was compared to CMD 90 ($P = 0.04$) and CMD 45 (P0.04). No significant difference was observed between CMD 90 and CMD 45 ($P=0.9$) also between Control and D-gal ($P = 0.1$).

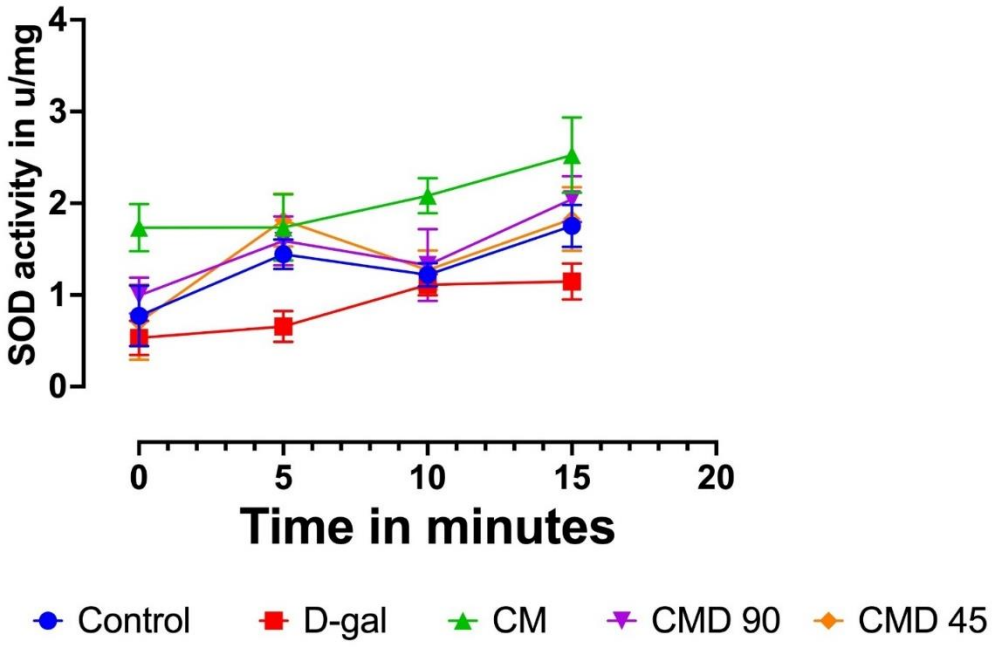

Figure 4.19.The effects of *C.molle* and D-galactose on superoxide dismutase activity. Data represented as mean ± SEM (n=8).

4.8.2 Effects of *C.molle* and D-galactose on Catalase activity and GPx activity

4.8.2.1 Catalase activity

Hydrogen peroxide is transformed by catalase into intramolecular oxygen and water. Catalase activity among the groups were observed to be significantly different (F4, 33 = 5.256, P= 0.002, Figure 4.20A). A multiple comparison test (Kruskal-wallis test) showed that D -galactose has significantly lower catalase activity compared to CM (P=0.026) and CMD 90 (P=0.012) groups. However, when CMD 45 (P=0. 69) and Control (P=0.25) groups were compared to D-galactose group, no significant difference was observed.

4.8.2.2 The Glutathione peroxidase (GPx) activity

The GPx (Figure 4.20B), ANOVA results showed a significant difference among the groups (F4, 36= KS statistics 15.11, P=0.0045) with the significant difference observed when the CM group is compared to Control (P=0.043), D-gal (P-0.0030), CMD 45 (P=0.0245) groups. When CM is compared to CMD 90 no significant difference was observed.

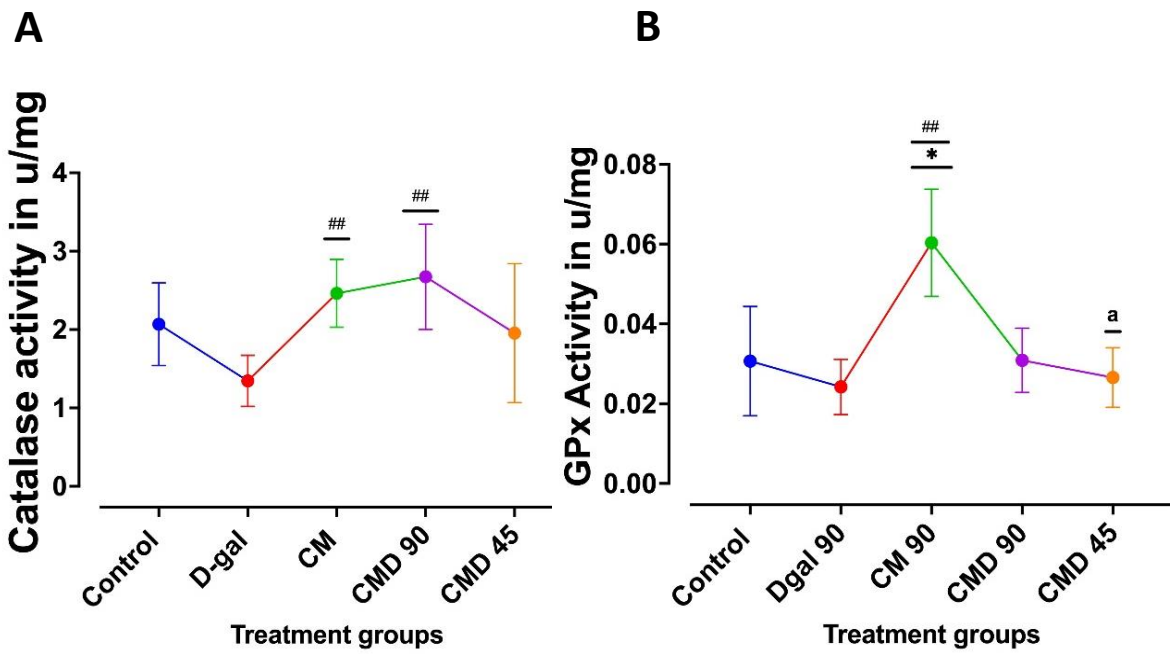

Figure 4.20. The effects of *C.molle* and D-galactose on Catalase activity (A) and Glutathione Peroxidase activity (B).Data represented as mean ± SEM (n=8). Significant difference $^{\#\#}P < 0.01$, $^{\#}P < 0.05$ vs. D-gal,* $P < 0.05$ vs Control, a < 0.05 vs CM.

4.9 Correlations

4.9.1 Correlation between the TNF alpha and Lipid peroxidation (TBARS)

The Pearson correlation analysis between TNF alpha and Lipid peroxidation shown in Figure 4.21 showed positive correlation in levels of TNF alpha and Lipid peroxidation ($r = 0.55$, R^2 0.31, $P < 0.0001$).

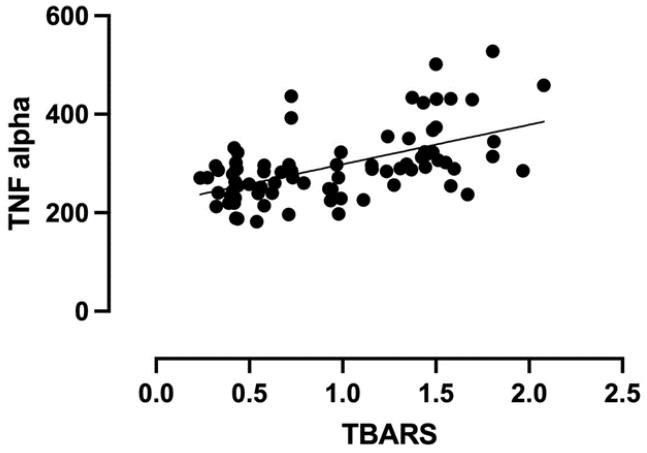

Figure 4.21. Correlations between TBARS and TNF alpha.

4.9.2 Correlation between Tumor Necrosis factor alpha and antioxidant enzymes

4.9.2.1 Correlation between SOD activity, TNF alpha and Lipid peroxidation.

The Pearson correlation analysis between SOD activity, TNF alpha and Lipid peroxidation shown in Figure 4.22 revealed that levels of Lipid peroxidation and SOD activity (r = -0.24, R^2 0.059, P < 0.033; Figure 4.22A) and correlation between levels of TNF alpha and SOD activity (r = -0.39, R^2 = 0.157, P =0.0004; Figure 4.22B) were negatively correlated.

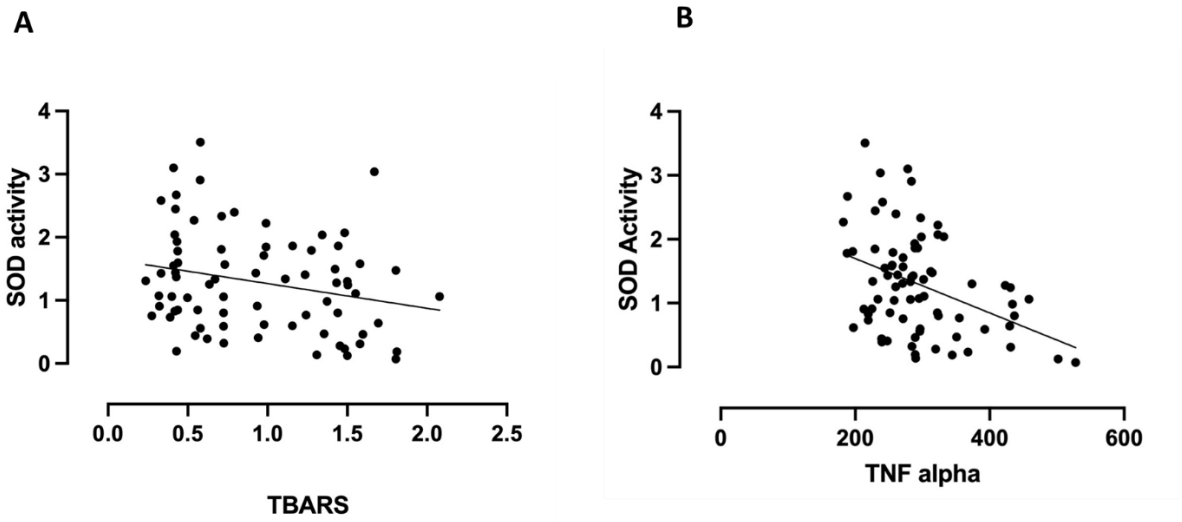

Figure 4.22. The correlation between superoxide activity, TBARS and TNF alpha.

4.9.2.2 The correlation between catalase enzyme, TBARS and TNF alpha.

The Pearson correlation analysis between catalase activity, TNF alpha and Lipid peroxidation shown in Figure 4.22 revealed that levels of Lipid peroxidation and catalase activity ($r = -0.55$, R^2 0.30, $P < 0.0003$; Figure 4.23A) and correlation between levels of TNF alpha and Catalase activity ($r = -0.35$, $R^2 = 0.122$, $P = 0.027$; Figure 4.23B) were negatively correlated.

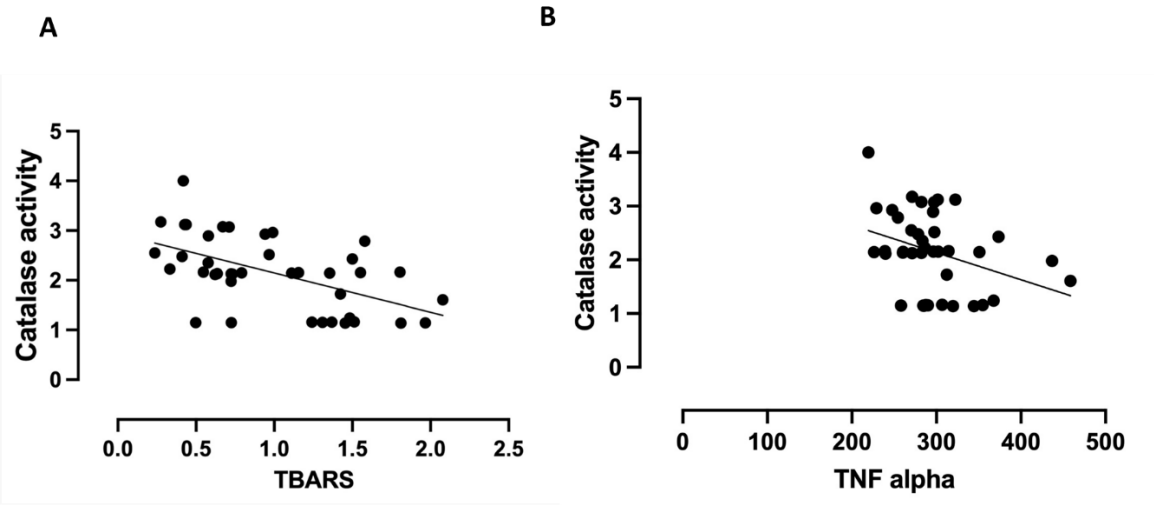

Figure 4.23. Correlation between catalase enzyme, TBARS and TNF alpha.

4.9.2.3 The correlation between Glutathione peroxidase (GPx), GSH, TBARS and TNF alpha.

The Pearson correlation analysis between GPx activity, GSH, TNF alpha and Lipid peroxidation shown in Figure 4.22 revealed that levels of Lipid peroxidation and GPx activity (r = -0.025, R^2 0.0006, P = 0.88; Figure 4.24A) and correlation between levels of TNF alpha and GPx activity (r = -0.33, R^2 = 0.114, P =0.044; Figure 4.24B) were negatively correlated. Also the strong negative correlation between the non-enzymatic antioxidant GSH and lipid peroxidation (r = -0.26, P = 0.12, R^2 = 0.061, Figure 4.22C) and TNF alpha (r = -0.37, P = 0.019, R^2 = 0.14, Figure 4.22D) was observed.

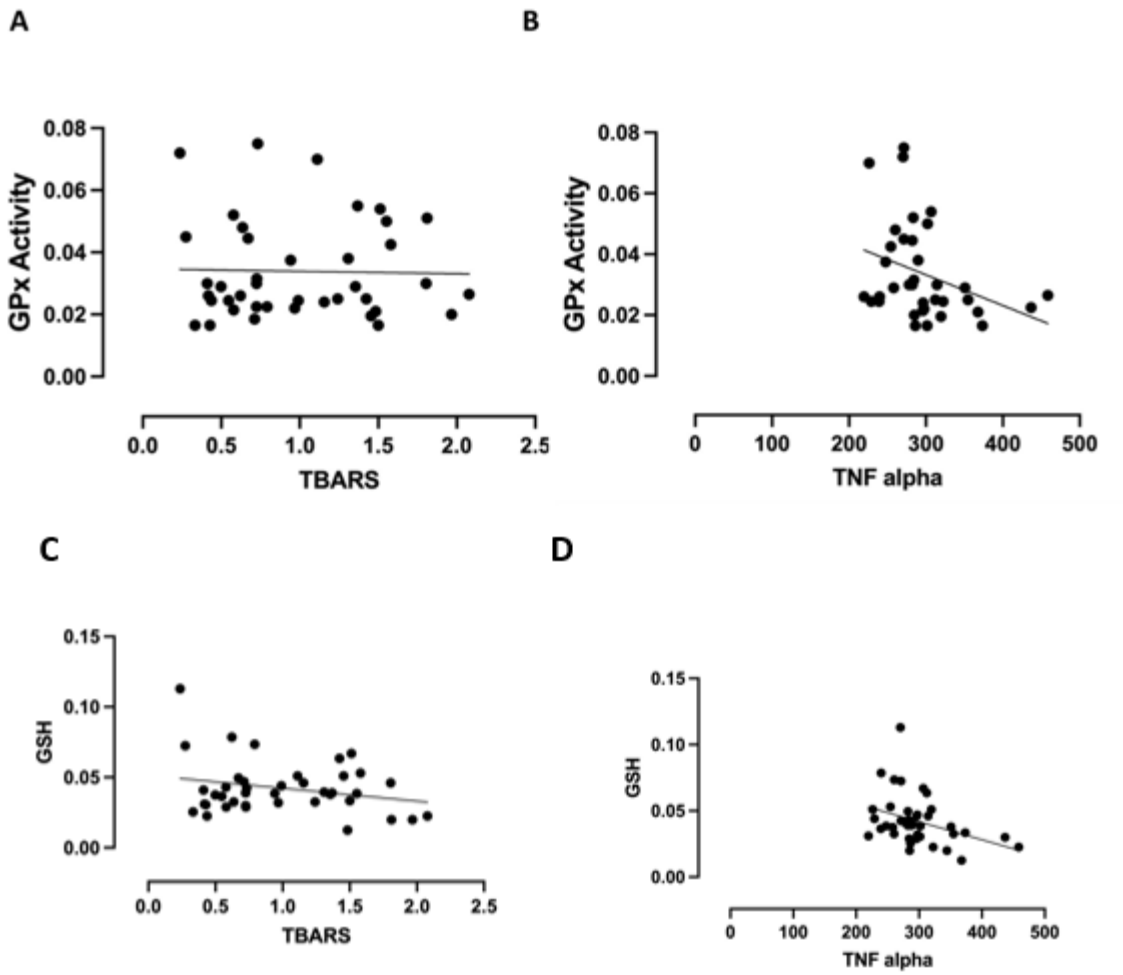

Figure 4.*24*. Correlation between Glutathione peroxidase (GPx), TBARS and TNF alpha (A and B) and correlation between Glutathione (GSH), TBARS and TNF alpha .

4.10 Effects of *C.molle* and D-galactose administration on brain weight

The findings in Table 4.4 revealed that there was no discernible variation in the brain weight. ($F_{4, 25}=1.199$, $P=0.335$). However, the brain coefficients showed significant difference among the groups $F_{4,25} = 7.46$, $P=0.0004$). The multiple comparison test showed that the CM group's brain coefficient was noticeably higher compared to the Control ($P =0.003$), D-gal group $P=0.0027$, CMD 90 group ($P= 0.0206$) and CMD 45 group ($P= 0.0049$).

Table 4.4 Effect of *Combretum molle* and D- galactose administration on brain weight

Treatment Groups	**Brain weight**	**Brain coefficient**
Control	2.25 ± 0.018	0.40 ± 0.0096§§§
D-gal	2.24 ± 0.030	0.41 ± 0.0056§§
CM	2.22 ± 0.094	0.47 ± 0.015
CMD 90	2.15 ± 0.018	0.42 ± 0.0083§
CMD 45	2.21 ± 0.044	0.41 ± 0.0089§§

All data are expressed as mean ± SEM, n = 10. $^{\#}p < 0.05$ or $^{\#\#}p < 0.01$ vs the **Control** group, *****$p < 0.05$ or ******$p < 0.01$ vs **D-galactose only (D-gal)** group, $^{\S}p < 0.05$ or $^{\S\S}p< 0.01$ or $^{\S\S\S}p < 0.001$ vs ***C.molle*** **(CM)** only group.

4.11 Effects of *C. molle* and D-galactose administration on the Hippocampal volumes and the total dentate gyrus

All the treatment groups were represented by the photomicrographs in Figure 4.25. Photomicrograph A represents the control group, B represents D-galactose group, C represents the *C. molle* group, D represents CMD 90 group and E represents the CMD 45 group. The hippocampal volume and Dentate gyrus were measured using Image J software and there was a substantial difference ($F_{4,145} = 3.59$, $P = 0.0079$) in the hippocampus volumes, as shown by the results in Figure 4.26A. The multiple comparison test revealed that the hippocampus volume of the D-gal group was substantially lower ($P=0.0046$) than that of the CM group. The average volumes in Table 4. 29 in Appendix C showed significantly high hippocampal volumes in CM (6.20), CMD 90 (5.57), CMD 45 (5.09), Control (4.78) with D-gal (4.05) having the lowest volumes from all other groups. The average total dentate gyrus volume in Table 4.28 in Appendix C showed CM (2.60), CMD 90 (2.46), CMD 45 (2.43), Control (2.05) had significantly higher volumes ($F_{4,145} = 3.82$, $P = 0.0055$, Figure 4.26B) compared to D-gal group (1.55).

Figure 4.25. Photomicrographs showing the structure of Hippocampus stained with the cresyl violet. The photomicrographs were taken at 2.5x magnification and the scale bar was set at 250 µm. The volumes of the hippocampus (HP) in mm^3 and dentate gyrus (DG) in mm^3 were measured with Image J.

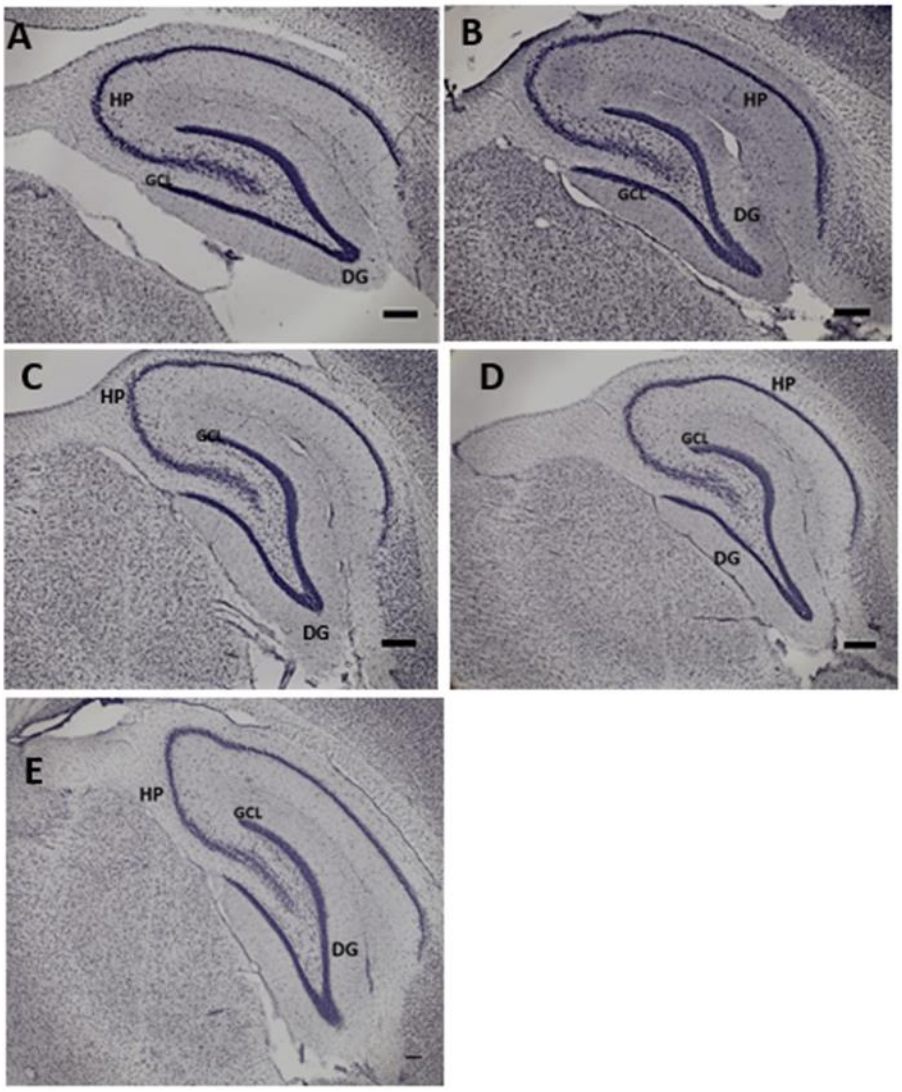
A
HP
GCL
DG
B
HP
GCL
DG
C
HP
GCL
DG
D
HP
GCL
DG
E
HP
GCL
DG

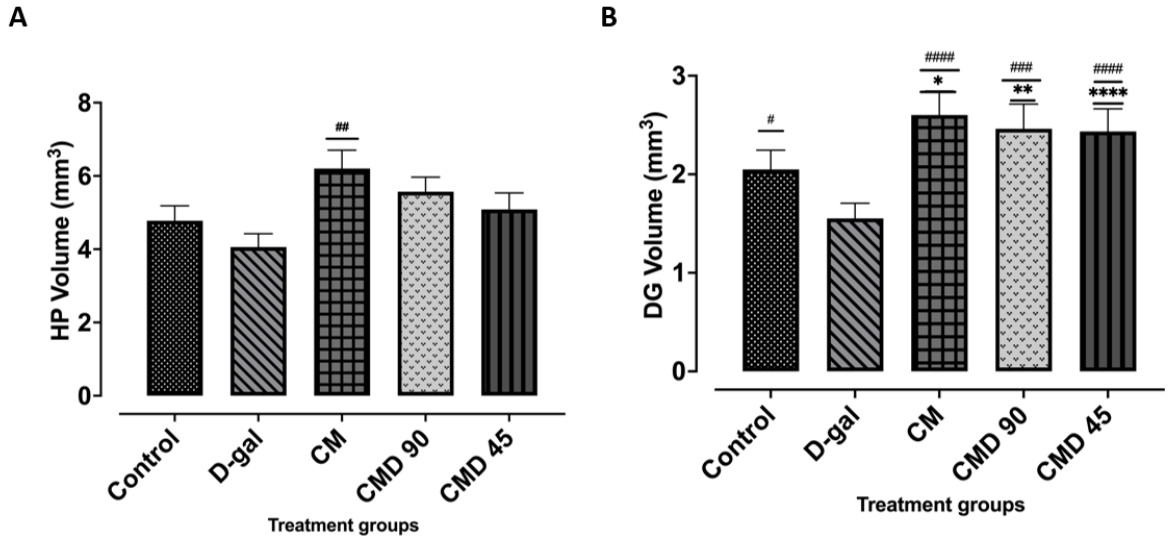

Figure 4.26. The total Hippocampal volume and Dentate Gyrus volume. Data represented as mean ± SEM (n=150). Significant difference set at P< 0,05 was obtained by ANOVA followed by Turkeys multiple comparison test for normally distributed data and were expressed as $^{\#\#\#\#}$P < 0 .0001, $^{\#\#\#}$P <0.001, $^{\#\#}$P < 0.01, $^{\#}$P< 0.05 vs. **D-gal group**; ****P < 0.0001, ***P<0,001, **P< 0.01, *P< 0.05 vs. **Control group**.

4.12 Quantification of Ki-67 Proliferative Cells and Doublecortin Immunoreactive Cells in the Dentate Gyrus of the Hippocampus.

4.12.1 Effects of D-galactose and C. molle on cell proliferation in the SGZ of the Dentate Gyrus

Throughout the cell cycle, except for the resting phase, the Ki-67 protein is expressed. Cell proliferation in the SGZ was measured in this study using Ki-67 immunostaining (Figure 4.27). Most of the groups showed significant variation in cell proliferation ($F_{4,205} = 14,51$; $P < 0,0001$; Figure 4.27). The results in Table 4.31 in Appendix C and figure 4.27 showed that the average number of proliferating cells in the D-gal group (3.8) was significantly lower than the Control group (5.8) ($P = 0,0077$), *C. molle* group (8.4) ($P < 0,0001$) and CMD 90 (8.0) ($P < 0,0001$). Additionally, number of Ki67 proliferative cells was significantly higher in the *C. molle* group ($P = 0,0026$) when compared to control. No significant difference was observed in the CMD 45 (4.8) ($P = 0,1841$) indicating the effect of D-galactose on cell proliferation. Similarly, no significance was observed between the Control and CMD 45 ($P = 0,7638$).

Figure 4.27. Photomicrographs showing the expression Ki67 cells in the dentate gyrus (DG) of the Hippocampi of the five treatment groups. The groups are represented as follows A-B belong to Control group, C-D belong to D-gal group, E-F belong to CM group, G-H belong to CMD 90 group and I-J belong to the CMD 45 group. The Photomicrographs A, C, E, G and I were captured at x10 magnification while photomicrographs B, D, F, H, and J indicated the area marked by box and were captured x40 magnification.

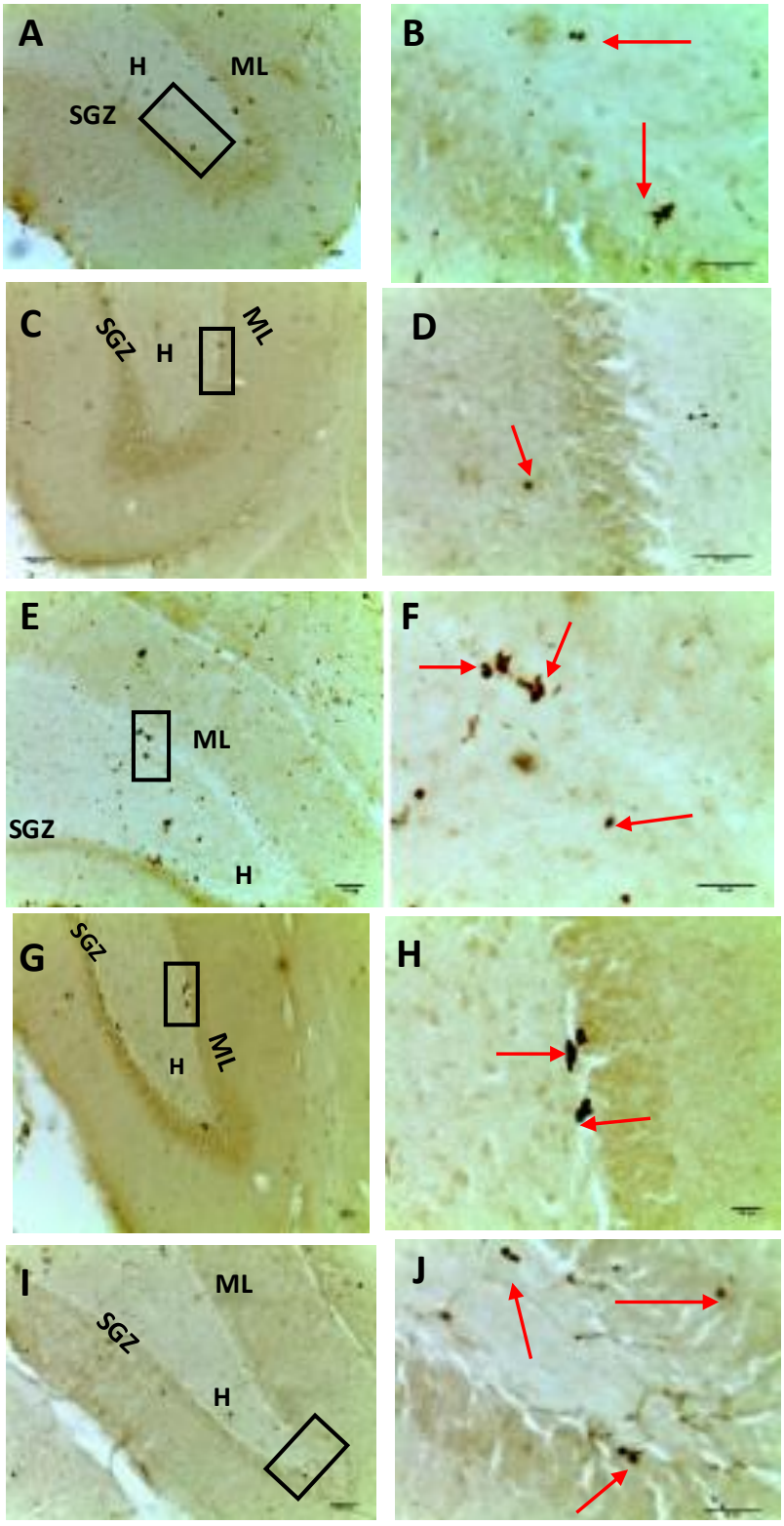
A
H
ML
SGZ
B
C
SGZ
H
ML
D
E
ML
SGZ
H
F
G
SGZ
H
ML
H
I
ML
SGZ
H
J

4.12.2 Quantitative analysis of Ki-67 proliferative cells

Figure 4.28 and Table 4.31 in Appendix C demonstrate a considerably higher number of Ki-67 proliferative cells in the CM (8.3), CMD 90 (8.0), Control (5.8) and CMD 45 (4.8) when compared to the D-gal (3.8). In comparison to the control, The CM ($p< 0.0056$) and CMD 90 ($p< 0.032$) group had a high number of Ki-67 cells while the CMD 45 ($p< 0.62$) was not significantly different. In comparison to the D-gal, The CM and CMD 90 group had significantly higher number of Ki-67 ($p<0.0001$).

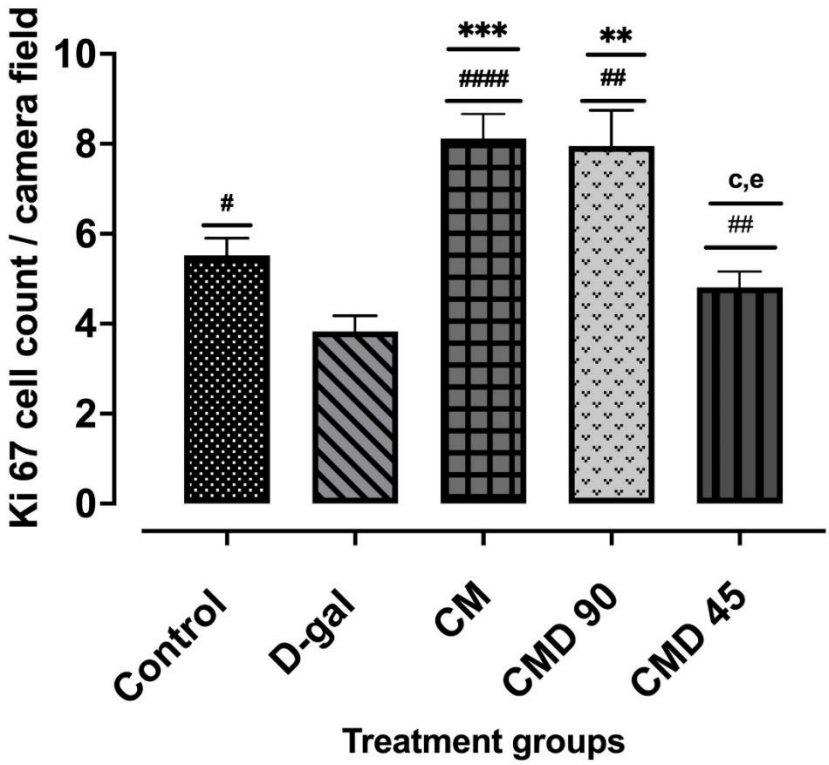

Figure 4.28. Effects of C. molle and D-galactose administration on the number Ki67 proliferative cells in the Dentate Gyrus of the Hippocampus. Data represented as mean ± SEM (n=210) sections. Significant difference expressed as $^{####}P < 0.0001$, $^{###}P < 0.001$, $^{##}P < 0.01$, $^{#}P < 0.05$ vs. **D-gal group**; ***P<0,001, **P< 0.01, *P< 0.05 vs. **Control group**. c < 0.01 vs **CM**; e < 0.001 vs **CMD 90**.

4.12.3 Correlations between Ki-67 proliferative cell count, BDNF and GSH

Figure 4.29 shows the results of a Pearson correlation analysis between the quantity of proliferating Ki-67 cells, BDNF, and GSH. The results revealed the correlation between the number of Ki-67 cells and BDNF ($r = -0.015$, R^2 0.0002, $P = 0.93$; Figure 4.29A) and correlation between the number of Ki-67 cells and GSH ($r = -0.39$, $R^2 = 0.149$, $P = 0.014$; Figure 4.29B) were negatively correlated.

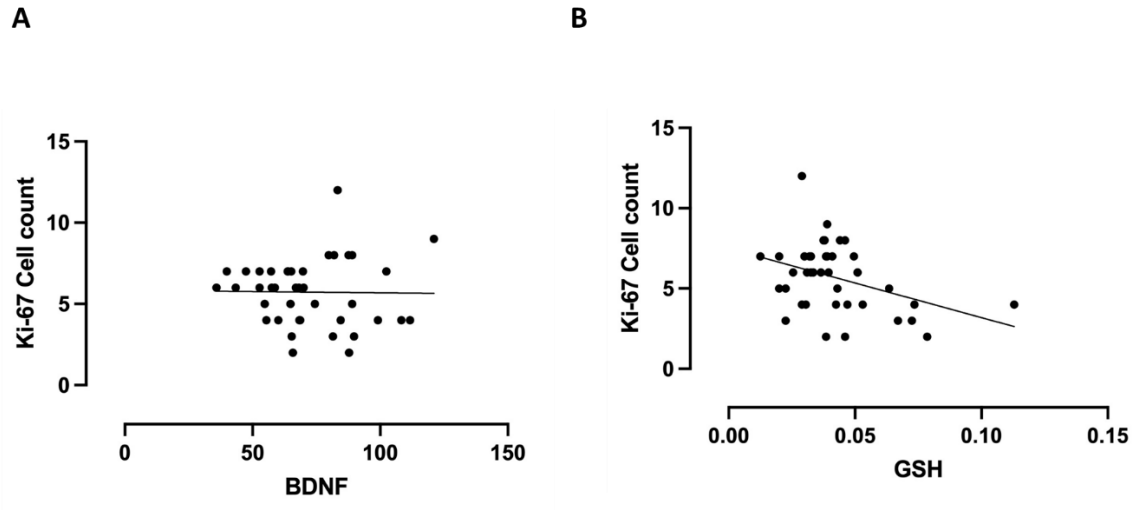

Figure 4.29 Correlations between Ki67 proliferative cell count BDNF and GSH

4.12.4 Qualitative analysis of DCX Immature neurons.

The DCX immunoreactive cells are expressed throughout the dentate gyrus of the hippocampal structure, as shown by the photomicrographs in Figure 4.30 (A-J). The immunoreactive cells were dispersed along the DG's SGZ, with some DCX cells extending their axon and dendrites to the GCL layer while others had an immature axon. The DG of CM (E-F) group had a larger expression of DCX immunoreactive cells than the D-gal (B-C) group, which had less cells that were sparsely dispersed in the SGZ.

Figure 4.30. Photomicrographs showing the expression DCX cells in the dentate gyrus (DG) of the Hippocampi of the five treatment groups. The groups are represented as follows: A – B belong to Control group, C-D belong to D-gal group, E-F belong to CM group, G- H belong to CMD 90 group and I-J belong to the CMD 45 group. The Photomicrographs A, C, E, G and I were captured at x10 magnification while photomicrographs B, D, F, H, and J at x40 magnification.

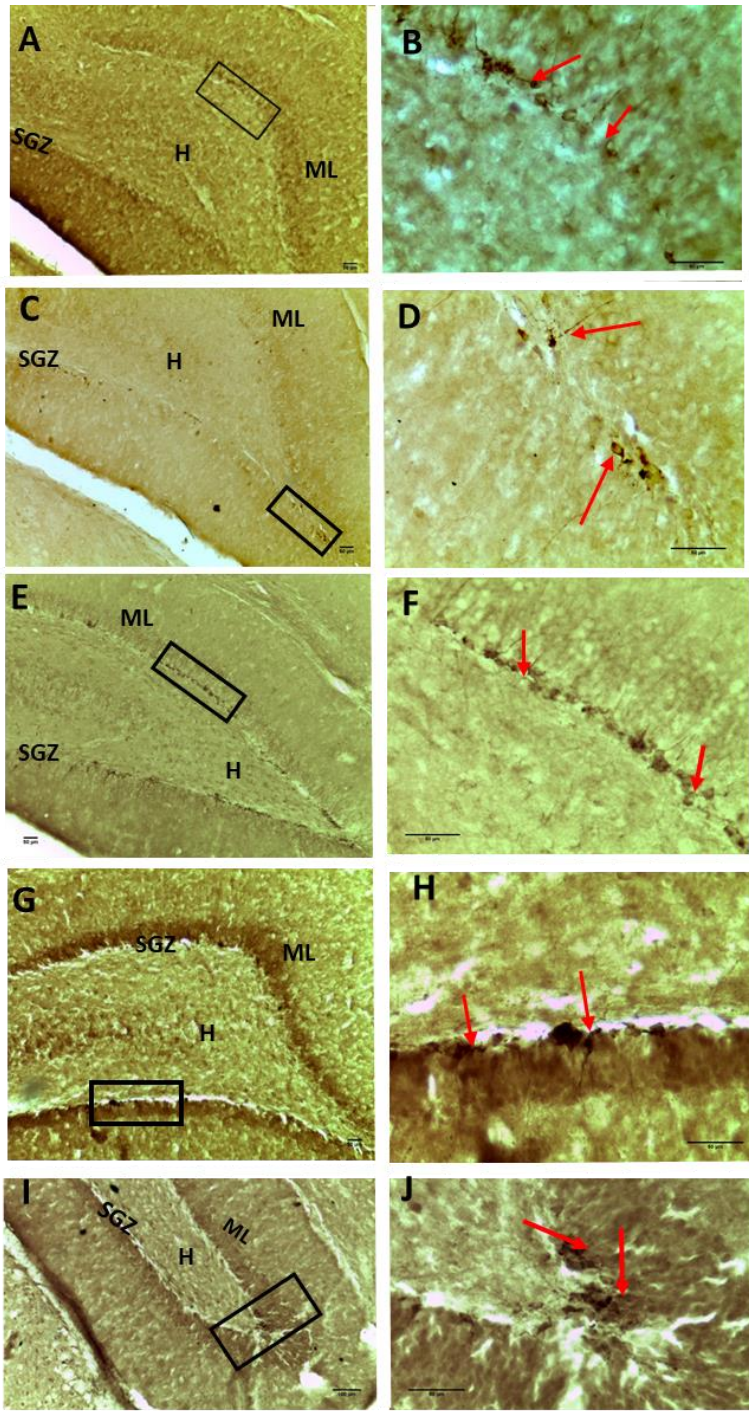
A
SGZ
H
ML
B
C
ML
SGZ
H
D
E
ML
SGZ
H
F
G
SGZ
ML
H
H
I
SGZ
ML
H
J

4.12.5 Quantitative analysis of Immature neurons

Differences in the expression of DCX immunoreactive cells in the dentate gyrus of the hippocampus were shown by the results in Figure 4.31 and Table 4.30 in Appendix C. The number of DCX positive cells in the CM (68.24) group was the highest compared to CMD 90 (51.69), CMD 45 (50.14) with more significantly lower number of cells observed when compared to Control (45.95) ($P = 0.0041$) and D-gal group (32.17) ($P< 0.0001$).

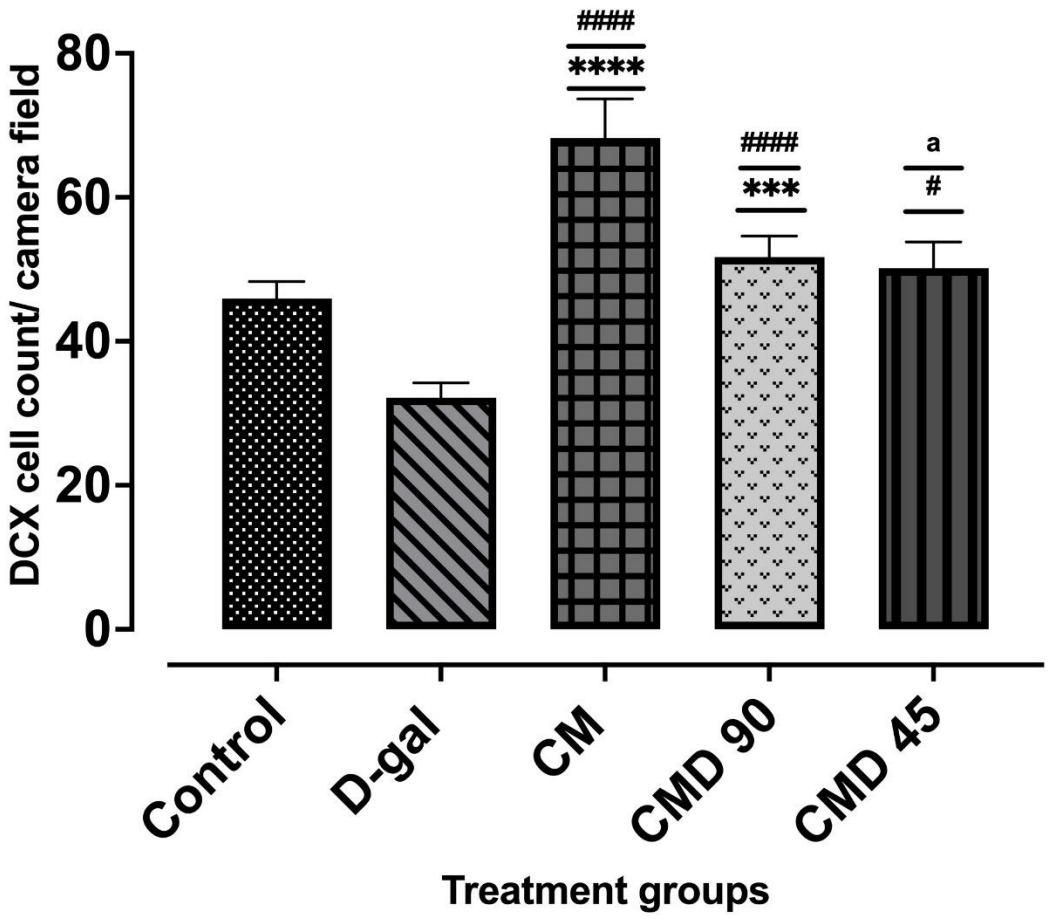

Figure 4.31 Effects of *C. molle* and D-galactose administration on the number of DCX immunoreactive cells in the Dentate Gyrus of the Hippocampus. Data represented as mean ± SEM (n=210) sections. Significant difference expressed as $^{\#\#\#\#}P < 0.0001$, $^{\#\#\#}P < 0.001$, $^{\#\#}P < 0.01$, $^{\#}P < 0.05$ vs. **D-gal group**; ****P < 0.0001, ***P<0,001 vs. **Control group**. a< 0.05 vs **CM**.

4.12.6 Correlations Between the DCX cell count, BDNF and GSH.

The Pearson correlation analysis between the DCX positive cells, BDNF and GSH shown in Figure 4.32. The correlation between DCX cells and BDNF ($r = 0.28$, R^2 0.076, $P = 0.085$; Figure 4.32A) and correlation between the number of DCX cells and GSH ($r = 0.15$, $R^2 = 0.024$, $P = 0.34$; Figure 4.32B) were positively correlated.

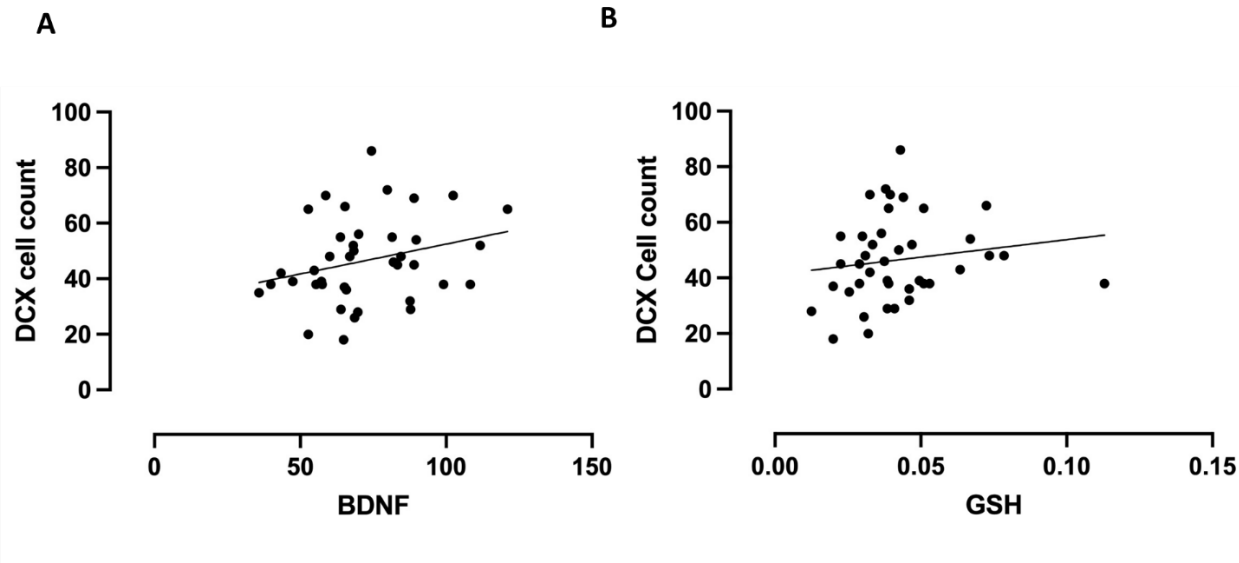

Figure 4.32 Correlations between the DCX cell count, BDNF and GSH

4.12.7 Qualitative analysis of Ki67 proliferative cells in the Subventricular zone of the cerebral cortex

According to the results in Figure 4.33 (A-J) showed the layers of 2 to 3 Ki-67 cells expressed in the SVZ of cerebral cortex. The density of cells was lesser on the D-gal group (B-C) as some areas of the SVZ were devoid of cells compared to the CM, CMD 90 and CMD 45.

Figure 4.33 Photomicrographs showing the expression Ki67 cells in the SVZ of the cortices of all the treatment groups. The groups are represented as follows: A – B belong to Control group, C-D belong to D-gal group, E-F belong to CM group, G- H belong to CMD 90 group and I-J belong to the CMD 45 group. The Photomicrographs A, C, E, G and I were captured at x10 magnification while photomicrographs B, D, F, H, and J at x40 magnification.

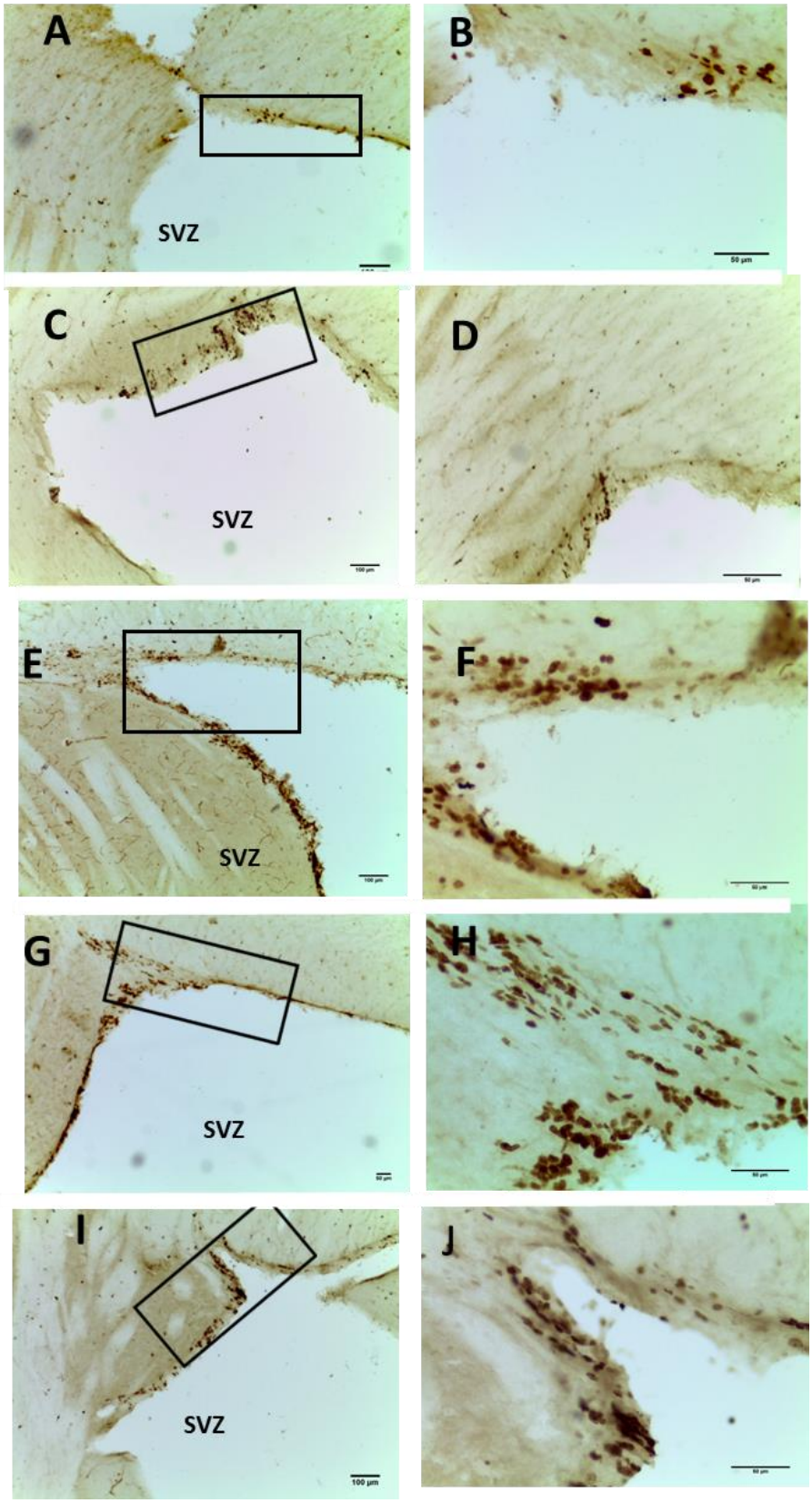
A
SVZ
B
C
SVZ
D
E
SVZ
F
G
SVZ
H
I
SVZ
J

4.12.8 Qualitative analysis of DCX immunoreactive cells in the SVZ of the cerebral cortex

The results as shown in Figure 4.34 (A-J) in SVZ of cerebral cortex of all the treatment groups. There were scantly distributed cells in D-gal compared to the Control (A-B) CM (E-F), CMD 90 (G-H) and CMD 45 (I-J).

Figure 4.34. Photomicrographs showing the expressions DCX immunopositive cells in the SVZ of the cortices of all the treatment groups. The groups are represented as follows: A – B belong to Control group, C-D belong to D-gal group, E-F belong to CM group, G- H belong to CMD 90 group and I-J belong to the CMD 45 group. The Photomicrographs A, C, E, G and I were captured at x10 magnification while photomicrographs B, D, F, H, and J at x40 magnification.

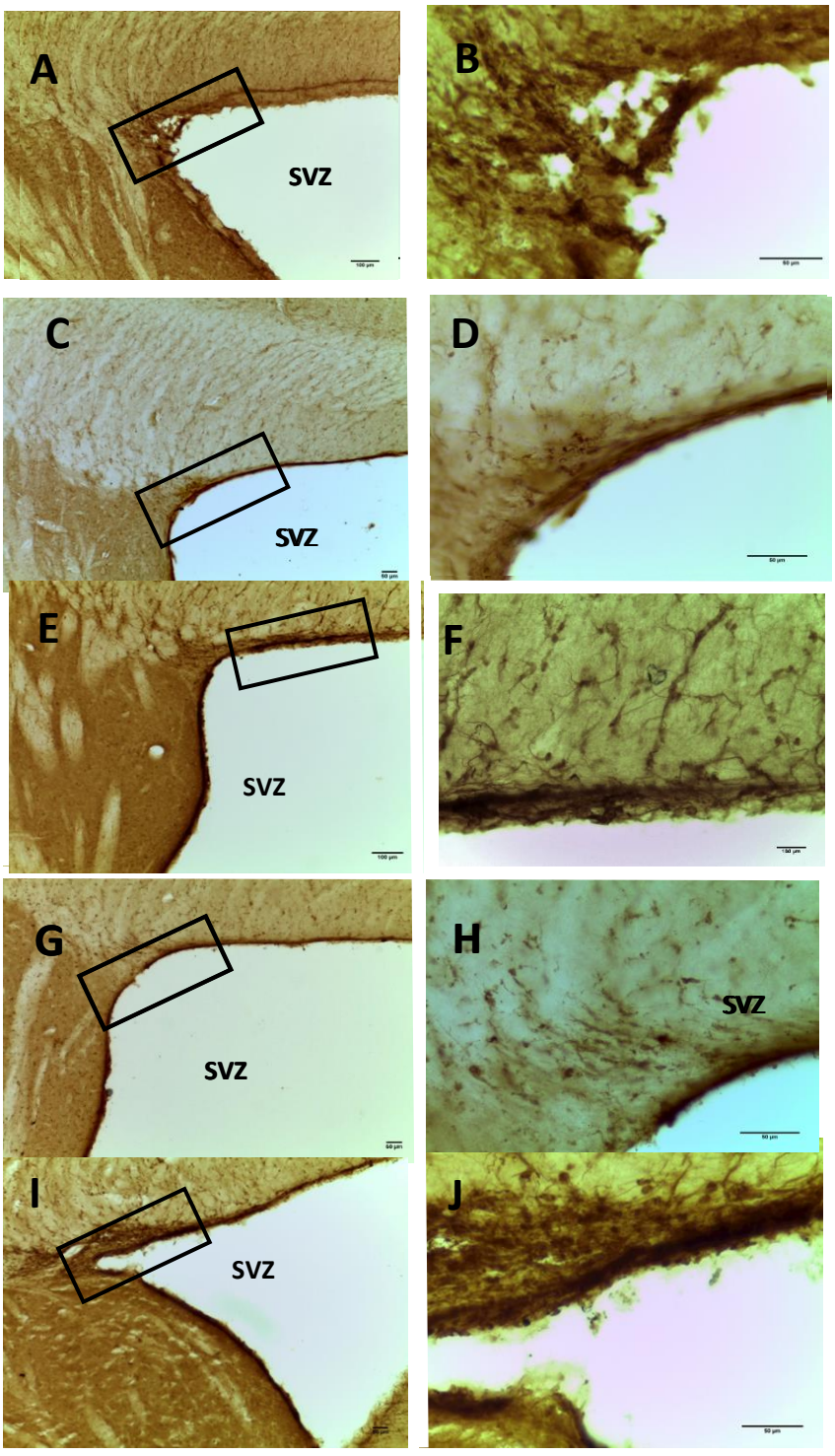
A
SVZ
B
C
SVZ
D
E
SVZ
F
G
SVZ
H
SVZ
I
SVZ
J

5 CHAPTER 5

5.1 DISCUSSION

Aging is a biological process that cannot be halted and is defined by a general and progressive decline in physiological activity. Many age- related changes manifest even in the absence of age-related pathological conditions, hence it is important to differentiate the effects of aging in the absence of ongoing disease from the effects of age-related disease. Screening of natural biologically active antiaging products has gained much momentum in research (Gen-Xiang et al., 2010, Argyropoulou et al., 2013, Yessuf, 2015, Lin et al., 2018, Li et al., 2019, Chen et al., 2022, Liu, 2022). Plant-derived bioactive compounds due to their free radical scavenging capability have been found to protect against various age-related diseases. Traditional African medicine makes considerable use of *Combretum molle (C.molle)* to cure a variety of human afflictions. *Combretum molle* is reported to have abundance of secondary metabolites including flavonoids, saponins, tannins, glycosides and anthraquinones (Bhatnagar et al., 2012, Ntshaka et al., 2020, Hamza et al., 2021). The phytochemical screening of the extract revealed positive secondary metabolites belonging to the flavonoids. Flavonoids are plant polyphenols found in herbs, vegetables, and fruits (Bohm, 1998, Pietta, 2000). Flavonoids are subdivided into different subgroups depending on the attachment of the carbon of the C ring to B ring (Panche et al., 2016).

Astragalin (kaempferol-3-O-β-D-glucoside), Myricetin-3-Galactoside and Quercetin are classified as flavonols while (+)-Catechin is classified as Flavanols (Harborne and Mabry, 2013, Panche et al., 2016, Bohm, 1998). Astragalin (kaempferol 3-glucoside) compound is well known for its diversified pharmacological applications such as anti-inflammatory, antioxidant, neuroprotective, cardioprotective properties by regulating enzymes including AchE and SOD (Riaz et al., 2018, Imraan et al., 2019). A study, revealed that astragalin prevents neurodegeneration by lowering ROS levels, inhibiting lipid peroxidation, and boosting SOD and GPx activities in *C.elegans* (Riaz et al., 2018). Flavanols, like catechins which are substances present in the *C.molle* and are primarily present in beverages like green tea, and are said to have reduced the levels of reactive thiobarbituric acid inC57BL/6J mice as well as averted the decrease in serum glutathione peroxidase and total superoxide dismutase activities (Li et al., 2010). A flavonol glycoside called

hyperoside, which is also present in the C. molle extract, has been shown to raise superoxide dismutase (SOD) levels and reduce malondialdehyde (MDA) levels in the myocardium (Raza et al., 2018).

In this study, the effects of *C. molle'*s antioxidant and neuroprotective activities on the D-galactose-induced rat brain were examined. The Sprague Dawley (SD) rats had their general health checked daily, and they were weighed once a week during the treatment period. There were no appreciable differences in the initial body weights. However, the final body weight was different with the CM and the CMD 90 group having lower body weights compared to the Control, CMD 45 and D-gal groups and the percentage of weight gain were higher in the latter groups than the former. In contrast to the result of this study, reduced final body weights were observed on the D-galactose induced animal models such as the male Kunming mice (Wang et al., 2021, Liu et al., 2018), female Kunming mice (Tang et al., 2013), NMRI mice (Kaviani et al., 2017) and Charles Foster rats (Firdaus et al., 2020). Several investigations on D-galactose induced animal models concurred with the findings of this study as they observed increased weight in their D-gal treated animals and lower weight gain on animals treated with various plant extracts, such as walnut septum extracts (Rusu et al., 2020) raw cacao powder (Yoo and Kim, 2021), *Garnodema lucidum rhodia* compound, (Yuan et al., 2020), malto (*Panax Ginseng extract) (*Shah et al., 2019). The reduced weight gain in the animals administered with *Combretum molle* and the combination treatment might be attributed to the pharmacological action of *C. molle* as reported by Miaffo et al (2014) on the hypo lipidemic properties of the plant which he attributes to the presence of the active secondary metabolites in the *C. molle*. Another possible mechanism might be the antidiabetic activity of the *C.molle* plant played a huge role in the SD rats metabolism, hence prevented the build-up of fats (Miaffo et al., 2014, Miaffo et al., 2019, Hamza et al., 2021).

The SD rat's locomotory activity and non-cognitive behaviour was investigated through the open field test to evaluate the effect of the extract on locomotory activity, the animals were not affected by the extract as they were very active throughout the open field test session. The animals were quite active throughout the open field test session, showing that the extract had no influence on their locomotory and anxiety like behaviours. The

rats' spontaneous physical activity was evaluated using their locomotor activity, which can be influenced by a variety of factors including age, diet, heredity, and the functioning of the hypothalamus (Bolivar et al., 2000, Tatem et al., 2014). In this study line crossing was used to assess the rat's locomotor activity of the and rearing frequency (vertical locomotor and exploring activity). For all treatment groups, there was no statistically significant change in the frequency of line crossing and rearing. The findings of this study agree with the observation by Haider et al (2015) who observed no difference in the locomotor activity on Albino Wistar rat that were administered with high dose of D-galactose and Saline for one week. Although this study was subacute, other Chronic D-galactose induced aging studies such as Wei et al., (2005) who investigated the locomotor activity and behaviour of C57BL/J6 mice following eight weeks of D-galactose subcutaneous injections and reported decreased locomotor activity. A more recent investigation by Prajit et al. (2020) on SD rats fed with D-galactose (50mg/kg/ip) and Chrysin extract observed no significant variation in the locomotor activity. In contrast, Firdaus et al., (2020) observed reduced locomotor activity and exploratory behaviour on D-galactose treated rats. Although aging was a factor in this study, none of the animals spent most of their time not moving, as most of them spent less than 5s in an inactive state (freezing). The findings of this study are the same as the result of a study by Kumar et al., (2011) who reported that chronic administration of D-galactose and *Centella asciatica* (CA) did not influence locomotory activity as compared to the naïve group. In our study, animals spent most of their time moving around the open field maze. If they were stationery, they were involved in grooming themselves. The grooming in the rats plays a role in animal body care (Spruijt et al.,1992). The findings of this study revealed a substantial difference in how each group groomed themselves, with the D-galactose group spending less time grooming themselves than the CM and CMD 90 groups. Similar to our findings, Sun et al., (2007) investigated the effect of Quercetin on behaviour and special memory and reported that animals administered with D-galactose spent less time grooming themselves when compared to animals that received Quercetin. Also, Liu et al., 2018 observed reduction in grooming behaviour in D -galactose induced mouse when compared to mouse administered with walnut seed coat. Grooming behaviour in mammals indicates the animal ability to care for itself. The grooming process is also used

by animals as means cleaning itself, also in cases of wound and getting rid of bacteria and pathogens from its body (Spruijt et al, 1992). Simonelli and Celis, 1999 observed age related changes in grooming behaviour and reported age related decrease in grooming behaviour in old rats, while the young rats show highest grooming behaviour. The findings of this study attribute the reduced grooming in D-galactose group to the effect of accelerated aging induced by D-galactose. Freezing is referred to as immobility in the presence of aversive stimuli, and it is used as an operational measure of fear (Brandao et al., 2008). In this study, there was no discernible difference in freezing behaviour for all the groups, this indicates that there was less fear of the novel environment, and the animals were ready to freely explore.

The NORT and OLT were used to evaluate recognition (non-spatial) and spatial memory respectively. In the current study, non-spatial and spatial cognitive function impairment caused by D-galactose was assessed using NORT and OLT to determine whether C. molle improved the impairment. Recalling prior events or experiences is a component of recognition memory (Tuscher et al., 2014, Denniger et al., 2018) and depends on coordinated function between the hippocampus and cortical areas (Genzel et al., 2019, Hattiangady et al., 2014). The task capitalizes on the rodent's ability to identify a novel object. The NORT was used to evaluate recognition memory by substituting out one of the familiar objects for a brand-new one. According to this study's findings, the animals in the D-gal group had recognition memory impairment as they spent lesser time with the novel object. This was also confirmed by the discrimination index (DI), all the groups were significantly different in comparison to the D-gal groups. The D-gal group's DI was negative while for all other groups was positive. The Discrimination index is often used when the investigators do not set the minimum criteria for active exploration time but instead set a maximum trial time regardless of the amount of active exploration time (Tuscher et al., 2014). In this study maximum trial time (10 minutes) was set to evaluate the total exploration time of the object. Studies on cognitive behaviour indicated that preference for novel object is indicated by positive value (above 0 value) of discrimination index while the preference for familiar object (below 0) and a value of 0 indicated no

preference of either object (Tuscher et al., 2014, Denniger et al., 2018, Genzel et al., 2019). Exploration of object A and B was not significantly different between the groups during the habituation phases of NORT and OLT. During the testing phase, a negative DI was observed in both NORT and OLT for the D-gal group indicating that D-gal was the cause of the deterioration of spatial and non-spatial memory. Additionally, the D-gal group had less than 50% total investigation time (TIT) with the novel object or at the novel location, while for other groups, TIT was significantly more than 50 %. This demonstrates that the animals that received D-gal experienced memory loss both for spatial and non-spatial, but that was reversed for groups that were administered with C. *molle* either at 45 or 90 days.

Similar to our findings, a study by Liu et al., (2018) revealed improved cognition, organ indices, antioxidant enzymes, and decreased body weights in rats given walnut seed coat and kernel. Hawary et al., (2021) for example, found that macadamia nuts and leaves corrected the cognitive impairment caused by D-galactose. Contrary to our results, the study by Wang et al., (2009) reported differences in the object recognition test and object location test in Swiss Albino mice administered with D-galactose and saline. Because the D-galactose-treated mice still spent more time examining the unfamiliar object than the novel one during the object recognition test, the study found that the degree of impairment of novel recognition and object location was not equal. This demonstrated that these mice retained their ability to distinguish between familiar and novel objects using their sample phase recognition memory.

Oxidative stress is brought on by prolonged D-galactose exposure., which leads to mitochondrial malfunction, intracellular neuronal damage, accelerating aging, and affects age-related cognitive decline (Park et al., 2011, Shwe et al., 2017). D-galactose at high dosages efficiently suppresses the expression of the protein associated to nerve growth factors, leading to the degeneration of nerve cells and a reduction in acetylcholine levels in specific brain regions. (Haider et al., 2015, Mehta et al., 2017). Acetylcholinesterase (AChE) is activated by chronic D-galactose treatment, which causes a significant reduction in Ach levels in the brain as a result of cholinergic neuron dysfunction (Mehta et al., 2017., Hyoeun and Hyun-Sook., 2021). By measuring the levels of Ach and AchE

in the cortex and hippocampus, we were able to investigate into the effects on the cholinergic system. In comparison to rats in the D-gal group, the CM and CMD 90 group had higher levels of Ach in their cortex and hippocampus. By measuring the levels of Ach and AchE in the cortex and hippocampus, we were able to gain insight into the effects on the cholinergic system. Comparing the rats in CM and CMD 90 group to the D-gal group, there were higher levels of Ach in the cortex and hippocampus in the CM and CMD 90. The AchE enzyme activity which declines with age in the brain, is one of the key indicators of cholinergic function (Wang et al., 2016). To reverse the deficits in Ach neurotransmission, cholinesterase inhibitors have been used to increase the availability of cortical Ach by inhibiting enzymatic catabolism of Ach. Plant extracts such as *Ginkgo biloba* (Abd-Elhady et al., 2013), Stevia (*Stevia rebaudiana Bertoni*) (Zhao et al., 2019), Piperine (Wang et al., 2020), walnut (Rusu et al., 2020), *Moringa oleifera* (Jamari et al., 2020), Cacao powder (Yoo and Kim., 2021), *Centella asiatica* (Firdaus et al., 2022) and *Sarcococca saligna* (Saleem et al., 2022), were reported to lower acetylcholine esterase in D-galactose induced aging rat and mice models. *C.molle* corrected the D-gal-induced AchE changes at either 45 or 90 days, which is consistent with the findings of the previous studies. The AchE levels were significantly lower in the CM group and CMD 90 in the cortex and hippocampus when compared to D-galactose only group. The findings of this study confirms the *C.molle* ‘s potential as an AchE inhibitor which was initially confirmed by Elufioye et al., (2010) and Dodehe et al (2010) who performed in vitro studies on *C.molle* leaves, and reported its anticholinesterase activity.

The expression of neurotrophic factors, which play a role in neuroprotection and are crucial for the sustained survival and maintenance of neurons, declines throughout brain aging, which compromises neurotropic factors like BDNF (Bathina and Das., 2015, Nam et al., 2019, Molinari et al., 2020). Increased ROS interact with BDNF, resulting in an imbalance that degenerates brain tissue (Lalo et al.,2020). Hippocampus, substantia nigra, amygdala, and frontal cortex are brain regions implicated in aging that are vulnerable to ROS (Yoo et al., 2012). In this study, there were increased levels of BDNF for the *C. molle* (CM) and *C.molle* plus D-galactose (CMD 90) group both in the cortex and hippocampus compared to the D-galactose only (D-gal 90). This confirms that *C.molle* has a potential to be used as a supplement to enhance endogenous BDNF levels

in an aging brain. A study by Molinari et al., (2020) reported that through its receptor TrkB and regulating the expression of apolipoprotein E, exogenous BDNF (BDNF SKA) is able to stimulate the synthesis of endogenous BDNF in the body on its own. Results of Another study by Wu et al., (2020) reported that chronic subcutaneous perfusion of BDNF reversed microglial activation which is a factor in the etiology of numerous neurodegenerative diseases. The mechanism of how the *C.molle* enhance the endogenous BDNF levels is yet to be understood. According to a Nam et al., (2014) study, plant compounds, such as *Curcumin Longa*, raised BDNF levels and counteracted the effects of D-galactose-induced aging.

The production of excessive oxygen species induces cellular damage which accelerates aging (von Bernhardi et al., 2010). D-galactose increase leads to imbalance between reactive oxygen species regeneration and clearance eventually to functional decline in the brain tissue. Brain GSH reduces in aging which eventually causes a decline in endogenous protection against free radicals. GSH is synthesised by conjugation of glutamate on cysteine (Ghosh et al.,2014). The levels of GSH were observed to be increased in the CM and CMD 90. The *C.molle* may have activated GSH synthesis pathway by adding cysteine into the pathway. Various studies demonstrated that high levels of D-galactose cause reduction in SOD, GSH and catalase activity (Anand et al., 2012, Wang et al., 2012, Kaviani et al, 2017; Shah et al., 2019, Yuan et al., 2020; Rusu et al., 2020). MDA the key indicator of oxidative damage which enhances the generation of reactive oxygen species (ROS) indirectly. Another important antioxidant enzyme Glutathione peroxidase which originates from unsaturated fatty acids due to is formed when the GSH is oxidised by Hydrogen peroxide in the GSH transporter system (Ighodaro and Akinloye, 2018). In this study, the CM and CMD 90 groups had significantly higher levels of SOD, GPx, and catalase in the brain tissue, with SOD and GPx activity being much higher in the CM group. This indicates that CM alone is protective against effects of aging, also the combination treatment CMD 90 showed that *C.molle* can reverse the effects of aging brought on by D-galactose. Various studies have shown that plant-based extracts have proven to be effective in ameliorating the effects of D-galactose induced oxidative stress by increasing brain antioxidant capacity. Studies such as Anand et al., (2012) used Chrysin against D-galactose oxidative stress, Sun et al., (2007) used

Quercetin to enhance brain antioxidant capacity. Wang et al., 2012 used *Colla corii asini* and reported it to improve antioxidant activities and reduce MDA in mice. More recent study by Sha et al., (2019) demonstrated that Maltol and the co-treatment of Maltol and D-galactose increased GSH levels, CAT and SOD activities and reduced MDA on D-galactose induced aging. The effects of aging by D-galactose significantly increased MDA, the product of oxidative stress, compared with animals that were administered with *C.molle* (CM) and *C.molle* plus D-galactose (CMD 90) groups for 45 or 90 days. MDA levels were significantly decreased in the cortex and in the hippocampus when compared to D-galactose groups. The correlation analysis between the levels of lipid peroxidation and antioxidant enzymes revealed a strong negative correlation between the antioxidant enzymes SOD and CAT including the non-enzymatic antioxidant GSH. However, for the GPx a weak negative correlation was observed.

Prolonged activity of proinflammatory cytokines is known to negatively affect cellular functions and structures. Proinflammatory cytokines such as TNF- alpha are associated with neurodegenerative disorders (Cutter et al., 2020). TNF alpha inhibitors are used for treatment inflammatory conditions (Macdonalds et al., 2003). The results of this study showed elevated levels of TNF alpha in the cortex and hippocampus of D-gal group compared to other groups. In the hippocampus, the CMD 45 group had significantly higher levels of TNF alpha compared to the control, CM and CMD 90 but lower than that of D-gal group. This shows that the administration of the *C.molle* after induction with D-gal 45 days was improved. The correlation analysis between the levels of TNF alpha revealed a strong negative correlation between the antioxidant enzymes SOD, CAT and GPx including the non-enzymatic antioxidant GSH. A research report by Naude et al., (2014) revealed that deletion of TNFR 2 impairs novel object recognition, spatial memory recognition motor performance and can increase anxiety-like behaviour in young adult mice whereas in aged mice impairment of recognition and spatial memory was observed both in TNFR1 and TNFR 2 deletion. In our study rats that had high levels of TNF had impairment of both recognition memory and spatial memory as revealed by the results of NORT and OLT respectively. Another report on human subjects revealed that TNF-α were longitudinally associated with declines in gray matter volume (Cutter et al., 2020). In our study animals administered with D-gal showed the highest level of TNF-α and the lowest

hippocampal and dentate gyrus volume compared to other groups. Which suggests that the D-galactose contributed to the decline in the size of the hippocampus and dentate gyrus.

Memory is strongly affected by neurogenesis, which takes place in the SGZ of the DG and SVZ of the cortex. This phenomenon is linked to the self-renewal of new mature neurons and neural stem cells (NSCs) in the SGZ. (Klempin and Kempermann, (2007), Ihunwo and Pillay, 2007). All phases of cell division, excluding the G0 phase, are marked by an increase in the protein Ki-67, suggesting that this protein is connected to cell proliferation (Murray et al, 2020). DCX, a protein that controls microtubules and the actin skeleton in neuronal cell migration, is only expressed by immature neurons. In this study, different phases of neurogenesis were assessed using the markers Ki-67 and DCX (cell proliferation and immature neurons, respectively. According to various studies, D-gal reduces neurogenesis by raising oxidative stress (Cui et al., 2006, Yoo et al., 2012, Zhu et al., 2014, Chen et al., 2018, Nam et al., 2019, Prajit et al., 2020, Mahdi et al., 2021., Saenno et al., 2022). The results of the current investigation showed that D-gal reduced neurogenesis, as seen by drops in the percentages of DCX-and Ki-67-positive cells in the D-gal group. Studies reported that D-gal promotes lipid peroxidation, which destroys Ki-67 and DCX (Shah et al ., 2019, Prajit et al., 2020). D-gal impaired antioxidant enzyme activities and decreases cell proliferation (Awaei et al., 2021 and Wang et al., 2020). In this study, the rates of adult neurogenesis in the *C. molle*-treated groups were significantly higher than those in the Control and D-galactose groups. Compared to the D-gal group, the DG of the CM and CMD 90 group had a higher expression of DCX and Ki-67 immunoreactive cells. Ki-67 cell expression was comparable between CMD 90 and CMD45, decreased when compared to the *C. molle* alone group, but elevated when compared to the D-gal group. Comparatively to the other groups, the D-galactose group showed the lowest expression of Ki-67 immunoreactive cells in the subventricular zone. In the SVZ of the D-gal, neither interneurons nor DCX cells were found. The correlation analysis revealed a strong positive correlation between the rate of DCX cells, BDNF and GSH, however for the Ki-67 cell count a weak negative correlation was observed when compared to BDNF levels with a strong negative correlation when compared to GSH. This

suggests that both BDNF and GSH do not have strong association with the levels of immature neurons but not with Ki-67 proliferative cells.

The majority of *C.molle* investigations were in vitro and concentrated on the toxicity and phytochemical content of different *C.molle* extracts. *Curcumin Longa* reversed the effects of D-galactose-induced aging by boosting cell proliferation and neuroblast differentiation in adult mice, according to studies on other plant material, such as the study by (Nam et al., 2019). These findings concur with ours, supporting the notion that *C. molle* protect against D-galactose-induced aging.

6 CHAPTER 6

6.1 6.1 CONCLUSIONS

This investigation proved that *C. molle* offers defence against memory loss. D-gal administration caused cognitive deficits in the animals, while *C. molle* co-treatment lessened these deficits. Moreover, we discovered no variations in the groups' locomotor activity, indicating that the animals were not physically hindered from conducting the behavioural assessments. The rate of weight gain was not as rapid in the animals that were administered with *C.molle* at 90 days (CM and CMD 90) despite the animals feeding behaviour. This suggest that *C.molle* had a role in suppression of fat build up in the animals. By lowering MDA levels and enhancing the antioxidant enzyme activities of SOD, CAT, and GPx, as well as non-enzymatic antioxidants like GSH, the *C. molle* proved successful in preventing the formation of oxidative stress. Additionally, treatment of *C. molle* shown promising potential as an AchE inhibitor, enhancing cholinergic neurotransmission by decreasing AchE activity and increasing Ach levels.

In this study, endogenous BDNF levels were found to be higher in the animal groups given *C. molle*, which is crucial for the survival and maintenance of neurons. As a final finding, this study also found that co-treatment with *C. molle* for 45 or 90 days was effective in reducing the impairment of adult neurogenesis induced by D-gal, as seen by the increased proliferation of cells, immature neurons, the dentate gyrus and hippocampal volumes.

6.2 Limitation to the study

The rate of cell death was not ascertained because caspase 3 and TUNNEL antibodies did not produce positive results across all the groups despite following the manufacturer's protocol and using various dilutions during optimization. Most of research done on *C.molle* is mostly in vitro studies hence it is was difficult to compare most of our results with what is existing in the literature.

7 REFERENCES

ABD-ELHADY, R. M., ELSHEIKH, A. M. & KHALIFA, A. E. 2013. Anti-amnestic properties of Ginkgo biloba extract on impaired memory function induced by aluminum in rats. *International journal of developmental neuroscience,* 31**,** 598-607.

ADEWUNMI, C. O. & OJEWOLE, J. A. O. 2004. Safety of traditional medicines, complementary and alternative medicines in Africa. *African journal of traditional, complementary and alternative medicines,* 1**,** 1-3.

ALCALÁ-BARRAZA, S. R., LEE, M. S., HANSON, L. R., MCDONALD, A. A., FREY, W. H. & MCLOON, L. K. 2010. Intranasal delivery of neurotrophic factors BDNF, CNTF, EPO, and NT-4 to the CNS. *Journal of drug targeting,* 18**,** 179-190.

ALTMAN, J. 1969. Autoradiographic and histological studies of postnatal neurogenesis. IV. Cell proliferation and migration in the anterior forebrain, with special reference to persisting neurogenesis in the olfactory bulb. *Journal of Comparative Neurology,* 137**,** 433-457.

ALY, H. F., METWALLY, F. M. & AHMED, H. H. 2011a. Neuroprotective effects of dehydroepiandrosterone (DHEA) in rat model of Alzheimer's disease. *Acta Biochimica Polonica,* 58.

ALY, H. F., METWALLY, F. M. & AHMED, H. H. 2011b. Neuroprotective effects of dehydroepiandrosterone (DHEA) in rat model of Alzheimer's disease. *Acta Biochim Pol,* 58**,** 513-20.

ANAND, K. V., MOHAMED JAABIR, M. S., THOMAS, P. A. & GERALDINE, P. 2012. Protective role of chrysin against oxidative stress in d-galactose-induced aging in an experimental rat model. *Geriatrics & gerontology international,* 12**,** 741-750.

ARANCIBIA, S., SILHOL, M., MOULIÈRE, F., MEFFRE, J., HÖLLINGER, I., MAURICE, T. & TAPIA-ARANCIBIA, L. 2008. Protective effect of BDNF against beta-amyloid induced neurotoxicity in vitro and in vivo in rats. *Neurobiology of disease,* 31**,** 316-326.

ARGYROPOULOU, A., ALIGIANNIS, N., TROUGAKOS, I. P. & SKALTSOUNIS, A.-L. 2013. Natural compounds with anti-ageing activity. *Natural product reports,* 30**,** 1412-1437.

AYDıN, A. F., ÇOBAN, J., DOĞAN-EKICI, I., BETÜL-KALAZ, E., DOĞRU-ABBASOĞLU, S. & UYSAL, M. 2016a. Carnosine and taurine treatments diminished brain oxidative stress and apoptosis in D-galactose aging model. *Metab Brain Dis,* 31**,** 337-45.

AYDıN, A. F., ÇOBAN, J., DOĞAN-EKICI, I., BETÜL-KALAZ, E., DOĞRU-ABBASOĞLU, S. & UYSAL, M. 2016b. Carnosine and taurine treatments diminished brain oxidative stress and apoptosis in D-galactose aging model. *Metabolic brain disease,* 31**,** 337-345.

AYDıN, A. F., ÇOBAN, J., DOĞAN-EKICI, I., BETÜL-KALAZ, E., DOĞRU-ABBASOĞLU, S. & UYSAL, M. 2016c. Carnosine and taurine treatments diminished brain oxidative stress and apoptosis in D-galactose aging model. *Metabolic brain disease,* 31**,** 337-345.

AZMAN, K. F. & ZAKARIA, R. 2019. D-Galactose-induced accelerated aging model: an overview. *Biogerontology,* 20**,** 763-782.

BABB, D. A., PEMBA, L., SEATLANYANE, P., CHARALAMBOUS, S., CHURCHYARD, G. J. & GRANT, A. D. 2007. Use of traditional medicine by HIV-infected individuals in South Africa in the era of antiretroviral therapy. *Psychology, health & medicine,* 12**,** 314-320.

BARONCELLI, L., BRASCHI, C., SPOLIDORO, M., BEGENISIC, T., SALE, A. & MAFFEI, L. 2010. Nurturing brain plasticity: impact of environmental enrichment. *Cell Death & Differentiation,* 17**,** 1092-1103.

BATHINA, S. & DAS, U. N. 2015. Brain-derived neurotrophic factor and its clinical implications. *Archives of Medical Science,* 11**,** 1164-1178.

BHATNAGAR, S., SAHOO, S., MOHAPATRA, A. K. & BEHERA, D. R. 2012. Phytochemical analysis, antioxidant and cytotoxic activity of medicinal plant Combretum roxburghii (Family: Combretaceae). 4**,** 193-202.

BOHM, B. A. 1998. *Introduction to flavonoids*, Harwood academic publishers.

BRUNO, S. & DARZYNKIEWICZ, Z. 1992. Cell cycle dependent expression and stability of the nuclear protein detected by Ki-67 antibody in HL-60 cells. *Cell proliferation,* 25**,** 31-40.

BUDNI, J., PACHECO, R., DA SILVA, S., GARCEZ, M. L., MINA, F., BELLETTINI-SANTOS, T., DE MEDEIROS, J., VOSS, B. C., STECKERT, A. V. & DA SILVA VALVASSORI, S. 2016. Oral administration of d-galactose induces cognitive impairments and oxidative damage in rats. *Behavioural brain research,* 302**,** 35-43.

CACCI, E., CLAASEN, J. H. & KOKAIA, Z. 2005. Microglia-derived tumor necrosis factor-α exaggerates death of newborn hippocampal progenitor cells in vitro. *Journal of neuroscience research,* 80**,** 789-797.

CAI, N., WU, Y. & HUANG, Y. 2022. Induction of accelerated aging in a mouse model. *Cells,* 11**,** 1418.

CAMERON, H. A. & MCKAY, R. D. 2001. Adult neurogenesis produces a large pool of new granule cells in the dentate gyrus. *Journal of comparative neurology,* 435**,** 406-417.

CARDOSO, A., MAGANO, S., MARRANA, F. & ANDRADE, J. P. 2015. d-Galactose high-dose administration failed to induce accelerated aging changes in neurogenesis, anxiety, and spatial memory on young male Wistar rats. *Rejuvenation research,* 18**,** 497-507.

CAROCHO, M. & FERREIRA, I. C. 2013. A review on antioxidants, prooxidants and related controversy: natural and synthetic compounds, screening and analysis methodologies and future perspectives. *Food Chem Toxicol,* 51**,** 15-25.

CHEN, H., DONG, L., CHEN, X., DING, C., HAO, M., PENG, X., ZHANG, Y., ZHU, H. & LIU, W. 2022. Anti-aging effect of phlorizin on D-galactose–induced aging in mice through antioxidant and anti-inflammatory activity, prevention of apoptosis, and regulation of the gut microbiota. *Experimental Gerontology,* 163**,** 111769.

CHU, W.-M. 2013. Tumor necrosis factor. *Cancer letters,* 328**,** 222-225.

CRAMER, S. C., SUR, M., DOBKIN, B. H., O'BRIEN, C., SANGER, T. D., TROJANOWSKI, J. Q., RUMSEY, J. M., HICKS, R., CAMERON, J. & CHEN, D. 2011. Harnessing neuroplasticity for clinical applications. *Brain,* 134**,** 1591-1609.

CUI, X., WANG, L., ZUO, P., HAN, Z., FANG, Z., LI, W. & LIU, J. 2004. D-galactose-caused life shortening in Drosophila melanogaster and Musca domestica is associated with oxidative stress. *Biogerontology,* 5**,** 317-325.

CUI, X., ZUO, P., ZHANG, Q., LI, X., HU, Y., LONG, J., PACKER, L. & LIU, J. 2006. Chronic systemic D-galactose exposure induces memory loss, neurodegeneration, and oxidative damage in mice: Protective effects of R-α-lipoic acid. *Journal of neuroscience research,* 83**,** 1584-1590.

CURRAIS, A. & MAHER, P. 2013. Functional consequences of age-dependent changes in glutathione status in the brain. *Antioxidants & redox signaling,* 19**,** 813-822.

DEI, R., TAKEDA, A., NIWA, H., LI, M., NAKAGOMI, Y., WATANABE, M., INAGAKI, T., WASHIMI, Y., YASUDA, Y., HORIE, K., MIYATA, T. & SOBUE, G. 2002. Lipid peroxidation and advanced glycation end products in the brain in normal aging and in Alzheimer's disease. *Acta Neuropathologica,* 104**,** 113-122.

DENNINGER, J. K., SMITH, B. M. & KIRBY, E. D. 2018. Novel object recognition and object location behavioral testing in mice on a budget. *JoVE (Journal of Visualized Experiments)***,** e58593.

DONG, Y., DEKENS, D. W., DE DEYN, P. P., NAUDÉ, P. J. & EISEL, U. L. 2015. Targeting of tumor necrosis factor alpha receptors as a therapeutic strategy for neurodegenerative disorders. *Antibodies,* 4**,** 369-408.

DORSZEWSKA, J. 2013. Cell biology of normal brain aging: synaptic plasticity–cell death. *Aging clinical and experimental research,* 25**,** 25-34.

DOUGLASS, R. 2015. The aging of Africa: Challenges to African development. *African Journal of Food, Agriculture, Nutrition and Development,* 16**,** 1-15.

ELOFF, J., KATERERE, D. & MCGAW, L. 2008. The biological activity and chemistry of the southern African Combretaceae. *Journal of Ethnopharmacology,* 119**,** 686-699.

ERICKSON, K. I., PRAKASH, R. S., VOSS, M. W., CHADDOCK, L., HEO, S., MCLAREN, M., PENCE, B. D., MARTIN, S. A., VIEIRA, V. J. & WOODS, J. A. 2010. Brain-derived neurotrophic factor is associated with age-related decline in hippocampal volume. *Journal of Neuroscience,* 30**,** 5368-5375.

FATTMAN, C. L., SCHAEFER, L. M. & OURY, T. D. 2003. Extracellular superoxide dismutase in biology and medicine. *Free Radical Biology and Medicine,* 35**,** 236-256.

FIGIEL, I. 2008. Pro-inflammatory cytokine TNF-alpha as a neuroprotective agent in the brain. *Acta Neurobiol Exp (Wars),* 68**,** 526-534.

FIRDAUS, Z., SINGH, N., PRAJAPATI, S. K., KRISHNAMURTHY, S. & SINGH, T. D. 2022. Centella asiatica prevents D-galactose-Induced cognitive deficits, oxidative stress and neurodegeneration in the adult rat brain. *Drug and Chemical Toxicology,* 45**,** 1417-1426.

FLOYD, R. A. & HENSLEY, K. 2002. Oxidative stress in brain aging: Implications for therapeutics of neurodegenerative diseases. *Neurobiology of Aging,* 23**,** 795-807.

FUCHS, E. & FLÜGGE, G. 2014. Adult neuroplasticity: more than 40 years of research. *Neural plasticity,* 2014.

GEN-XIANG, M., HONG-BIN, D., LONG-GUO, Y., DIAN-DONG, L., LI, Y.-Y. Y. & ZHEN, W. 2010. Protective role of salidroside against aging in a mouse model induced by D-galactose. *Biomedical and Environmental Sciences,* 23**,** 161-166.

GHOSH, D., LEVAULT, K. R. & BREWER, G. J. 2014. Relative importance of redox buffers GSH and NAD (P) H in age-related neurodegeneration and Alzheimer disease-like mouse neurons. *Aging cell,* 13**,** 631-640.

GU, F., CHAUHAN, V. & CHAUHAN, A. 2015. Glutathione redox imbalance in brain disorders. *Current Opinion in Clinical Nutrition & Metabolic Care,* 18**,** 89-95.

GYASI, R. M. & PHILLIPS, D. R. 2020. Aging and the rising burden of noncommunicable diseases in sub-Saharan Africa and other low-and middle-income countries: a call for holistic action. *The Gerontologist,* 60**,** 806-811.

HAIDER, S., LIAQUAT, L., SHAHZAD, S., SADIR, S., MADIHA, S., BATOOL, Z., TABASSUM, S., SALEEM, S., NAQVI, F. & PERVEEN, T. 2015. A high dose of short term exogenous d-galactose administration in young male rats produces symptoms simulating the natural aging process. *Life Sciences,* 124**,** 110-119.

HAIDER, S., SALEEM, S., PERVEEN, T., TABASSUM, S., BATOOL, Z., SADIR, S., LIAQUAT, L. & MADIHA, S. 2014. Age-related learning and memory deficits in rats: role of altered brain neurotransmitters, acetylcholinesterase activity and changes in antioxidant defense system. *Age,* 36**,** 9653.

HAIDER SAIDA, SALEEM SADIA, PERVEEN TAHIRA, TABASSUM SAIQA, BATOOL ZEHRA, SADIR SADIA, LIAQUAT LARAIB & SYEDA, M. 2014 Age-related learning and memory deficits in rats: role of altered brain neurotransmitters, acetylcholinesterase activity and changes in antioxidant defense system. *Age* 36**,** 9653-.

HAMZA, R. Z., AL-BAQAMI, N. M., KHOJAH, E., MANSOUR, A. M., E. AL-MOTAANI, S., A. AL-SALMI, F. & EL-MEGHARBEL, S. M. 2021. Possible Antioxidant and Antidiabetic Effects of Combretum Molle Extract in a Diabetes Mellitus Experimental Model in Male Rats. *Natural Product Communications,* 16**,** 1934578X211043964.

HARBORNE, J. B. & MABRY, T. J. 2013. The flavonoids: advances in research.

HE, W., ABODERIN, I. & ADJAYE-GBEWONYO, D. 2020. Africa aging: 2020. US Government Printing Office.

HERMES-LIMA, M., CARREIRO, C., MOREIRA, D. C., POLCHEIRA, C., MACHADO, D. P. & CAMPOS, É. G. 2012. Glutathione status and antioxidant enzymes in a crocodilian species from the swamps of the Brazilian Pantanal. *Comparative Biochemistry and Physiology Part A: Molecular & Integrative Physiology,* 163**,** 189-198.

HO, S.-C., LIU, J.-H. & WU, R.-Y. 2003. Establishment of the mimetic aging effect in mice caused by D-galactose. *Biogerontology,* 4**,** 15-18.

HSIEH, H.-M., WU, W.-M., AND & HU, M.-L., . 2009. Soy isoflavones attenuate oxidative stress and improve parameters related to aging and Alzheimer's disease in C57BL/6J mice treated with D-galactose. *Food and Chemical Toxicology,,* 47(3), pp.625-632.

HSIEH, H.-M., WU, W.-M. & HU, M.-L. 2009. Soy isoflavones attenuate oxidative stress and improve parameters related to aging and Alzheimer's disease in C57BL/6J mice treated with D-galactose. *Food and Chemical Toxicology,* 47**,** 625-632.

HUA, X., LEI, M., ZHANG, Y., DING, J., HAN, Q., HU, G. & XIAO, M. 2007. Long-term D-galactose injection combined with ovariectomy serves as a new rodent model for Alzheimer's disease. *Life sciences,* 80**,** 1897-1905.

HUSSAIN, S., SLIKKER JR, W. & ALI, S. 1995. Age-related changes in antioxidant enzymes, superoxide dismutase, catalase, glutathione peroxidase and glutathione in different regions of mouse brain. *International Journal of Developmental Neuroscience,* 13**,** 811-817.

IGHODARO, O., MACDONALD, & AKINLOYE, O., ADEBOYE, 2018. First line defence antioxidants-superoxide dismutase (SOD), catalase (CAT) and glutathione peroxidase (GPX): Their fundamental role in the entire antioxidant defence grid. . *Alexandria journal of medicine,* 54**,** 287-293.

IHUNWO, A. & PILLAY, S. 2007. Neurogenic sites in the adult mammalian central nervous system. *Res J Biol Sci,* 2**,** 170-177.

ISKUSNYKH, I. Y., ZAKHAROVA, A. A. & PATHAK, D. 2022. Glutathione in brain disorders and aging. *Molecules,* 27**,** 324.

JAMARI, H., ROFIEE, M. S., JOHARI, R. J., SALLEH, M. Z. & KEK, T. L. 2020. Standardised Extracts of Moringa Oleifera and Centella Asiatica Enhanced the Antioxidant Activity, Learning and Memory Effects by Inhibiting Acetylcholinesterase Activity in D-Galactose Induced Ageing Rats. *Pertanika Journal of Science & Technology,* 28.

JI, Z.-H., LIU, C., ZHAO, H. & YU, X.-Y. 2015. Neuroprotective effect of biatractylenolide against memory impairment in D-galactose-induced aging mice. *Journal of Molecular Neuroscience,* 55**,** 678-683.

JIA, Y., GALL, C. M. & LYNCH, G. 2010. Presynaptic BDNF promotes postsynaptic long-term potentiation in the dorsal striatum. *Journal of Neuroscience,* 30**,** 14440-14445.

KATOH-SEMBA, R., TAKEUCHI, I. K., SEMBA, R. & KATO, K. 1997. Distribution of brain-derived neurotrophic factor in rats and its changes with development in the brain. *Journal of neurochemistry,* 69**,** 34-42.

KAUSHIK, S. & KAUR, J. 2003. Chronic cold exposure affects the antioxidant defense system in various rat tissues. *Clinica Chimica Acta,* 333**,** 69-77.

KEE, N., SIVALINGAM, S., BOONSTRA, R. & WOJTOWICZ, J. 2002. The utility of Ki-67 and BrdU as proliferative markers of adult neurogenesis. *Journal of neuroscience methods,* 115**,** 97-105.

KLEMPIN, F. & KEMPERMANN, G. 2007. Adult hippocampal neurogenesis and aging. *European archives of psychiatry and clinical neuroscience,* 257**,** 271-280.

KNIGHT, J. A. 2001. The biochemistry of aging. *Advances in clinical chemistry,* 35**,** 1-62.

KNUSEL, B., BECK, K. D., WINSLOW, J. W., ROSENTHAL, A., BURTON, L. E., WIDMER, H. R., NIKOLICS, K. & HEFTI, F. 1992. Brain-derived neurotrophic factor administration protects basal forebrain cholinergic but not nigral dopaminergic neurons from degenerative changes after axotomy in the adult rat brain. *Journal of Neuroscience,* 12**,** 4391-4402.

KUMAR, A., PRAKASH, A. & DOGRA, S. 2010. Naringin alleviates cognitive impairment, mitochondrial dysfunction and oxidative stress induced by D-galactose in mice. *Food and Chemical Toxicology,* 48**,** 626-632.

KUMAR, A., PRAKASH, A. & DOGRA, S. 2011. Centella asiatica attenuates D-galactose-induced cognitive impairment, oxidative and mitochondrial dysfunction in mice. *International journal of Alzheimer's disease,* 2011.

KUMAR, A., SINGH, B. K., AHMAD, I., SHUKLA, S., PATEL, D. K., SRIVASTAVA, G., KUMAR, V., PANDEY, H. P. & SINGH, C. 2012. Involvement of NADPH oxidase and glutathione in zinc-induced dopaminergic neurodegeneration in rats: similarity with paraquat neurotoxicity. *Brain research,* 1438**,** 48-64.

LALO, U., BOGDANOV, A., MOSS, G. W. & PANKRATOV, Y. 2020. Astroglia-derived BDNF and MSK-1 mediate experience-and diet-dependent synaptic plasticity. *Brain Sciences,* 10**,** 462.

LEE, J., KOO, N. & MIN, D. B. 2004. Reactive oxygen species, aging, and antioxidative nutraceuticals. *Comprehensive reviews in food science and food safety,* 3**,** 21-33.

LEI, M., HUA, X., XIAO, M., DING, J., HAN, Q. & HU, G. 2008a. Impairments of astrocytes are involved in the d-galactose-induced brain aging. *Biochemical and Biophysical Research Communications,* 369**,** 1082-1087.

LEI, M., SU, Y., HUA, X., DING, J., HAN, Q., HU, G. & XIAO, M. 2008b. Chronic systemic injection of D-galactose impairs the septohippocampal cholinergic system in rats. *Neuroreport,* 19**,** 1611-1615.

LI, C., TAN, F., YANG, J., YANG, Y., GOU, Y., LI, S. & ZHAO, X. 2019. Antioxidant effects of Apocynum venetum tea extracts on d-galactose-induced aging model in mice. *Antioxidants,* 8**,** 381.

LI, G., SCULL, C., OZCAN, L. & TABAS, I. 2010. NADPH oxidase links endoplasmic reticulum stress, oxidative stress, and PKR activation to induce apoptosis. *Journal of Cell Biology,* 191**,** 1113-1125.

LIN, L., YANG, K., ZHENG, L., ZHAO, M., SUN, W., ZHU, Q. & LIU, S. 2018. Anti-aging effect of sea cucumber (Cucumaria frondosa) hydrolysate on fruit flies and d-galactose-induced aging mice. *Journal of Functional Foods,* 47**,** 11-18.

LIN, M. T. & BEAL, M. F. 2006. Mitochondrial dysfunction and oxidative stress in neurodegenerative diseases. *Nature,* 443**,** 787.

LIU, C.-M., ZHENG, Y.-L., LU, J., ZHANG, Z.-F., FAN, S.-H., WU, D.-M. & MA, J.-Q. 2010. Quercetin protects rat liver against lead-induced oxidative stress and apoptosis. *Environmental toxicology and pharmacology,* 29**,** 158-166.

LIU, J.-K. 2022. Antiaging agents: Safe interventions to slow aging and healthy life span extension. *Natural Products and Bioprospecting,* 12**,** 18.

LOBO, V., PATIL, A., PHATAK, A. & CHANDRA, N. 2010. Free radicals, antioxidants and functional foods: Impact on human health. *Pharmacognosy reviews,* 4**,** 118.

LONG, J., WANG, X., GAO, H., LIU, Z., LIU, C., MIAO, M., CUI, X., PACKER, L. & LIU, J. 2007. D-galactose toxicity in mice is associated with mitochondrial dysfunction: protecting effects of mitochondrial nutrient R-alpha-lipoic acid. *Biogerontology,* 8**,** 373-381.

LU, H.-K., HSIEH, C.-C., HSU, J.-J., YANG, Y.-K. & CHOU, H.-N. 2006. Preventive effects of Spirulina platensis on skeletal muscle damage under exercise-induced oxidative stress. *European journal of applied physiology,* 98(2), pp.220-226.

LU, J., WU, D.-M., HU, B., CHENG, W., ZHENG, Y.-L., ZHANG, Z.-F., YE, Q., FAN, S.-H., SHAN, Q. & WANG, Y.-J. 2010. Chronic administration of troxerutin protects mouse brain against D-galactose-induced impairment of cholinergic system. *Neurobiology of learning and memory,* 93**,** 157-164.

LU, J., WU, D.-M., ZHENG, Z.-H., ZHENG, Y.-L., HU, B. & ZHANG, Z.-F. 2011. Troxerutin protects against high cholesterol-induced cognitive deficits in mice. *Brain,* 134**,** 783-797.

LU, J., ZHENG, Y.-L., WU, D.-M., LUO, L., SUN, D.-X. & SHAN, Q. 2007. Ursolic acid ameliorates cognition deficits and attenuates oxidative damage in the brain of senescent mice induced by D-galactose. *Biochemical pharmacology,* 74**,** 1078-1090.

MALABOU, C. 2009. *What should we do with our brain?*, Fordham Univ Press.

MANGA, F. N., EL KHATTABI, C., FONTAINE, J., BERKENBOOM, G., DUEZ, P., NZUNZU, J. L. & POCHET, S. 2012. Vascular effects and antioxidant activity of two Combretum species from Democratic Republic of Congo. *Journal of ethnopharmacology,* 142**,** 194-200.

MAPIYE, S. 2019. *Analysis of antibacterial activity of Terminalia Sericea and Combretum Imberbe two combretaceae species from Namibia.* University of Namibia.

MARIANI, E., POLIDORI, M., CHERUBINI, A. & MECOCCI, P. 2005. Oxidative stress in brain aging, neurodegenerative and vascular diseases: an overview. *Journal of Chromatography B,* 827**,** 65-75.

MASOKO, P., PICARD, J., HOWARD, R., MAMPURU, L. & ELOFF, J. 2010. In vivo antifungal effect of Combretum and Terminalia species extracts on cutaneous wound healing in immunosuppressed rats. *Pharmaceutical Biology,* 48**,** 621-632.

MATTSON, M. P. 2004. Pathways towards and away from Alzheimer's disease. *Nature,* 430**,** 631-639.

MATTSON, M. P. & ARUMUGAM, T. V. 2018. Hallmarks of brain aging: adaptive and pathological modification by metabolic states. *Cell metabolism,* 27**,** 1176-1199.

MCDANIEL, K. L., PADILLA, S., MARSHALL, R. S., PHILLIPS, P. M., PODHORNIAK, L., QIAN, Y. & MOSER, V. C. 2007. Comparison of acute neurobehavioral and cholinesterase inhibitory effects of N-methylcarbamates in rat. *Toxicological sciences,* 98**,** 552-560.

MCGAW, L., RABE, T., SPARG, S., JÄGER, A., ELOFF, J. & VAN STADEN, J. 2001. An investigation on the biological activity of Combretum species. *Journal of ethnopharmacology,* 75**,** 45-50.

MEISSNER, A., VISANJI, N. P., MOMEN, M. A., FENG, R., FRANCIS, B. M., BOLZ, S. S. & HAZRATI, L. N. 2015. Tumor necrosis factor-α underlies loss of cortical dendritic spine density in a mouse model of congestive heart failure. *Journal of the American Heart Association,* 4**,** e001920.

MIAFFO, D., NTCHAPDA, F., WANSI, S. L., POUALEU, S. L. K. & KAMANYI, A. 2019. Aqueous extract of Combretum molle boughs ameliorates hyperglycaemia and hyperlipidemia in sucrose-induced insulin resistant rats. *Journal of Herbmed Pharmacology,* 8**,** 328-332.

MIAFFO, D., POUALEU, S. L. K. & KAMANYI, A. 2014. Antidiabetic activity of the methanol and acetone extracts of twigs of Combretum molle in dexamathasone induced-insulin resistance in rats. *World Journal of Pharmaceutical Sciences***,** 955-965.

MIRANDA, M., MORICI, J. F., ZANONI, M. B. & BEKINSCHTEIN, P. 2019. Brain-derived neurotrophic factor: a key molecule for memory in the healthy and the pathological brain. *Frontiers in cellular neuroscience***,** 363.

MITCHELL, E. & WALKER, R. 2020. Global ageing: successes, challenges and opportunities. *British Journal of Hospital Medicine,* 81**,** 1-9.
MITCHELL, S. J., SCHEIBYE-KNUDSEN, M., LONGO, D. L. & DE CABO, R. 2015. Animal models of aging research: implications for human aging and age-related diseases. *Annu. Rev. Anim. Biosci.,* 3**,** 283-303.
MITTLER, R. 2017. ROS Are Good. *Trends in Plant Science,* 22**,** 11-19.
MIZUNO, M., YAMADA, K., HE, J., NAKAJIMA, A. & NABESHIMA, T. 2003. Involvement of BDNF receptor TrkB in spatial memory formation. *Learning & memory,* 10**,** 108-115.
MOLINARI, C., MORSANUTO, V., RUGA, S., NOTTE, F., FARGHALI, M., GALLA, R. & UBERTI, F. 2020. The role of BDNF on aging-modulation markers. *Brain Sciences,* 10**,** 285.
MORRIS, J. C. & CUMMINGS, J. 2005. Mild cognitive impairment (MCI) represents early-stage Alzheimer's disease. *Journal of Alzheimer's Disease,* 7**,** 235-239.
MORRIS, J. C., STORANDT, M., MILLER, J. P., MCKEEL, D. W., PRICE, J. L., RUBIN, E. H. & BERG, L. 2001. Mild cognitive impairment represents early-stage Alzheimer disease. *Archives of neurology,* 58**,** 397-405.
MOSER, J. S., SCHRODER, H. S., HEETER, C., MORAN, T. P. & LEE, Y.-H. 2011. Mind your errors: Evidence for a neural mechanism linking growth mind-set to adaptive posterror adjustments. *Psychological science,* 22**,** 1484-1489.
NAIR, J., AREMU, A. & VAN STADEN, J. 2012. Anti-inflammatory effects of Terminalia phanerophlebia (Combretaceae) and identification of the active constituent principles. *South African Journal of Botany,* 81**,** 79-80.
NAM, S. M., SEO, M., SEO, J.-S., RHIM, H., NAHM, S.-S., CHO, I.-H., CHANG, B.-J., KIM, H.-J., CHOI, S.-H. & NAH, S.-Y. 2019. Ascorbic acid mitigates D-galactose-induced brain aging by increasing hippocampal neurogenesis and improving memory function. *Nutrients,* 11**,** 176.
NAUDE, P. J., DOBOS, N., VAN DER MEER, D., MULDER, C., PAWIRONADI, K. G., DEN BOER, J. A., VAN DER ZEE, E. A., LUITEN, P. G. & EISEL, U. L. 2014. Analysis of cognition, motor performance and anxiety in young and aged tumor necrosis factor alpha receptor 1 and 2 deficient mice. *Behavioural brain research,* 258**,** 43-51.
NKOMOZEPI P. MAZENGENYA P, I. A. 2019. <Age related changes in Ki-67 and DCX expression in mice.pdf>. *International Journal of Developmental Neuroscience,* 72**,** 36-47.
OGBERA, A., DADA, O., ADELEYE, F. & JEWO, P. 2010. Complementary and alternative medicine use in diabetes mellitus. *West African journal of medicine,* 29.
OJEWOLE, J. A. 2008. Cardiovascular effects of mollic acid glucoside, a 1α-hydroxycycloartenoid saponin extractive from Combretum molle R Br ex G Don (Combretaceae) leaf: cardiovascular topic. *Cardiovascular journal of Africa,* 19**,** 128-134.
ORTÍ-CASAÑ, N., ZUHORN, I. S., NAUDÉ, P. J., DE DEYN, P. P., VAN SCHAIK, P. E., WAJANT, H. & EISEL, U. L. 2022. A TNF receptor 2 agonist ameliorates neuropathology and improves cognition in an Alzheimer's disease mouse model. *Proceedings of the National Academy of Sciences,* 119**,** e2201137119.

OZIOMA, E.-O. J. & CHINWE, O. A. N. 2019. Herbal medicines in African traditional medicine. *Herbal medicine,* 10**,** 191-214.

PAN, W., BANKS, W. A., FASOLD, M. B., BLUTH, J. & KASTIN, A. J. 1998. Transport of brain-derived neurotrophic factor across the blood–brain barrier. *Neuropharmacology,* 37**,** 1553-1561.

PANCHE, A. N., DIWAN, A. D. & CHANDRA, S. R. 2016. Flavonoids: an overview. *Journal of nutritional science,* 5**,** e47.

PARK, D.-S., LEE, S.-H., CHOI, Y.-J., BAE, D.-K., YANG, Y.-H., YANG, G.-E., KIM, T.-K., YEON, S.-H., HWANG, S.-Y. & JOO, S.-S. 2011. Improving effect of silk peptides on the cognitive function of rats with aging brain facilitated by D-galactose. *Biomolecules & Therapeutics,* 19**,** 224-230.

PAUDYAL, V., SUN, S., HUSSAIN, R., ABUTALEB, M. H. & HEDIMA, E. W. 2022. Complementary and alternative medicines use in COVID-19: A global perspective on practice, policy and research. *Research in Social and Administrative Pharmacy,* 18**,** 2524-2528.

PELTZER, K., PREEZ, N. F.-D., RAMLAGAN, S. & FOMUNDAM, H. 2008. Use of traditional complementary and alternative medicine for HIV patients in KwaZulu-Natal, South Africa. *BMC public health,* 8**,** 1-14.

PETERS, R. 2006. Ageing and the brain. *Postgrad Med J,* 82**,** 84-8.

PIETTA, P.-G. 2000. Flavonoids as antioxidants. *Journal of natural products,* 63**,** 1035-1042.

PRAJIT, R., SRITAWAN, N., SUWANNAKOT, K., NAEWLA, S., ARANAROCHANA, A., SIRICHOAT, A., PANNANGRONG, W., WIGMORE, P. & WELBAT, J. U. 2020. Chrysin Protects against Memory and Hippocampal Neurogenesis Depletion in D-Galactose-Induced Aging in Rats. *Nutrients,* 12**,** 1100.

RAMASAMY, R., VANNUCCI, S. J., YAN, S. S. D., HEROLD, K., YAN, S. F. & SCHMIDT, A. M. 2005. Advanced glycation end products and RAGE: a common thread in aging, diabetes, neurodegeneration, and inflammation. *Glycobiology,* 15**,** 16R-28R.

RATTAN, S. 2008. Biological Aging: Methods and Protocols. *Biogerontology,* 9**,** 137-137.

REHMAN, S. U., SHAH, S. A., ALI, T., CHUNG, J. I. & KIM, M. O. 2017. Anthocyanins reversed D-galactose-induced oxidative stress and neuroinflammation mediated cognitive impairment in adult rats. *Molecular neurobiology,* 54**,** 255-271.

RENDEIRO, C., VAUZOUR, D., KEAN, R. J., BUTLER, L. T., RATTRAY, M., SPENCER, J. P. & WILLIAMS, C. M. 2012. Blueberry supplementation induces spatial memory improvements and region-specific regulation of hippocampal BDNF mRNA expression in young rats. *Psychopharmacology,* 223**,** 319-330.

RITCHIE, H. & ROSER, M. 2019. Age structure. *Our World in Data*.

RUSU, M. E., GEORGIU, C., POP, A., MOCAN, A., KISS, B., VOSTINARU, O., FIZESAN, I., STEFAN, M.-G., GHELDIU, A.-M. & MATES, L. 2020. Antioxidant effects of walnut (Juglans regia L.) kernel and walnut septum extract in a D-galactose-induced aging model and in naturally aged rats. *Antioxidants,* 9**,** 424.

SAENNO, R., DORNLAKORN, O., ANOSRI, T., KAEWNGAM, S., SIRICHOAT, A., ARANAROCHANA, A., PANNANGRONG, W., WIGMORE, P. & WELBAT, J. U. 2022. Caffeic Acid Alleviates Memory and Hippocampal Neurogenesis Deficits in Aging Rats Induced by D-Galactose. *Nutrients,* 14**,** 2169.

SALEEM, U., CHAUHDARY, Z., ISLAM, S., ZAFAR, A., KHAYAT, R. O., ALTHOBAITI, N. A., SHAH, G. M., ALQARNI, M. & SHAH, M. A. 2023. Sarcococca saligna ameliorated D-galactose induced neurodegeneration through repression of neurodegenerative and oxidative stress biomarkers. *Metabolic Brain Disease,* 38**,** 717-734.

SÁNCHEZ-HUERTA, K., SALDAÑA-SALINAS, R. D., BUSTAMANTE-NIEVES, P. E., JIMÉNEZ, A., CORZO-CRUZ, A., MARTÍNEZ-VARGAS, M., GUEVARA-GUZMÁN, R., VELASCO, I. & ESTUDILLO, E. 2022. Sucrose Consumption during Late Adolescence Impairs Adult Neurogenesis of the Ventral Dentate Gyrus without Inducing an Anxiety-like Behavior. *International Journal of Molecular Sciences,* 23**,** 14176.

SARTER, M. 2004. <Animal cognition.pdf>. *Neuroscience and Biobehavioral Reviews,* 28**,** 645-650.

SCHLIEBS, R. & ARENDT, T. 2006. The significance of the cholinergic system in the brain during aging and in Alzheimer's disease. *Journal of neural transmission,* 113**,** 1625-1644.

SEN, S. & CHAKRABORTY, R. 2011. The role of antioxidants in human health. *Oxidative stress: diagnostics, prevention, and therapy.* ACS Publications.

SHOHAMI, E., GINIS, I. & HALLENBECK, J. M. 1999. Dual role of tumor necrosis factor alpha in brain injury. *Cytokine & growth factor reviews,* 10**,** 119-130.

SHOHAYEB, B., DIAB, M., AHMED, M. & NG, D. C. H. 2018. Factors that influence adult neurogenesis as potential therapy. *Translational neurodegeneration,* 7**,** 1-19.

SHWE, T., PRATCHAYASAKUL, W., CHATTIPAKORN, N. & CHATTIPAKORN, S. C. 2018. Role of D-galactose-induced brain aging and its potential used for therapeutic interventions. *Experimental gerontology,* 101**,** 13-36.

SILHOL, M., ARANCIBIA, S., PERRIN, D., MAURICE, T., ALLIOT, J. & TAPIA-ARANCIBIA, L. 2008. Effect of aging on brain-derived neurotrophic factor, proBDNF, and their receptors in the hippocampus of Lou/C rats. *Rejuvenation research,* 11**,** 1031-1040.

SOBECKI, M., MROUJ, K., COLINGE, J., GERBE, F., JAY, P., KRASINSKA, L., DULIC, V. & FISHER, D. 2017. Cell-Cycle Regulation Accounts for Variability in Ki-67 Expression LevelsKi-67 Expression and the Cell Cycle. *Cancer research,* 77**,** 2722-2734.

SOFOWORA, A. 1996. Research on medicinal plants and traditional medicine in Africa. *The Journal of Alternative and Complementary Medicine,* 2**,** 365-372.

SOHAL, R. S., ARNOLD, L. A. & SOHAL, B. H. 1990. Age-related changes in antioxidant enzymes and prooxidant generation in tissues of the rat with special reference to parameters in two insect species. *Free Radical Biology and Medicine,* 9**,** 495-500.

SONG, X., BAO, M., LI, D. & LI, Y. M. 1999. Advanced glycation in D-galactose induced mouse aging model. *Mechanisms of ageing and development,* 108**,** 239-251.

SRIDHARAMURTHY, N., ASHOK, B. & YOGAN, R. 2012. Evaluation of Antioxidant and Acetyl Cholinesterase inhibitory activity of Peltophorum pterocarpum in Scopolamine treated Rats. *International journal of drug development and research,* 4.

STAFFORD, G. I., PEDERSEN, M. E., VAN STADEN, J. & JÄGER, A. K. 2008. Review on plants with CNS-effects used in traditional South African medicine against mental diseases. *Journal of ethnopharmacology,* 119**,** 513-537.

SUH, J. H., SHENVI, S. V., DIXON, B. M., LIU, H., JAISWAL, A. K., LIU, R.-M. & HAGEN, T. M. 2004. Decline in transcriptional activity of Nrf2 causes age-related loss of glutathione synthesis, which is reversible with lipoic acid. *Proceedings of the National Academy of Sciences,* 101**,** 3381-3386.

TARTT, A. N., FULMORE, C. A., LIU, Y., ROSOKLIJA, G. B., DWORK, A. J., ARANGO, V., HEN, R., MANN, J. J. & BOLDRINI, M. 2018. Considerations for assessing the extent of hippocampal neurogenesis in the adult and aging human brain. *Cell Stem Cell,* 23**,** 782-783.

THOENEN, H. 1995. Neurotrophins and neuronal plasticity. *Science,* 270**,** 593-598.

TREMBOVLER, V., BEIT-YANNAI, E., YOUNIS, F., GALLILY, R., HOROWITZ, M. & SHOHAMI, E. 1999. Antioxidants attenuate acute toxicity of tumor necrosis factor-alpha induced by brain injury in rat. *Journal of interferon & cytokine research,* 19**,** 791-795.

VAZ, M., SILVA, V., MONTEIRO, C. & SILVESTRE, S. 2022. Role of aducanumab in the treatment of Alzheimer's disease: Challenges and Opportunities. *Clinical Interventions in Aging***,** 797-810.

VON BERNHARDI, R., BERNHARDI, L. E.-V. & EUGENÍN, J. 2017. What is neural plasticity? *The plastic brain***,** 1-15.

VON BERNHARDI, R., TICHAUER, J. E. & EUGENÍN, J. 2010. Aging-dependent changes of microglial cells and their relevance for neurodegenerative disorders. *Journal of Neurochemistry,* 112**,** 1099-1114.

VON BOHLEN UND HALBACH, O. 2011. Immunohistological markers for proliferative events, gliogenesis, and neurogenesis within the adult hippocampus. *Cell and tissue research,* 345**,** 1-19.

VON BOHLEN UND HALBACH, O., ZACHER, C., GASS, P. & UNSICKER, K. 2006. Age-related alterations in hippocampal spines and deficiencies in spatial memory in mice. *Journal of neuroscience research,* 83**,** 525-531.

WAJANT, H., PFIZENMAIER, K. & SCHEURICH, P. 2003. Tumor necrosis factor signaling. *Cell Death & Differentiation,* 10**,** 45-65.

WAJANT, H. & SIEGMUND, D. 2019. TNFR1 and TNFR2 in the Control of the Life and Death Balance of Macrophages. *Frontiers in cell and developmental biology,* 7**,** 91.

WANG, C., CAI, Z., WANG, W., WEI, M., KOU, D., LI, T., YANG, Z., GUO, H., LE, W. & LI, S. 2019. Piperine attenuates cognitive impairment in an experimental mouse model of sporadic Alzheimer's disease. *The Journal of nutritional biochemistry,* 70**,** 147-155.

WANG, C., SHEN, Z., YU, J., YANG, J., MENG, F., JIANG, X. & ZHU, C. 2020. Protective effects of enzyme degradation extract from Porphyra yezoensis against oxidative stress and brain injury in d-galactose-induced ageing mice. *British Journal of Nutrition,* 123**,** 975-986.

WANG, Y.-J., LU, J., WU, D.-M., ZHENG, Z.-H., ZHENG, Y.-L., WANG, X.-H., RUAN, J., SUN, X., SHAN, Q. & ZHANG, Z.-F. 2011. Ursolic acid attenuates lipopolysaccharide-induced cognitive deficits in mouse brain through suppressing

p38/NF-κB mediated inflammatory pathways. *Neurobiology of learning and memory,* 96**,** 156-165.
WANG, Y., BRANICKY, R., NOË, A. & HEKIMI, S. 2018. Superoxide dismutases: Dual roles in controlling ROS damage and regulating ROS signaling. *Journal of Cell Biology,* 217**,** 1915-1928.
WATI, H., KUDO, K., QIAO, C., KUROKI, T. & KANBA, S. 2006. A decreased survival of proliferated cells in the hippocampus is associated with a decline in spatial memory in aged rats. *Neuroscience letters,* 399**,** 171-174.
WEI, H., LI, L., SONG, Q., AI, H., CHU, J. & LI, W. 2005a. Behavioural study of the D-galactose induced aging model in C57BL/6J mice. *Behav Brain Res,* 157**,** 245-51.
WEI, H., LI, L., SONG, Q., AI, H., CHU, J. & LI, W. 2005b. Behavioural study of the D-galactose induced aging model in C57BL/6J mice. *Behavioural brain research,* 157**,** 245-251.
WEI, Y., LIU, D., ZHENG, Y., LI, H., HAO, C. & OUYANG, W. 2017. Protective effects of kinetin against aluminum chloride and D-galactose induced cognitive impairment and oxidative damage in mouse. *Brain research bulletin,* 134**,** 262-272.
WICKENS, A. P. 2001. Ageing and the free radical theory. *Respiration physiology,* 128**,** 379-391.
WILLIAMS, G., MOLINA-HOLGADO, F. & DOHERTY, P. 2008. Tandem repeat peptide strategy for the design of neurotrophic factor mimetics. *CNS & Neurological Disorders-Drug Targets (Formerly Current Drug Targets-CNS & Neurological Disorders),* 7**,** 110-119.
WU, S.-Y., PAN, B.-S., TSAI, S.-F., CHIANG, Y.-T., HUANG, B.-M., MO, F.-E. & KUO, Y.-M. 2020. BDNF reverses aging-related microglial activation. *Journal of neuroinflammation,* 17**,** 1-18.
XU, X.-H. & ZHAO, T.-Q. 2002. Effects of puerarin on D-galactose-induced memory deficits in mice. *Acta Pharmacologica Sinica,* 23**,** 587-590.
YAMADA, J. & JINNO, S. 2019. Potential link between antidepressant-like effects of ketamine and promotion of adult neurogenesis in the ventral hippocampus of mice. *Neuropharmacology,* 158**,** 107710.
YAMADA, K., MIZUNO, M. & NABESHIMA, T. 2002. Role for brain-derived neurotrophic factor in learning and memory. *Life sciences,* 70**,** 735-744.
YELTEKIN, A. Ç., UCAR, A., PARLAK, V., ÖZGERIŞ, F. B., TÜRKEZ, H., ESENBUĞA, N., ATAMANALP, M. & ALAK, G. 2022. Borax exerts protective effect against ferrocene-induced neurotoxicity in Oncorhynchus mykiss. *Journal of Trace Elements in Medicine and Biology,* 72**,** 126996.
YESSUF, A. M. 2015. Phytochemical extraction and screening of bio active compounds from black cumin (Nigella sativa) seeds extract. *American Journal of Life Sciences,* 3**,** 358-364.
YIN, F., SANCHETI, H., PATIL, I. & CADENAS, E. 2016. Energy metabolism and inflammation in brain aging and Alzheimer's disease. *Free Radical Biology and Medicine,* 100**,** 108-122.
YOO, H. & KIM, H.-S. 2021. Cacao powder supplementation attenuates oxidative stress, cholinergic impairment, and apoptosis in d-galactose-induced aging rat brain. *Scientific Reports,* 11**,** 1-11.

YOUSUF, S., ATIF, F., AHMAD, M., HODA, N., ISHRAT, T., KHAN, B. & ISLAM, F. 2009. Resveratrol exerts its neuroprotective effect by modulating mitochondrial dysfunctions and associated cell death during cerebral ischemia. *Brain research,* 1250**,** 242-253.

ZAMBÓN, D., QUINTANA, M., MATA, P., ALONSO, R., BENAVENT, J., CRUZ-SÁNCHEZ, F., GICH, J., POCOVÍ, M., CIVEIRA, F. & CAPURRO, S. 2010. Higher incidence of mild cognitive impairment in familial hypercholesterolemia. *The American journal of medicine,* 123**,** 267-274.

ZHANG, C., ZHANG, N., LI, Z., TIAN, Y., ZHANG, L. & ZHENG, B. 2016. Antioxidant Efficacy of Protein Hydrolysates from Large Yellow Croaker (Pseudosciaena crocea) in D-galactose-Induced Aging Mice. *Journal of Aquatic Food Product Technology,* 26**,** 1-12.

ZHANG, C., ZHANG, N. N., LI, Z. Y., TIAN, Y. T., ZHANG, L. T. & ZHENG, B. D. 2017. Antioxidant Efficacy of Protein Hydrolysates from Large Yellow Croaker (Pseudosciaena crocea) in D-galactose-Induced Aging Mice. *Journal of Aquatic Food Product Technology,* 26**,** 17-28.

ZHANG, Q., LI, X., CUI, X. & ZUO, P. 2005. D-galactose injured neurogenesis in the hippocampus of adult mice. *Neurological research,* 27**,** 552-556.

ZHANG, X.-L., AN, L.-J., BAO, Y.-M., WANG, J.-Y. & JIANG, B. 2008. d-galactose administration induces memory loss and energy metabolism disturbance in mice: Protective effects of catalpol. *Food and Chemical Toxicology,* 46**,** 2888-2894.

ZHANG, X. L., JIANG, B., LI, Z. B., HAO, S. & AN, L. J. 2007. Catalpol ameliorates cognition deficits and attenuates oxidative damage in the brain of senescent mice induced by d-galactose. *Pharmacology Biochemistry and Behavior,* 88**,** 64-72.

ZHANG, Y. & PARDRIDGE, W. M. 2001. Neuroprotection in transient focal brain ischemia after delayed intravenous administration of brain-derived neurotrophic factor conjugated to a blood-brain barrier drug targeting system. *Stroke,* 32**,** 1378-1384.

ZHANG, Z.-F., FAN, S.-H., ZHENG, Y.-L., LU, J., WU, D.-M., SHAN, Q. & HU, B. 2009. Purple sweet potato color attenuates oxidative stress and inflammatory response induced by d-galactose in mouse liver. *Food and chemical toxicology,* 47**,** 496-501.

ZHAO, L., YANG, H., XU, M., WANG, X., WANG, C., LIAN, Y., MEHMOOD, A. & DAI, H. 2019. Stevia residue extract ameliorates oxidative stress in d-galactose-induced aging mice via Akt/Nrf2/HO-1 pathway. *Journal of Functional Foods,* 52**,** 587-595.

ZHEN, Y. Z., LIN, Y. J., LI, K. J., ZHANG, G. L., ZHAO, Y. F., WANG, M. M., WEI, J. B., WEI, J. & HU, G. 2016a. Effects of rhein lysinate on D-galactose-induced aging mice. *Exp Ther Med,* 11**,** 303-308.

ZHEN, Y. Z., LIN, Y. J., LI, K. J., ZHANG, G. L., ZHAO, Y. F., WANG, M. M., WEI, J. B., WEI, J. & HU, G. 2016b. Effects of rhein lysinate on D-galactose-induced aging mice. *Experimental and therapeutic medicine,* 11**,** 303-308.

ZHONG, F., LIU, L., WEI, J.-L., HU, Z.-L., LI, L., WANG, S., XU, J.-M., ZHOU, X.-F., LI, C.-Q. & YANG, Z.-Y. 2019. Brain-derived neurotrophic factor precursor in the hippocampus regulates both depressive and anxiety-like behaviors in rats. *Frontiers in Psychiatry,* 9**,** 776.

ZHU, J., MU, X., ZENG, J., XU, C., LIU, J., ZHANG, M., LI, C., CHEN, J., LI, T. & WANG, Y. 2014. Ginsenoside Rg1 prevents cognitive impairment and hippocampus senescence in a rat model of D-galactose-induced aging. *PloS one,* 9**,** e101291.

ZHU YUANGUI , CARVEY PAUL & ZAODUNG, L. 2006. <Age-related changes in glutathione and glutathione-related.pdf>. *Brain Research,* 1090**,** 35-44.

8 APPENDICES

8.1 Appendix A

8.1.1 Ethics Clearance and Extension

STRICTLY CONFIDENTIAL

ANIMAL ETHICS SCREENING COMMITTEE (AESC)

CLEARANCE CERTIFICATE NO. 2017/08/51/C

APPLICANT: Mrs T Fasemore

SCHOOL: Anatomical Sciences
DEPARTMENT:
LOCATION:

PROJECT TITLE: Evaluation of antioxidant properties and neuroprotective effects of combretum Molle methanolic leaf extract in D-galactose treated Sprague Dawley rats

Number and Species

50 Sprague Dawley rats

Approval was given for the use of animals for the project described above at an AESC meeting held on 2017/08/29. This approval remains valid until 2019/11/12.
Unreported changes to the application may invalidate the clearance given by the AESC
An annual progress report must be provided

The use of these animals is subject to AESC guidelines for the use and care of animals, is limited to the procedures described in the application form and is subject to any additional conditions listed below:

Signed: _____ (Chairperson: AESC) Date: 23 November 2017

I am satisfied that the persons listed in this application are competent to perform the procedures therein, in terms of Section 23 (1) (c) of the Veterinary and Para-Veterinary Professions Act (19 of 1982)

Signed: _____ (Registered Veterinarian) Date: 23 November 2017

cc: Supervisor: Professor F Mbajiorgu
Director: CAS

Works 2000\lain0015\AESCCert.wps

AREC 2017 M&E

Please note that only typewritten applications will be accepted.

UNIVERSITY OF THE WITWATERSRAND

ANIMAL RESEARCH ETHICS COMMITTEE
MODIFICATIONS AND EXTENSIONS TO EXPERIMENTS

a. Name: Thandi Mamorapelo Dorothy Fasemore

b. School and email address: School of Anatomical Sciences

c. Experiment to be modified / extended

	AREC/AESC NO		
Original AESC number	**2017/08/51/C**		
Other M&Es : Yes			

d. Project Title: **Evaluation of antioxidant properties and neuroprotective effects of methanolic leaf extract of *Combretum molle* in D-galactose-induced aging model of Sprague Dawley rats.**

		No.	Species
e.	Number and species of animals originally approved:	50	SD Rats
f.	Number of additional animals previously allocated on M&Es:	50	SD Rats
g.	Total number of animals allocated to the experiment to date:	50	SD Rats
h.	Number of animals used to date:	50	SD Rats

i. Specific modification / extension requested:

The ethics approval of the study is expiring on the **12th November 2019**. I hereby request for extension of ethics as the study is still ongoing until December 2022.

j. Motivation for modification / extension:

Due to unforeseen delays the experiments did not take place at the expected time. At the moment the animals are currently undergoing treatment at the Wits Central animal Services (CAS) and other parts of the study such as behavioural study will still need to be conducted after treatment. Then after termination organs will be harvested for further analysis thus I request the ethics to be extended until **31st December 2022.**

Date: **5th September 2019** Signature:

RECOMMENDATIONS Extension of time until december 2022

Date: 3/10/2019 Signature: Chairman, AREC pp

8.2 Appendix B

8.2.1 Protocols steps for Assays

8.2.1.1 Elisa kits Assay Procedure summary for BDNF and AchE (Sandwich method)

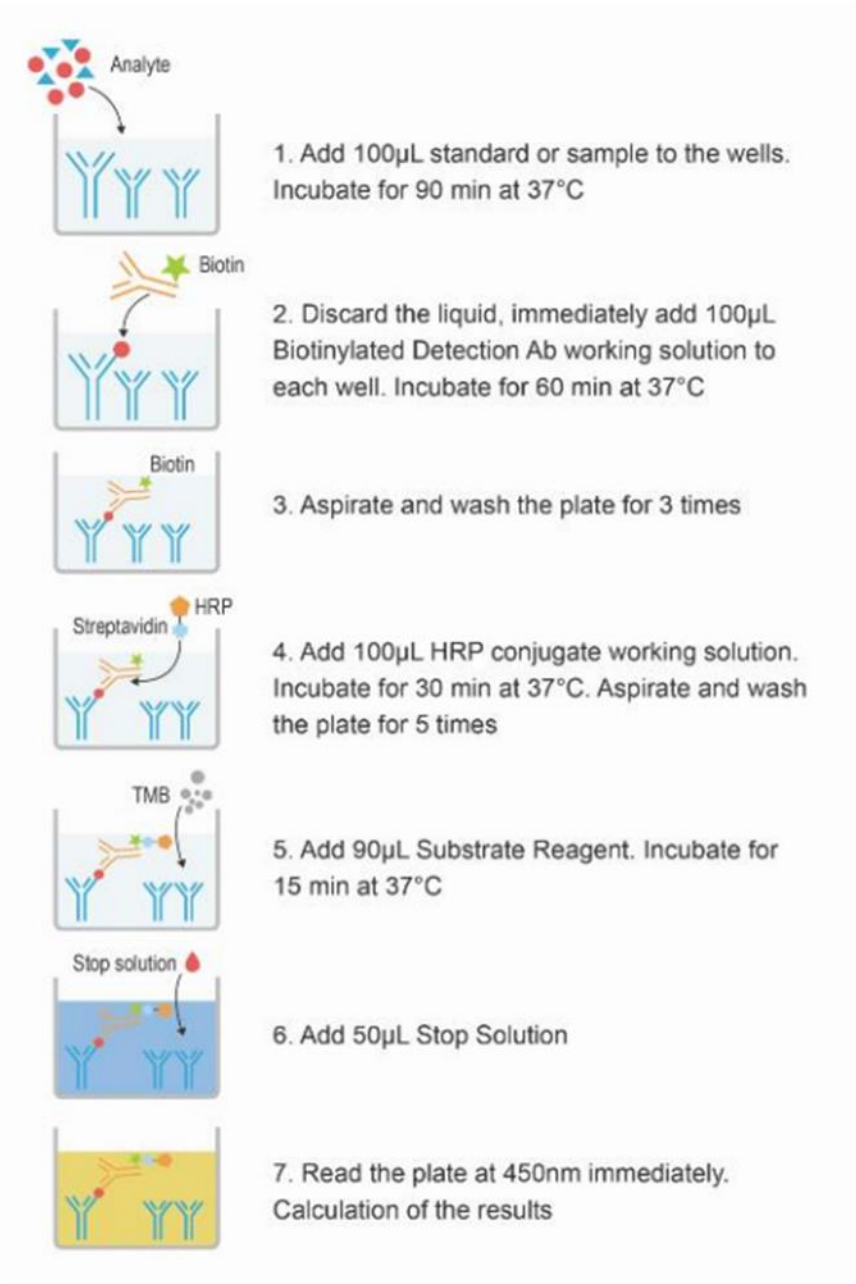

Figure 3.1 Elisa kit assay procedure summary for BDNF and AchE

8.2.1.2 Elisa kits Assay Procedure summary for Ach (Competitive method)

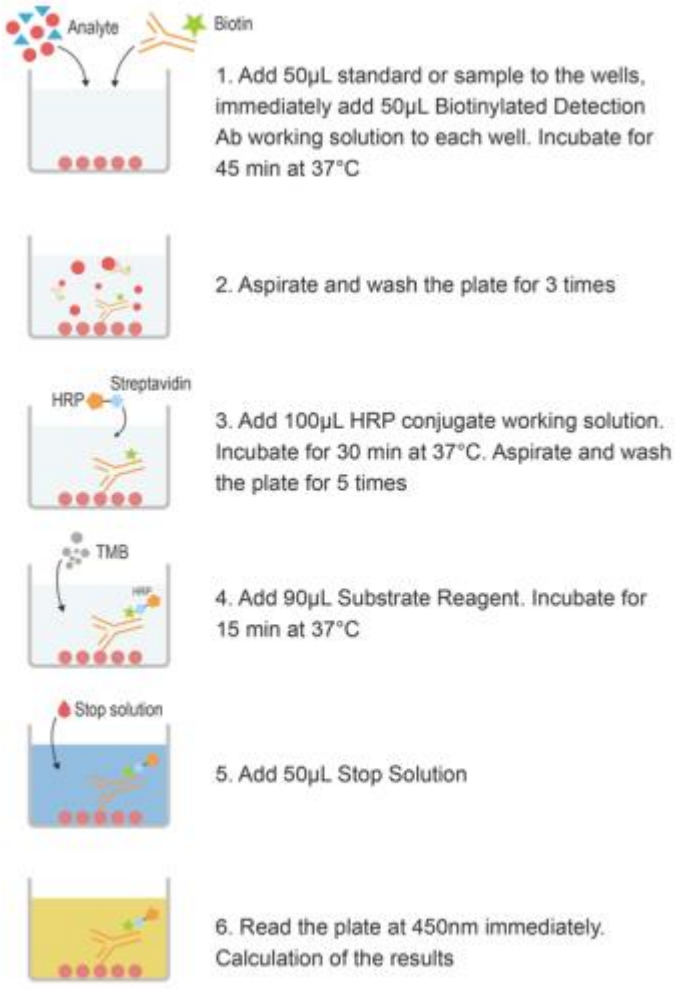

Figure 3.2 Elisa kits assay procedure summary for Ach.

8.3 Appendix C

8.3.1 Descriptive statistics

Table 4.2 Weekly averages of water intake. Values represent mean ± SEM.

Week	Control	D-gal	CM	CMD 90	CMD 45
1	103.7 ± 6.41	117.4 ± 11.87	129.0 ±15.49	107,997 ±8,731	99,600 ± 1,503
2	132.4 ± 14.66	109.7± 8.35	138. 4± 13.73	114,227 ±7,126	125,214±7,840
3	122.0 ± 15.48	129.8 ± 5.06	137.0 ± 15.29	125,407 ±7,156	113,629±9,520
4	122.3 ± 8.14	168.4 ± 7.10	145.9 ± 14.62	128,563 ±10,437	138,681±11,080
5	149.7 ± 4.99	114.19±12.04	163.2 ± 15.18	158,807 ±8,295	144,043±8,775
6	143.2 ± 11.91	129.7 ± 16.61	165.7 ± 13.86	131,829 ±10,831	167,190±14,879
7	143.4 ± 9.98	124.7± 12.79	160.9 ± 11.06	152,143 ±14,689	146,771±12,680
8	143.9 ± 23.26	131.5 ± 16.53	129.4 ± 23.79	142,829 ±16,498	132,414±22,873
9	147.7 ± 20.94	150.5 ± 13.68	141.0 ± 12.75	123,786 ±22,511	138,243±20,680
10	171.9 ± 19.31	154.7 ± 19.00	119.6 ± 7.14	139,734 ±8,201	154,429±23,139
11	148.3 ± 7.71	150.0 ± 9.57	157.3± 15.95	137,976 ±6,772	128,238±23,896
12	159.7 ± 18.93	155.9 ± 10.19	115.8 ± 34.56	136,458 ±21,425	131,552±16,657
13	159.9 ± 8.06	140.6 ± 25.86	136.9 ± 22.84	185,421 ±31,654	155,510±22,713
14	152.3 ± 12.49	166.1 ± 25.86	168.5 ± 45.92	150,234 ±9,043	138,833±19,161
15	176.6 ± 16.39	154.2 ± 30.04	129.4 ± 15.91	134,700 ±15,020	154,883±17,529

Table 4.3. Weekly averages for food intake per week. Values represent mean ± SEM.

Week	Control	D-gal	CM	CMD 90	CMD 45
1	106,479±44,393	103,833±19,282	147,832±80,000	101,994±33,702	130,223±48,457
2	88,657±32,290	80,900±29,105	120,095±46,809	77,871±36,888	94,406±13,197
3	82,714±33,293	110,560±52,585	127,517±70,366	110,790±22,626	67,720±18,123
4	131,171±38,668	152,665±106,933	137,245±92,840	144,866±82,611	136,579±47,343
5	154,502±11,767	128,227±43,452	140,962±31,318	131,822±29,368	139,344±10,878
6	107,221±19,907	97,933±16,028	118,545±48,514	108,900±16,258	114,435±25,477
7	67,211±19,389	73,914±20.197	94,357±50,356	70,600±20,555	92,854±42,062
8	77,194±17,249	97,814±17,781	95,486±43,684	74,711±20,406	91,569±31,759
9	111,663±16,383	140,986±28,284	110,271±35,346	114,789±7,893	111,289±30,055
10	112,329±10,130	88,864±16,649	106,160±43,616	104,940±24,807	101,426±43,812
11	119,829±12,086	130,429±23,960	95,986±30,897	112,564±20,117	105,497±34,556
12	119,588±33,855	127,048±43,457	139,879±52,678	106,633±28,097	105,856±45,921
13	89,414±20,483	120,470±38,295	130,550±116,892	93,786±36,750	123,195±38,520
14	125,574±15,957	96,176±42,367	119,888±25,814	132,855±27,701	109,496±12,650
15	96,333±7,630	68,782±26,824	104,024±59,410	65,602±21,789	57,555±23,064

Table 4.6. The descriptive statistics values grooming in the open field test.

TREATMENT GROUPS	MEAN	SD	SEM
CONTROL	4.667	1.633	0.67
D-GAL	4.500	1.378	0.56
CM	3.333	1.033	0.42
CMD 90	3.833	1.941	0.79
CMD 45	5.000	2.000	0.82

Table 4.7. The descriptive statistics values grooming in the open field test.

TREATMENT GROUPS	MEAN	SD	SEM
CONTROL	23.33	7.26	2.96
D-GAL	23.17	2.48	1.01
CM	36.67	6.38	2.60
CMD 90	42.67	10.50	4.29
CMD 45	22.83	6.40	2.61

Table 4.8. The descriptive statistics of time spent exploring object A during familiarization

TREATMENT GROUPS	MEAN	SD	SEM
CONTROL	21.50	4.76	1.94
D-GAL	21.67	3.20	1.31
CM	28.50	2.59	1.06
CMD 90	24.00	5.76	2.35
CMD 45	22.83	4.36	1.78

Table 4.9. The descriptive statistics of time spent exploring object B during familiarization phase.

TREATMENT GROUPS	MEAN	SD	SEM
CONTROL	18.83	2.48	1.01
D-GAL	18.83	4.45	1.82
CM	22.50	2.17	0.89
CMD 90	21.17	3.49	1.42
CMD 45	21.33	1.37	0.56

Table 4.10. Descriptive statistics of discrimination index in NORT during familiarization phase.

TREATMENT GROUPS	MEAN	SD	SEM
CONTROL	39.56	13.66	5.58
D-GAL	31.15	5.67	2.32
CM	44.63	9.28	3.79
CMD 90	43.03	14.21	5.80
CMD 45	34.41	8.36	3.41

Table 4.11. Descriptive statistics of Total investigation time (TIT) in NORT during familiarization phase.

TREATMENT GROUPS	MEAN	SD	SEM
CONTROL	66.86	12.55	5.12
D-GAL	62.24	5.32	2.17
CM	69.81	8.70	3.55
CMD 90	71.23	7.36	3.01
CMD 45	66.54	4.82	1.96

Table 4.12. Descriptive statistics of time spent exploring object A (Novel) during NORT testing phase.

TREATMENT GROUPS	MEAN	SD	SEM
CONTROL	49.33	7.65	3.12
D-GAL	33.67	7.03	2.87
CM	53.83	9.15	3.74
CMD 90	48.83	9.13	3.73
CMD 45	33.80	10.41	4.25

Table 4.13. Descriptive statistics of time spent exploring object B (Familiar) during NORT testing phase.

TREATMENT GROUPS	MEAN	SD	SEM
CONTROL	22.00	4.82	1.97
D-GAL	24.67	2.81	1.15
CM	15.17	2.32	0.95
CMD 90	14.83	3.87	1.58
CMD 45	17.00	4.34	1.77

Table 4.14. Descriptive statistics values of discrimination index (DI) in NORT during testing phase

TREATMENT GROUPS	MEAN	SD	SEM
CONTROL	6.64	15.17	6.191
D-GAL	-19.26	17.13	6.995
CM	26.40	23.03	9.401
CMD 90	16.05	22.44	9.162

CMD 45	16.61	18.53	7.566

Table 4.15. Descriptive statistics of Total investigation time (TIT) NORT during testing phase.

TREATMENT GROUPS	MEAN	SD	SEM
CONTROL	53.32	7.58	3.10
D-GAL	40.37	8.57	3.50
CM	63.20	11.51	4.70
CMD 90	54.40	13.41	5.48
CMD 45	58.30	9.27	3.78

Table 4.16. Descriptive statistics of time spent at Location A during OLT Familiarization phase.

TREATMENT GROUPS	MEAN	SD	SEM
CONTROL	25.60	8.11	3.62
D-GAL	21.20	4.66	2.08
CM	23.17	4.58	1.87
CMD 90	24.50	5.45	2.72
CMD 45	21.67	3.39	1.38

Table 4.17. Descriptive statistics of time spent at Location B during OLT Familiarization phase.

TREATMENT GROUPS	MEAN	SD	SEM
CONTROL	22.80	8.53	3.81
D-GAL	28.00	6.05	3.03
CM	20.17	3.19	1.30
CMD 90	16.00	1.63	0.82
CMD 45	21.00	6.67	2.98

Table 4.18. Descriptive statistics of Discrimination index (DI) during OLT Familiarization phase

TREATMENT GROUPS	MEAN	SD	SEM
CONTROL	19.50	1.87	0.76
D-GAL	19.50	2.88	1.18
CM	25.00	3.74	1.53
CMD 90	21.50	1.87	0.76
CMD 45	20.00	3.84	1.57

Table 4.19. Descriptive statistics of Total investigation time (TIT) during OLT Familiarization phase

TREATMENT GROUPS	MEAN	SD	SEM
CONTROL	53.02	3.61	1.47
D-GAL	48.09	5.24	2.14
CM	54.14	3.02	1.23
CMD 90	57.30	7.35	2.99
CMD 45	49.14	10.99	4.49

Table 4.20. Descriptive statistics values of Time spent in Location A (Novel) in OLT during testing phase.

TREATMENT GROUPS	MEAN	SD	SEM
CONTROL	21.80	5.17	2.31
D-GAL	16.00	1.83	0.91
CM	24.00	3.54	1.58
CMD 90	25.80	3.63	1.63
CMD 45	23.80	3.03	1.36

Table 4.21. Descriptive statistics values of Time spent in Location B (Familiar) in OLT during testing phase.

TREATMENT GROUPS	MEAN	SD	SEM
CONTROL	19.50	4.76	1.95
D-GAL	27.20	4.15	1.86
CM	15.33	2.73	1.12
CMD 90	16.50	4.04	1.65
CMD 45	17.50	3.94	1.61

Table 4.22. Descriptive statistics values of Discrimination Index (DI) in OLT during testing phase.

TREATMENT GROUPS	MEAN	SD	SEM
CONTROL	6.97	26.69	10.90
D-GAL	-7.80	26.52	10.83
CM	27.92	9.29	4.16
CMD 90	37.79	6.39	2.86
CMD 45	13.95	8.09	3.62

Table 4.23. Descriptive statistics values of Total investigation time (TIT) in OLT during testing phase.

TREATMENT GROUPS	MEAN	SD	SEM
CONTROL	52.38	6.39	2.61
D-GAL	46.83	6.94	3.10
CM	63.96	4.65	2.08
CMD 90	67.07	5.67	2.53
CMD 45	55.14	5.02	2.05

Table 4.24. Summary of the mean values of Ach and AchE

TREATMENT GROUPS	CORTEX		HIPPOCAMPUS	
	AchE	Ach	AchE	Ach
Control	3.73 ± 0.16	32.51 ± 1.30	3.80 ± 0.28	33.33 ± 0.83
Dgal 90	3.91 ± 0.17	31.63 ± 0.88	3.98 ± 0.11	32.59 ± 1.48
CM 90	2.57± 0.068	45.74 ± 0.82	2.61 ± 0.083	37.48 ± 0.78
CMD 90	2.65 ± 0.088	44.48 ± 1.71	3.04 ± 0.072	37.28 ± 0.58
CMD 45	3.40 ± 0.22	35.93 ± 0.92	3.66 ± 0.14	34.09 ± 0.16

Table 4.25. Summary of mean values of Oxidative stress biomakers GSH and MDA including BDNF

GROUPS	CORTEX			HIPPOCAMPUS		
	BDNF	GSH	MDA	BDNF	GSH	MDA
Control	55.08±5.58	0.030±0.0045	1.57±0.063	54.18±2.88	0.041±0.0033	1.06±0.11
Dgal 90	57.13±4.55	0.025±0.0046	1.61±0.12	51.83±5.16	0.028±0.0048	1.63±0.077
CM 90	93.81±8.25	0.068±0.0045	0.92±0.055	95.21±6.83	0.076±0.0025	0.44±0.050
CMD 90	92.33±8.40	0.044±0.0048	1.04±0.11	86.88±6.67	0.045±0.0073	0.45±0.031
CMD 45	57.57±3.18	0.035±0.0025	1.23±0.10	63.39±7.44	0.039±0.0045	1.08±0.20

Table 4.26 Mean and SEM of Tumor Necrosis Alpha.

TREATMENT GROUPS	CORTEX	HIPPOCAMPUS
Control	304.6 ± 4.12	245.9 ± 12.88
D-gal	363.9 ± 21.77	446.4 ± 15.82
CM	267.6 ± 7.31	231.5 ± 11.37
CMD 90	262.1 ± 15.02	243.1 ± 14.33
CMD 45	284.3 ± 8.22	302.4 ± 10.91

Table 4.27. Mean and SEM of Antioxidant enzyme activity.

TREATMENT GROUPS	SOD 0MINS	SOD 5MINS	SOD 10MINS	SOD 15MINS	CATALASE	GPX
CONTROL	2.02 ± 0.68	2.17 ± 0.31	1.23 ± 0.15	1.37 ± 0.10	2.07 ± 0.2	0.03 ± 0.01
D-GAL	2.11 ± 0.74	1.87 ± 0.33	0.77 ± 0.35	0.86 ± 0.18	1.35 ± 0.12	0.02 ± 0.003
CM 90	2.23 ± 0.41	1.71 ± 0.37	1.58 ± 0.22	1.93 ± 0.22	2.46 ± 0.15	0.06± 0.005
CMD 90	1.38 ± 0.39	1.74 ± 0.30	1.26 ± 0.38	1.70 ± 0.18	2.67 ± 0.24	0.03 ± 0.003
CMD 45	1.96 ± 0.59	1.93 ± 0.23	1.08 ± 0.28	1.13 ± 0.16	1.96 ± 0.31	0.03 ± 0.003

Table 4.28. Descriptive statistics of Total DG volumes.

TREATMENT GROUPS	MEAN	SD	SEM
CONTROL	2.05	1.07	0.19
D-GAL	1.55	0.84	0.15
CM	2.60	1.34	0.24
CMD 90	2.46	1.37	0.25
CMD 45	2.43	0.25	0.23

Table 4.29. Descriptive statistics of Total HP volume.

TREATMENT GROUPS	MEAN	SD	SEM
CONTROL	4.78	2.23	0.41
D-GAL	4.05	1.99	0.36
CM	6.20	2.74	0.50
CMD 90	5.57	2.18	0.40
CMD 45	5.09	2.47	0.45

Table 4.30. Descriptive statistics of DCX cells in the DG

TREATMENT GROUPS	MEAN	SD	SEM
CONTROL	45.95	15.26	2.35
D-GAL	32.17	13.39	2.07
CM	68.24	35.11	5.42
CMD 90	51.69	19.04	2.94
CMD 45	50.14	23.66	3.65

Table 4.31. Descriptive statistics of Number of Ki67 in the DG

TREATMENT GROUPS	MEAN	SD	SEM
CONTROL	5.83	2.17	0.34
D-GAL	3.76	1.94	0.29
CM	8.36	3.90	0.60
CMD 90	7.95	5.15	0.79
CMD 45	4.81	2.28	0.35